ARSENIC IN A HIGH ARCTIC SOIL ECOSYSTEM ON DEVON ISLAND, NUNAVUT

A thesis submitted to the College of Graduate Studies and Research

In Partial Fulfillment of the Requirements for the Degree of

Master of Science

In the

Department of Soil Science

University of Saskatchewan

Saskatoon

By

Simone Levy

PERMISSION TO USE

In presenting this thesis in partial fulfillment of the requirements for a Postgraduate degree from the University of Saskatchewan, I agree that the Libraries of this University may make it freely available for inspection. I further agree that permission for copying of this thesis in any manner in whole or in part, for scholarly purposes may be granted by the professor or professors who supervised my thesis work or, in their absence, by the Head of the Department or the Dean of the College in which my thesis work was done. It is understood that any copyright or publication or use of this thesis or parts thereof for financial gain shall not be allowed without my written permission. It is also understood that due recognition shall be given to me and to the University of Saskatchewan in any scholarly use which may be made of any material in my thesis.

Requests for permission to copy or to make other use of material in this thesis in whole or in part should be addressed to:

Head of the Department of Soil Science
University of Saskatchewan
Saskatoon, Saskatchewan S7N 5A8

ABSTRACT

In this study, total As (T-As) levels in superpermafrost groundwater at a site in the High Arctic doubled over the course of the summer thaw. This increase was not due to snow input, as levels in snow were negligible. This increase in T-As did not correspond with a decrease in Eh, nor a rise in soluble Fe(II). It did, however, correspond with a shift in As speciation from arsenate to arsenite suggestive of reducing conditions. In the absence of predominant reducing conditions, the highly alkaline nature of the melting snow and concomitant large input of HCO_3^- may have played an important role in the increase of As in groundwater during the summer thaw.

Laboratory studies found that dissolved As (D-As) release under anaerobic conditions depended on the organic matter content of soil, with organic soils releasing D-As under reducing conditions and mineral soils sequestering D-As. In temperate soils, the release of D-As from organic soils is greatly accelerated due to the activity of anaerobic microbes. In northern soils, the same phenomenon may occur, with greater microbiological activity in organic soils where there is more labile C and nutrients than in mineral soil.

The sequestration of As in mineral soil is postulated to have occurred due to preferential sorption of arsenite to ferrihydrite or possibly to green rust minerals present under anaerobic conditions. Supporting this, arsenite sequestration occurred to a greater extent compared to arsenate, which is in agreement with the relative affinities of these two species for ferrihydrite.

Evidence from this study suggests that the As cycle on Truelove Lowland is dominated by the desorption of As due to HCO_3^- input each year during the spring melt

linked to the sorption of As to ferrihydrite or green rust present in underlying mineral soils. The sequential thawing of the soil's active layer and large inputs of HCO_3^- are unique to northern environments. Thus, this delicate balance of two sorbing processes should be born in mind in northern development. Large inputs of soluble organic matter or nutrients could cause increased solubilization and mobility of D-As during the summer thaw when soils become flooded.

ACKNOWLEDGEMENTS

I would like to thank my supervisor Dr. Steven Siciliano for his guidance throughout this project. I would also like to thank my supervisory committee, Drs. Derek Peak and Fran Walley for their advice along the way. Dr. Peak's assistance in sorting out the soil chemistry is greatly appreciated and Dr. Walley's support and encouragement really helped me to get through the tough bits. A special thanks also goes to Dr. Diane Knight for her help with my numerous statistics related questions.

Within Dr. Siciliano's research group I would particularly like to thank Alanna Dickson for her help and friendship along the way – Devon Island wouldn't have been the same without you! Thanks also to Wai Ma who was always willing to lend a hand. The use of Dr. Peak's lab and the assistance of his students, in particular Dani Xu and Pete Burnett, are greatly appreciated. I would also like to extend thanks to Dr. Germida for the use of his lab and supplies, and to Arlette Seib for her assistance on numerous occasions. Finally, I would like to thank everyone in the department of Soil Science for making it such a wonderful place to do an M.Sc., from office staff who go out of their way to arrange logistics, to all the professors who take time to get to know students individually.

This project was funded by NSERC-PGS-M, NSERC Discovery, NSERC Northern Research Internship Scholarship, the Polar Continental Shelf Project, and the Northern Scientific Training Program.

TABLE OF CONTENTS

LIST OF FIGURES

LIST OF TABLES

LIST OF ABBREVIATIONS

Arsenic abbreviations:

Arsenate	inorganic As in its oxidized form (H_3AsO_4, $H_2AsO_4^-$ and $HAsO_4^{2-}$)
Arsenite	inorganic As in its reduced form ($H_3AsO_3^0$, $H_2AsO_3^-$ and $HAsO_3^{2-}$)
D-As	aqueous As in a sample filtered through a 0.45μm filter
T-As	aqueous As concentration in an unfiltered sample

Other abbreviations:

AMD	acid mine drainage
ANOVA	analysis of variance
ATP	adenosine-5'-triphosphate
BAP	bathophenantholinedisulfonic acid disodium salt (98%)
CCA	chromated copper arsenic
DARB	dissimilatory arsenic-reducing bacteria
DFB	deferoxamine mesylate B
DIRB	dissimilatory iron-reducing bacteria
DMA	dimethyl arsenic
EXAFS	extended x-ray absorption fine structure
GLM	general linear model
HEPES	N-2-Hydroxyethylpiperazine-N'-2-ethanesulfonic acid
IBP	International Biological Project
LFS	lower foreslope
MMA	monomethyl arsenic
PDH	puruvate dehydrogenase
PVC	polyvinyl chloride
PZC	point of zero charge
RBC	raised beach crest
RPD	relative percent difference
SD	standard deviation
SE	standard error
SRB	sulfate-reducing bacteria
TiNTA	titanium(III) nitrilotriacetate
WHO	World Health Organization
WSM	wet sedge meadow

1.0 INTRODUCTION

Arsenic (As) is a known toxic contaminant with some forms of As having significant carcinogenic effects. Ingestion of As can also cause long term heart, liver, kidney and central nervous system damage (Vahter and Concha, 2001). Arsenic is ubiquitous, found in trace levels in the earth's atmosphere, waters, soils, and organisms (Nriagu, 1994). In the earth's crust, As is present at levels of up to several hundred mg kg^{-1}. The highest concentrations are found in marine shale materials, magmatic sulfides, and iron ores, where it occurs as arsenopyrite (FeAsS), realgar (AsS), and orpiment (As_2S_3) (Nriagu, 1994).

Elevated levels of As may be found in soils due to industrial activities such as mining and coal ash deposits, atmospheric fallout, pesticide application, and natural geological sources (Essington, 2004). Increasing development and human impact in Canada's North could lead to localized increases in As cycling in northern soil ecosystems (Mace, 1998). Therefore, it is important to determine baseline As levels in soil as well as understand natural biogeochemical cycling of As. There has been virtually no published research on As fate in northern ecosystems.

Arsenic exists in inorganic and organic forms and in different oxidation states (−3, 0, +3, +5). In soils, As exists primarily in two inorganic valence states, arsenate ($H_2AsO_4^-$, $HAsO_4^{2-}$) and arsenite ($H_3AsO_3^0$, $H_2AsO_3^-$) (Yang et al., 2005). Arsenate generally dominates under oxidizing conditions and arsenite dominates under reducing conditions (Sparks, 2003). While both forms of As have toxic effects in elevated doses, arsenite is

generally more toxic than arsenate (Hughes, 2002). In most soils, arsenite is also more mobile than arsenate (Masscheleyn et al., 1991).

In soil, arsenate and arsenite mainly sorb to the surface of soil colloidal particles. These particles can be oxides or hydroxide surfaces of Fe, Al and Mn, phyllosilicates, carbonates, or organic matter (Sadiq, 1995). Due to the negative charge of As oxyanions under most pH and redox conditions, positively charged surfaces offer the most favourable binding sites. Arsenic is most commonly associated with Fe minerals in soil, in large part due to the positive charge of Fe oxides and hydroxides below approximately pH 8 (Sadiq, 1995; Pfeifer et al., 2004; Yang et al., 2005). Under neutral to alkaline conditions, carbonates are common ligands for As (Romero et al., 2004), and in acidic conditions As can bind to Al oxides and hydroxides (Huang, 1975).

While Fe minerals provide numerous sorption sites for As, the redox-sensitive nature of both Fe and As can result in solubilization of As under certain environmental conditions (Masscheleyn et al., 1991; Sadiq, 1995). When As is solubilized, it becomes mobile and can migrate into waters used for human or wildlife consumption. In temperate soil ecosystems, solubilization of As follows flooding of soil as O_2 is consumed by aerobic microorganisms and conditions become reducing (Takahashi et al., 2004). Following depletion of O_2, anaerobic microbes, specifically dissimilatory iron-reducing bacteria (DIRB) use Fe(III) in Fe minerals as their terminal electron acceptors. The reduction of Fe(III) destabilizes the mineral, releasing sorbed As (Ahmann et al., 1997; Rochette et al., 1998; Cummings et al., 1999).

In the Canadian High Arctic, the summer thaw is a yearly phenomenon when temperatures warm sufficiently to melt overlying snow and thaw the soil, developing the active layer to depth. During this time there is a pulse of biological activity (Pfeifer et

al., 2004), and many biogeochemical reactions take place only during this time. Snowmelt usually occurs within approximately two weeks, and meltwater accumulates in depressional landscape positions (Ryden, 1977). During the development of the active layer, soils remain saturated by meltwater perched on the permafrost table. Soils in depressional areas are mainly Gleysolic with an overlying layer of organic material from decomposition of vegetation adapted to submerged soils including sedges, mosses and grasses (Muc and Bliss, 1977; Walker and Peters, 1977).

The hypothesis for this study was that saturation of soil during the summer thaw would promote reducing conditions, leading to solubilization of As. This study aimed to elucidate the mechanisms controlling As fate in a High Arctic soil ecosystem located on Truelove Lowland, Devon Island, Nunavut.

The project described in this thesis involved both a field and laboratory component. In the field, snow samples were taken for analysis of As content just before the major summer thaw event. While snow was melting, samples of ponded meltwater were collected for analysis of total As (T-As) and dissolved As (D-As, sample filtered through a 0.45μm filter) content. Within approximately two weeks of arriving at the site, all snow had melted and the active layer began to develop. Once approximately 30 cm of soil had thawed, wells to trap superpermafrost groundwater were inserted in the active layer. Wells were made of 5 cm diameter polyvinyl chloride (PVC) pipe with slits for entry of water and were isolated from surface water using bentonite chips. On a bi-daily basis Eh, pH and temperature were recorded from water that had accumulated in the wells. Wells were then purged of three volumes, depending on recharge velocity, and samples of recharged water were taken for analysis of T-As, D-As, arsenite, arsenate,

Fe(III), Fe(II), and sulfide. Prior to leaving the site, soil samples from four sites at the study location were collected for use in laboratory experiments.

Soils from Truelove Lowland were used in controlled environment experiments with manipulation of redox status at cold temperatures to determine whether redox status was affecting As partitioning in soil and groundwater. Soil slurries (1:40 soil to water ratio) were incubated in Nalgene® bottles ('microcosms') under aerobic and anaerobic headspace and shaken continuously at 10°C. Further experiments aimed to determine what would occur when soil slurries were spiked with As under aerobic and anaerobic conditions.

This thesis is presented in six chapters. This introduction (Chapter 1) is followed by a review of pertinent literature presented in Chapter 2. The literature review discusses As toxicity, As chemistry in soils, and environmental phenomena in the High Arctic that may affect As partitioning in soil and water. Chapters 3 and 4 comprise the main body of the thesis and detail the procedures and results obtained from field and laboratory investigations. In Chapter 3, the field site and environmental conditions during the field stay are described in detail. Levels of As in snow, meltwater and superpermafrost groundwater are presented along with environmental parameters (Eh, pH and temperature). Chemical and microbiological processes that may affect As partitioning are discussed.

Chapter 4 outlines the results of laboratory investigations looking at As partitioning in soil slurries incubated aerobically and anaerobically. A further microcosm experiment with an As spike provides useful information on As partitioning and speciation over time.

Chapter 5 summarizes the findings of the field and laboratory investigations. Conclusions are drawn as results of microcosm experiments are used to explain As partitioning in soil and superpermafrost groundwater at the field site.

Finally, Chapter 6 is a list of references and literature cited throughout the thesis.

2.0 LITERATURE REVIEW

2.1 Arsenic sources and uses

Arsenic is ubiquitous in the environment with a crustal abundance of 0.0001% (Nriagu, 1994). Though it is a relatively rare element, As is often found in very high concentrations in certain areas around the world depending on the deposition environment of soil and bedrock. Arsenic is commonly found with the ores of metals such as copper, lead, nickel, silver, and gold (Frankenberger, 2002). Arsenic is produced as a by-product of ore extraction, often in vast quantities.

Certain forms of As are very toxic and historically As was used as a poison. Before the mid-19th century when James Marsh devised the first chemical test for the presence of As in tissue, it was sometimes referred to as "inheritance powder" (Oremland and Stolz, 2003). In fact, there is debate as to whether Napoleon Bonaparte was poisoned by As (Lin et al., 2004). Ingestion of As causes health problems by affecting numerous organs including the skin, cardiovascular, nervous, hepatic, hematological, endocrine and renal systems, and can cause cancerous tumors to develop on the skin as well as in the bladder, liver, and kidneys (Smith et al., 1992; Nordstrom, 2002). Arsenic does not bioaccumulate as do other toxic metals such as mercury (Huang et al., 2005).

In lesser doses As has a long history of medical applications; before penicillin was developed, an As compound was used to treat syphilis and yaws (Rattner, 1943). Today, As trioxide (AsO_3) is used to treat human leukemia (Shigeno et al., 2005). Roxarsone,

an organoarsenic compound, is added to poultry feed to improve weight gain and feed efficiency and is used as an antibiotic and palliative agent for swine (O'Connor et al., 2005).

Arsenic also has several industrial applications. In the past, organic arsenicals were used extensively in herbicides and pesticides (Swiggart et al., 1972). Arsenic is used in combination with other materials in pigments, poison gases and insecticides (such as Paris Green, calcium arsenate and lead arsenate) and is well known from former use as a rat poison (Bartrip, 1992). Arsenic is used in ammunition manufacturing because it helps to create harder and rounder bullets (Koons and Grant, 2002). It is also used in small quantities in semi-conductor manufacturing, as a preservative in tanning and taxidermy, as well as on the exterior of wood, such as deck and playground materials (Ndiokwere, 1985).

Waste from any of the above applications can cause serious As contamination. For example, numerous orchards contain excessive amounts of As where As-containing pesticides were used over an extended period of time (Merwin et al., 1994), and As is known to leach out of ammunition that is not properly disposed (Nriagu, 1994). Arsenic contamination also results from improperly disposed solution for preservation of wood with chromated copper arsenate (CCA), and leaching of As from treated wood as it ages is a known mechanism of soil contamination (Ndiokwere, 1985; Cui et al., 2005).

Despite its numerous uses, far more As is produced than is able to be put to use in the world market. As mentioned previously, average As content in soil and rock is quite low; however, in areas containing metal deposits, As can be found in excessive quantities. One such example is at Spain's Aznalcollar/Los Frailes Ag-Cu-Pb-Zn mine, one ton of ore produces 28.35 g gold, 56.7 g silver, 9 kg of copper, and 81.72 kg of As

as a by-product (Hudson-Edwards et al., 2005)! If improperly stored, As from waste material can become mobile and enter surface and groundwater, causing widespread contamination.

The best example of this in the Arctic is the Royal Oak Giant Mine. The Giant Mine is located within the city limits of the city of Yellowknife in Canada's Northwest Territories. Mining began in 1948 with shallow underground excavation, followed by open pit mining in 1974. Since 1974, underground workings have been developed to 610 m. Waste rock was used as backfill and in construction of tailings dams and road surfacing.

The site is in the zone of discontinuous permafrost and surface relief at the site is less than 75 m. The main pathways of groundwater recharge include flow through old mine workings, unfilled drill holes, sub-vertical faults, and associated splays. Minimal groundwater recharge occurs during the spring melt because the frozen active layer acts as a barrier.

The gold recovered at Giant Mine is hosted in arsenopyrite (FeAsS). Over the past 50 years, an excess of approximately 237,000 tonnes of As trioxide (AsO_3) dust has been stored in old stopes and specially designed chambers in the shallow underground (Clark and Raven, 2004). Samples of AsO_3 or "baghouse dust" contain between 58 and 68% As. Concentrations of As in flowing drillholes and seeps near the storage chambers range from 0.1 to greater than 4 g L^{-1}. Groundwater contains an average As concentration of 16 mg L^{-1}, and the migration of As into groundwater presents a hazard to nearby groundwater users.

2.2 Arsenic toxicity

The acute toxicity of As is related to its chemical form and oxidation state. Arsenic exists in inorganic and organic forms and in different oxidation states (–3, 0, +3, +5). Arsenate is generally found in oxidizing environments, while arsenite is generally found in reducing environments (Nriagu, 1994). While both species of As can be quite toxic in sufficient doses, arsenite is considered more toxic than arsenate (Vahter and Concha, 2001). In the mouse, the oral LD_{50} of arsenite is 8 mg kg^{-1}, while that for arsenate is 22 mg kg^{-1} (Bencko et al., 1978). In the human adult, the lethal range of inorganic As is estimated at a dose of 1–3 mg As kg^{-1} (Ellenhorn, 1997). The characteristics of severe acute As toxicity in humans include gastrointestinal discomfort, vomiting, diarrhea, bloody urine, anuria, shock, convulsions, coma, and death (Ellenhorn, 1997).

Millions of people around the world are chronically exposured to As via drinking water (Anawar et al., 2003). The World Health Organization (WHO) has recently lowered the limit for D-As in drinking water from 50 to 10 μg L^{-1} (WHO, 2001). Improved cost-effective technologies will be required to remove D-As from drinking water to meet WHO guidelines and protect consumers from potential effects of As consumption.

Both arsenite and arsenate affect the production of adenosine-5'-triphosphate (ATP) with the toxicity of arsenite better understood compared to arsenate (Hughes, 2002). Arsenite is highly reactive with sulphur and readily reacts with thiol-containing molecules such as glutathione and cysteine. Arsenite causes toxic effects by binding to thiol groups, causing inhibition of important biochemical events (Scott et al., 1993). An example of this is the inhibition of pyruvate dehydrogenase (PDH) by arsenite. Pyruvate

dehydrogenase requires the cofactor lipoic acid, a dithiol, for enzymatic activity, and arsenite binds to lipoic acid (Szinicz and Forth, 1988). Pyruvate dehydrogenase is an integral part of the citric acid cycle, and inhibition of PDH may ultimately lead to decreased production of ATP. Inhibition of PDH may explain in part the depletion of carbohydrates observed in rats administered arsenite (Reichl et al., 1988; Szinicz and Forth, 1988).

Arsenate is an analogue of phosphate (PO_4^{3-}) and acts as a competing ligand in the numerous physiological reactions in which PO_4^{3-} participates. Arsenate interferes with the sodium pump and anion exchange transport system of human erythrocytes (Kenney and Kaplan, 1988). Another mode of toxic action is the uncoupling of formation of ATP when 'arsenolysis' replaces glycolysis. In one step of the glycolytic pathway, phosphate is linked enzymatically to D-glyceraldehyde-3-phosphate to form 1,3-biphospho-D-glycerate. Arsenate can replace phosphate in this reaction to form the anhydride 1-arsenato-3-phospho-D-glycerate. However, this anhydride is unstable and it hydrolyzes to arsenate and 3-phosphoglycerate (Dixon, 1997).

2.2.1 Detoxification mechamisms and methylation of As

In humans and other mammals, detoxification of As occurs via methylation, making the molecules less reactive with tissue components (Vahter and Concha, 2001). In higher eukaryotes, glutathione reduces arsenate to arsenite, which then accepts a methyl group from S-adenosylmethionine, producing monomethylarsonic acid (MMA^V) or dimethylarsonic acid (DMA^V) (Hughes, 2002). Monomethylarsonous acid (MMA^{III}) and dimethylarsinous acid (DMA^{III}) are proposed intermediates in the metabolism of As

and have recently been detected in the urine of humans chronically exposed to inorganic As in their drinking water (Aposhian, 1989). Binding of arsenite at nonessential sites in proteins may also be a detoxication mechanism (Aposhian, 1989).

In the environment, some species of bacteria and fungi are also able to methylate As as a mechanism of detoxification. The most well studied mechanism of detoxification and resistance is the ArsC system (Gadd, 1993). At least three different but structurally related arsenate reductases have convergently evolved in bacteria and fungi. ArsC, a small–molecular mass protein (13 to 16 kD), mediates the reduction of arsenate to arsenite in the cytoplasm. Although arsenite is more toxic, it can be excreted via an arsenite-specific transporter, ArsB (Rosen, 2002). In the soil ecosystem, methylated arsenicals are generally produced only when As is in great excess; therefore, methylated forms of As can be virtually discounted in uncontaminated systems (Sadiq, 1995; Turpeinen et al., 1999).

2.3 Arsenic speciation and sorption in soils

In soils, As exists primarily in two inorganic valence states, arsenate ($H_2AsO_4^-$, $HAsO_4^{2-}$) and arsenite ($H_3AsO_3^0$, $H_2AsO_3^-$) (Yang et al., 2005). The pKa_1 of arsenite as $H_3AsO_3^0$ is 9.20, pKa_2 is 12.13, and pKa_3 is 13.4 (Raven et al., 1998). The pKa_1 of arsenate as H_3AsO_4 is 2.19, pKa_2 is 6.94, and pKa_3 is 11.5 (Stumm and Morgan, 1996). Thus, in natural soil and water with pH between 6 and 9, arsenite exists primarily as neutral $H_3AsO_3^0$ and arsenate exists as mono- or divalent $H_2AsO_4^-$ or $HAsO_4^{2-}$.

Adsorption of As in soil mainly occurs on the surface of soil particles. These particles can be oxides or hydroxide surfaces of Fe, Al and Mn, phyllosilicates,

carbonates, or organic matter. Due to the negative charge of As oxyanions under most pH and redox conditions, As has a limited affinity for organic complexation and is not expected to form complexes with Cl^-, SO_4^{2-} or HCO_3^- (Sadiq, 1995).

Arsenite is generally considered to be more mobile in soil ecosystems than arsenate (Masscheleyn et al., 1991). Some authors suggest this is because arsenate sorbs to a host of soil solids, while arsenite is more discriminate and tends to bind strongly only to ferrihydrite (Sadiq, 1995; Manning et al., 1998; Raven et al., 1998).

Under reducing conditions, mixed Fe(II)/Fe(III) oxides often form in soil and sediment and are commonly referred to as "green rust minerals" (Randall et al., 2001). Green rust minerals consist of sheets of $(Fe(II))(OH)_6$ in which some of the Fe(II) is replaced by Fe(III), and are postulated to be an intermediate phase in the formation of iron oxides such as goethite, lepidocrite and magnetite (Su and Puls, 2004). Both arsenate and arsenite have been found to sorb substantially to green rust minerals. In a microcosm experiment to determine the sorption capacity of arsenate on green rust, sorption after 10 h was 92 to 94%. In a similar experiment, Lien and Wilkin (2005) observed a decrease in aqueous arsenite by a factor of 10 times after 50 h, and a decrease of 100 times after 200 h. The mechanism of removal has not been confirmed but is presumed to be via adsorption or co-precipitation.

The majority of As adsorption on particle surfaces is generally via outer-sphere complexation. Outer-sphere complexation occurs when the attraction between a metal and a ligand is strictly due to electrostatic forces. Inner-sphere complexes are defined as covalent linkages between the adsorbed ion and the reactive surface with no water of hydration between the adsorbed ion and the surface functional group (Sposito, 1984). Inner sphere complexation can occur well above the ligand's point of zero charge (PZC).

Inner-sphere complexes are expected to form when solution concentration of As is high, while outer-sphere complexes form when solution concentration is lower (Sparks, 2003).

With increasing reaction time, outer-sphere complexes can be transformed to more stable inner-sphere complexes, excluding the waters of hydration. Experiments by Fendorf et al. (2004) have shown that bioaccessibility of As decreases exponentially over 100 d of incubation, as outer-sphere complexes undergo transformation to inner-sphere complexes (Manning et al., 1998; Fendorf et al., 2004). Extended X-ray Absorption Fine-Structure Spectroscopy (EXAFS) data shows that over time, a bidentate binuclear bond forms between arsenate and goethite with a bond length of 3.24 Å (Figure 2.1).

Three types of bond can form between arsenate and geothite depending on surface coverage level. At high surface loading, bidentate binuclear complexes dominate, while monodentate bonds form at low surface coverage. At surface coverage near monolayer capacity, bidentate binuclear complexes dominate (Fendorf et al., 1997). Spectroscopic evidence for inner-sphere complexes between arsenite and geothite shows that bidentate binuclear complexes also form between arsenite and the geothite surface with a bond length of 3.38Å (Figure 2.1) (Manning et al., 1998).

Iron oxide surfaces in soil may develop electrical charge due to hydration, specific adsorption, changes in cation coordination, isomorphous substitution, and crystallinity. Hydrous Fe oxides/hydroxides are reported to have a PZC ranging from 7.9 to 9.0 with a mean around 8.0 (Dzombak and Morel, 1987). In most slightly alkaline, neutral or acidic soil solutions, Fe oxides will be positively charged and will be suitable ligands for anionic As. The PZC of Al-oxide/hydroxides is around pH 6 (Huang, 1975; Dzombak and Morel, 1987). Aluminium oxides play a more significant role as sorptives for As in

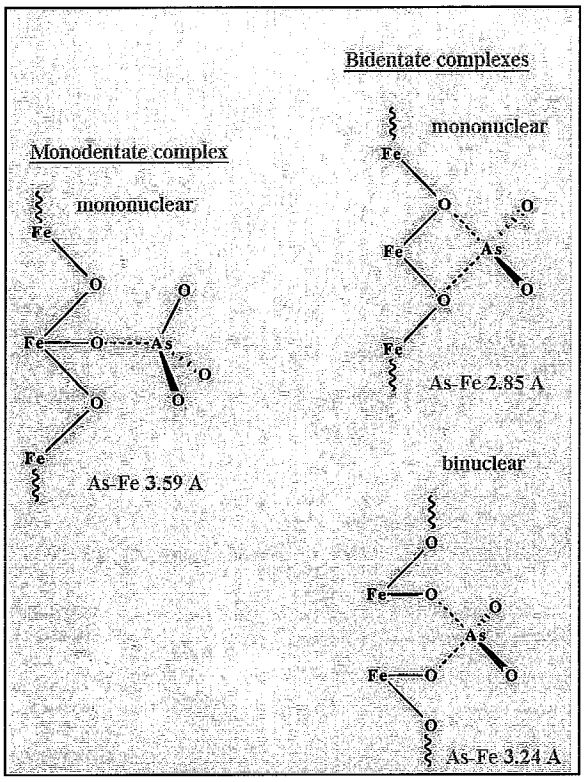

Figure 2.1 Schematic illustration of the surface structure of arsenate on goethite based on the local coordination environment determined with extended x-ray absorption fine structure (EXAFS) spectroscopy (adapted from Fendorf et al. (1997)).

acidic soils. Manganese oxide surfaces have a PZC around pH 2, and carry a negative charge in most soil solutions (McKenzie, 1981).

Clay minerals (phyllosilicates) have a variable charge due to protonation of surface oxygen and deprotonation of surface hydroxyl (Sparks, 2003). Complexation of As on the surface of clay particles depends on properties of particular clays. Figure 2.2 shows adsorption of arsenate on illite, kaolinite and montmorillonite over a pH range of 3 to 11.

The PZC of clay minerals varies considerably, ranging between pH 4 to 8 with a mean around pH 5 (Sadiq, 1995). In acidic soils when surfaces are positively charged, clays can be important ligands for As. Clay particle surfaces can also have Fe or Al coatings that provide positive binding sites for As (Manning et al., 1998; Goldberg and Johnston, 2001).

Carbonate minerals play an important role in As sorption in alkaline soils and especially in calcareous soils. The PZC values determined for one of the main carbonate minerals, calcite ($CaCO_3$), range from pH 7 to 10.8. The PZC for a particular mineral depends on the mineral type, state of crystallinity, hydration, impurities, precipitation of a new phase at the surface of the calcite crystal, differences in solution composition among experimental studies, and partial pressure of CO_2 (Stumm, 1992; Sadiq, 1995; Romero et al., 2004).

The range of PZC values for calcite suggests that it has a high potential for As retention in the natural environment. For example, Romero et al. (2004) found that retention of arsenate correlated with calcite content of aquifer material. Further, Rochette et al. (1998) found that the apparent solubility of arsenate complexes under oxic conditions decreased in the order $CaHAsO_4 = Na_2HAsO_4 \cdot 7H_20 > AlAsO_4 \cdot 2H_2O > MnHAsO_4 > FeAsO_4 \cdot 2H_2O$. This suggests that carbonate mineral-As complexes

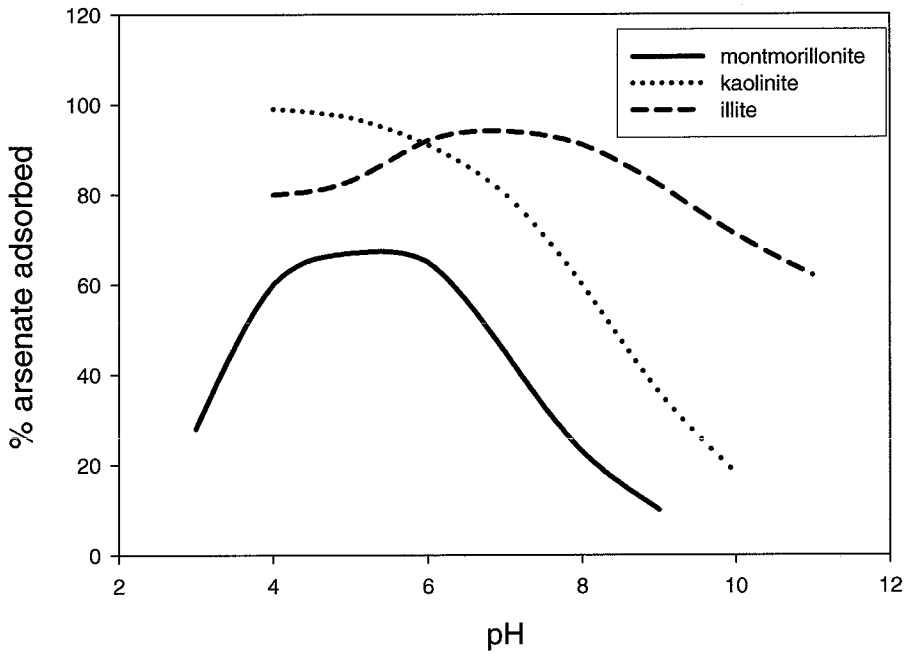

Figure 2.2 Adsorption of arsenate (%) to clays montmorillonite, kaolinite and illite over a range in pH (adapted from Manning and Goldberg (1996)).

are stable in aqueous solution and that if sufficient Ca is available, these complexes will form and persist.

2.3.1 Eh and microbial processes controlling As speciation

In soil, redox status is a dynamic process, often changing dramatically over a period of hours to days. In the study of soils redox potential is commonly referred to as Eh and is expressed in millivolts (mV). A decrease in Eh often follows the flooding of soil as water on the soil surface slows diffusion of O_2, limiting its availability for ecological processes requiring O_2 (Kirk, 2004). In a soil ecosystem, availability of O_2 through the soil profile depends heavily on physical properties including soil structure, pore space saturation and the depth and degree of oxygenation of overlying water.

Microbial processes and photosynthesis are the main processes requiring O_2, and in temperate ecosystems O_2 is consumed rapidly (Kirk, 2004). When supplies of O_2 have been exhausted, microbes turn to other molecules that can serve as terminal electron acceptors, reducing compounds such as NO_3^- to NO_2^-, Mn(IV) to Mn(II), Fe(III) to Fe(II), and arsenate to arsenite (Stumm and Morgan, 1996).

Oxygen is the most energetically favourable electron acceptor and has what can be described as the "greatest affinity for electrons" (Kirk, 2004). Once oxygen is consumed, microbes generally use alternative terminal electron acceptors in the order of energetic favourability (Zhender and Stumm, 1988). Table 2.1 outlines the sequence in which electron acceptors are used for dissimilatory reduction, assuming that molecular hydrogen is used as the electron donor (Newman et al., 1998). The free energy generated by the reduction of arsenate is expected to fall below that generated by

Table 2.1 Free energies of various electron acceptors coupled to H_2 oxidation (adapted from Newman et al., 1998).

Reaction	ΔG', kcal/mol e^-	Eh range (mV)
$\frac{1}{4}\ O_{2\,(g)} + \frac{1}{2}\ H_2 \rightarrow \frac{1}{2}\ H_2O$	-23.55[a]	350 – 600
$\frac{1}{3}\ NO_3^- + 1/5\ H^+ + \frac{1}{2}\ H_2 \rightarrow 1/10\ N_2(g) + 3/5\ H_2O$	-20.66[a]	200 – 500
$\frac{1}{2}\ MnO_2(s) + H^+ + \frac{1}{2}\ H_2 \rightarrow \frac{1}{2}\ Mn^{2+} + H_2O$	-22.48[b]	200 – 400
$\frac{1}{2}\ SeO_4^{2-} + \frac{1}{2}\ H^+ + \frac{1}{2}\ H_2 \rightarrow \frac{1}{2}\ HSeO_3^- + \frac{1}{2}\ H_2O$	-15.53[b]	200 – 400
$1/8\ NO_3^- + \frac{1}{4}\ H^+ + \frac{1}{2}\ H_2 \rightarrow \frac{1}{8}\ NH_4^+ + 3/8\ H_2O$	-13.42[a]	200 – 400
$\frac{1}{3}\ CrO_4^{2-} + 5/3\ H^+ + \frac{1}{2}\ H_2 \rightarrow \frac{1}{3}\ Cr^{3+} + 4/3\ H_2O$	-10.76[b]	100 – 300
$Fe(OH)_{3(am)} + 2H^+ + \frac{1}{2}\ H_2 \rightarrow Fe^{2+} + 3\ H_2O$	-10.4[b]	0 – 150
$\frac{1}{4}\ HSeO_3^- + \frac{1}{4}\ H^+ + \frac{1}{2}\ H_2 \rightarrow \frac{1}{4}\ Se^0 + \frac{3}{4}$ H2O	-8.93[b]	0 – 200
$\frac{1}{2}\ H_2AsO_4^- + \frac{1}{2}\ H^+ + \frac{1}{2}\ H_2 \rightarrow \frac{1}{2}\ H_3AsO_3 + \frac{1}{2}\ H_2O$	-5.51[c]	0 – 200
$\frac{1}{3}\ H_3AsO_3 + \frac{1}{2}\ H_2 \rightarrow \frac{1}{3}\ As^0 + H_2O$	-2.58[d]	-100 – (+100)
$\frac{1}{8}\ SO_4^{2-} + \frac{1}{8}\ H^+ + \frac{1}{2}\ H_2 \rightarrow \frac{1}{8}\ HS^- + \frac{1}{2}\ H_2O$	-0.10[a]	-200 - (-100)

$P_{H2} = 10^{-6.6}$ atm = 10 nM; $P_{N2} = 0.78$ atm; $P_{O2} = 0.21$ atm; pH = 7.0.
$[NO_3^-] = [NH_4^+] = [Mn^{2+}] = [Fe^{2+}] = [SeO_4^{2-}] = [HSeO_3^-] = [CrO_4^{2-}] = [Cr^{3+}] = [H_2AsO_4^-] = [H_3AsO_3] = [SO_4^{2-}] = [HS^-] = 1\mu M$.

[a]Calculated from Zhender and Stumm (1988)
[b]Calculated from Morel and Hering (1993)
[c]Calculated from Sadiz (1990)
[d]Calculated from Vanysek (1995)

reduction of NO_3^-, Mn(IV) and Fe(III). While direct arsenate respiration is expected to occur only after stronger oxidants have been depleted, the reduction of NO_3^-, Mn(IV) and especially Fe(III) can have important implications for As speciation and mobility.

The reduction of NO_3^- does not have a direct impact on As speciation. However, once NO_3^- has been depleted, certain microbes can synthesize the arsenate reductase enzyme required for reduction of arsenate to arsenite. This form of metabolism is termed dissimilatory As reduction with dissimilatory As-reducing bacteria (DARB) used to describe this class of microorganism (Oremland et al., 2000). There are no known microbes that are solely reducers of As; most DARB will preferentially reduce NO_3^- when it is available as it is more energetically favourable (Dowdle et al., 1996; Newman et al., 1998).

Sulfospirillum barnesii strain SES-3 is one of a number of arsenate respiring organisms that has been isolated and characterized (Laverman et al., 1995; Oremland et al., 2000). Although it remains to be proven, the gene encoding arsenate reductase in strain SES-3 is presumed to have a chromosomal locus. Supporting this assumption, when cells of strain SES-3 are grown in NO_3^- - containing medium, the ability to reduce arsenate is retained from one generation to the next (Laverman et al., 1995). The rate of arsenate reduction reaches a maximum at approximately 5 mM arsenate; at higher concentrations toxicity begins to slow growth (Dowdle et al., 1996).

Microbes classified as Dissimilatory Iron-Reducing Bacteria (DIRB) are able to use Fe(III) as their terminal electron acceptor. In soil, Fe(III) is most commonly encountered in oxide form, and arsenate and to some extent arsenite are commonly sorbed to iron oxides (Sparks, 2003). In general, when Fe(III) in Fe oxides is

reduced,arsenate and arsenite will desorb, and this may or may not be followed by reduction of arsenate (Cummings et al., 1999).

Similar to NO_3^- reducers, some DIRB species are able to reduce arsenate, while others are not. Certain microbes such as *Sulfurospirillum barnesii* are capable of anaerobic growth using Fe(III) or arsenate as their terminal electron acceptor and will reduce arsenate when it is sorbed to an Fe oxide surface (Zobrist et al., 2000). Other microbes, such as *Shewanella alga* BrY and *Geobacter metallireducens*, are able to reduce Fe(III) only (Cummings et al., 1999; Tadanier et al., 2005).

Indirectly, the reduction of sulfate by sulfate-reducing bacteria (SRB) can affect the state of As in the soil solution. Hydrogen sulfide (H_2S or HS^-) is produced when SRB reduce SO_4^{2-}, and can accumulate in reducing environments (Rittle et al., 1995). Hydrogen sulfide is a powerful reductant that can reduce arsenate to arsenite, followed by precipitation as (Fe)AsS complexes (Rochette et al., 2000). The reduction of arsenate by H_2S occurs as follows:

$$H_2AsO_4^- + H_2S + H^+ \leftrightarrow H_3AsO_3 + 1/8S_8 + H_2O \qquad (2.1)$$

The rate constant of this reaction proceeds 300 times faster at pH 4 than at pH 7. For example, within 33 h nearly complete conversion of arsenate to arsenite occurs at pH 4, while less than 10% is reduced at pH 7 with an initial H_2S:arsenate ratio of 10^4:1 (Rochette et al., 2000). Therefore, an acidic environment and a high concentration of H_2S would be required for reduction of arsenate to arsenite.

2.3.2 Arsenic solubilization in Acid Mine Drainage (AMD)

In general, soils have extremely high buffering capacities. Changes in the acidity of a soil ecosystem are usually the result of production of large amounts of concentrated H^+ ions either by oxidation of minerals, processes occurring in the rhizosphere or a large input of carbonate (Sparks, 2003). Since both arsenite and arsenate exist as hydrated ions, changes in pH can cause protonation and deprotonation as well as changes in speciation. Changes in pH can also cause mineral surfaces to which As is sorbed to become more or less negatively charged, potentially enhancing As mobility (Sparks, 2003). One example of dramatic changes in soil acidity occurs due to Acid Mine Drainage (AMD), a phenomenon common in the mining industry.

Under strongly reducing conditions (Eh < -100 mV), As can be precipitated with Fe and S minerals forming arsenopyrite (FeAsS) and related minerals. When an area is mined, waste rock containing these minerals is exposed to O_2, and reduced species of Fe, As and S are oxidized to Fe oxides, arsenate and SO_4^{2-}. While AMD does proceed without microbial action, it has been reported that sulphide oxidation catalysed by bacteria may have reaction rates six orders of magnitude (i.e. 1,000,000 times) greater than the same reactions in the absence of bacteria (Evangelou and Zhang, 1995). Oxidation of sulphur or sulphides for energy production is restricted to the bacterial genera *Thiobacillus*, *Thiomicrospira*, and *Sulfolobus.* These bacteria all produce sulphuric acid as a metabolic product (Groudeva et al., 2004).

Arsenic is mobilized when reduced species become oxidized, and sulfuric acid leaches As from waste rock to reduce the pH. The oxidation of arsenite to arsenate occurs via the following reactions:

$$As_2O_3 + 3H_2O \rightarrow 2H_3AsO_3^0 \quad (2.2)$$

$$H_3AsO_3^0 + H_2O \rightarrow H_2AsO_4^- + 3H^+ \quad (2.3)$$

Arsenate could complex with Fe oxides; however, the extremely acidic environment, with pH as low as 2, creates an environment conducive to mobilization of arsenate (Evangelou and Zhang, 1995). The leachate produced by AMD carrying toxic metals can enter nearby streams, rivers or seep into groundwater.

The stability phase diagram in Figure 2.3 illustrates how Eh and pH interact to control As speciation and potential sorption. The diagram was generated using data from the experiment described below and simple thermodynamic calculations (Masscheleyn et al., 1991). Briefly, when soils were incubated aerobically and arsenate was the predominant As species, As was coprecipitated [as arsenate] with Fe oxides and released upon their solubilization. Alkaline conditions and/or reduction of arsenate to arsenite led to a mobilization of As. Under moderately reduced conditions (0 - 100 mV), As solubility was controlled by the dissolution of Fe oxides.

Similarly, an experiment by Takahashi et al. (2004) in a temperate area (Japan) revealed that leachable As increased by seven times when soil was flooded versus dry due to reductive dissolution of Fe oxides. In the Arctic, the summer melt could cause the same phenomenon in depressional areas that become flooded. If this happens during a time of high flow, As could be released, transported in meltwater, and later re-adsorbed or precipitated when soils dried out, causing a concentration of As in depressed areas of the landscape.

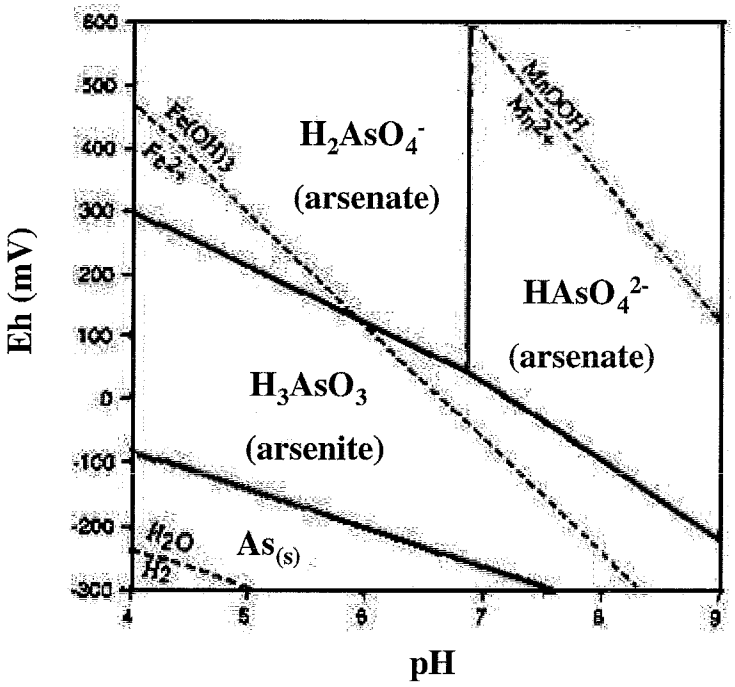

Figure 2.3 Stability field Eh-pH diagram for the As-H_2O system. Activities of As, Fe and Mn were all taken to be 10^{-4}. The designated species make up >50% of total As species. Lines represent the stability field for the Fe and Mn systems (dotted line) and arsenic (solid line) (adapted from Masscheleyn et al. (1991)).

2.4 The Arctic soil ecosystem

Soils in this thesis are classified and described according to 'The Canadian System of Soil Classification, Third Edition' (National Research Council, 1998). Soils in the High Arctic are generally of the Cryosolic order. Cryosols can be classed into the following three great groups: Turbic, Static or Organic. Turbic Cryosols develop primarily in fine-textured mineral material and have marked evidence of mixing of horizons, termed 'cryoturbation'. Static Cryosols develop primarily in well-drained coarse-textured mineral parent materials, or in a wide textural range of recently deposited or disturbed sediments where evidence of cryoturbation is still largely absent. They may have organic surface horizons less than 40 cm thick. Having an overlying organic horizon in excess of 40 cm differentiates organic Cryosols from Turbic and Static Cryosols. Turbic Cryosols are defined as having a permafrost layer within 2 m of the surface, while Static and Organic Cryosols have permafrost within 1m (Harris et al., 1988).

Repeated freezing and thawing of soil, particularly in Turbic Cryosols, has the effect of changing soil structure by affecting the arrangement of soil pores and particles. The expansion of ice and the contractions resulting from the suctions in unfrozen water has the effect of increasing pore size and compressing soil aggregates (Williams and Smith, 1989). Cryoturbation further alters soil structure. Thus, the freezing process could expose new surfaces that either retain or release As that is potentially available for reaction during the following summer thaw.

The summer thaw is particularly important in the context of As cycling. When air temperature warms sufficiently to melt overlying snow, two phenomena occur: 1) meltwater runs through the active layer, perched on the permafrost table, and 2) the

active layer simultaneously develops as thawing proceeds. Meltwater eventually collects in depressional areas and evaporates rapidly in the dry and often windy Arctic climate (Ryden, 1977). Rainfall events and meltwater from further development of the active layer in elevated landscape positions serve to replenish pooled water in depressional areas.

2.4.1. Microbes in cold temperatures

Microbiological processes do proceed in cold temperatures, albeit at reduced rates (Stapleton et al., 2005). Cold temperatures and low nutrient conditions give rise to a unique group of microorganisms known as psychrophiles, i.e. cold-loving microorganisms, and psychrotrophs, i.e. cold-requiring bacteria. Psychrophiles can grow at mesophilic temperatures whereas psychrotrophs cannot (Deming, 2002). Microbes in cold environments have specific adaptations including increased cell membrane lipid constituents to avoid solidification. This is especially important for maintaining the ability to transport substrates and nutrients under very cold, otherwise rigidifying conditions (Chattopadhyay and Jagannadham, 2001). Cold-specific enzymes with reduced activation energies must be synthesized by microbes in cold environments, and cold shock proteins must be available for homeostasis as the temperature drops (Sheridan et al., 2000). To date no psychrophilic DARB have been isolated (Oremland and Stolz, 2003), but the activities of certain genera of DIRB have been observed at cold temperatures.

In a study by Stapleton et al. (2005), isolates of the genus *Shewanella*, known for their Fe-reducing capability, were able to use a variety of electron acceptors including

oxygen, nitrate and metals coupled with the oxidation of several organic acids, glucose or hydrogen at temperatures down to 0°C. More specific to As chemistry, the *Shewanella* isolates were able to reduce Fe(III) at temperatures from 0 to 37°C, with a maximum rate between 14 and 20°C (Stapleton et al., 2005). Hence, the reduction of Fe(III) could proceed at cold temperatures encountered in the Arctic, possibly contributing to As solubilization upon soil flooding.

2.4.2. Arsenic biogeochemistry in an Arctic soil ecosystem

The cold climate and summer thaw in the Canadian High Arctic give rise to a distinct soil ecosystem in which to study the biogeochemistry of As. Given the lack of understanding of As biogeochemistry at cold temperatures, it is uncertain how reactions will proceed that affect As solubilization and speciation. During soil flooding that would normally induce reducing conditions in temperate soils, cold temperatures may inhibit microbial activity; alternatively, specially adapted microbes may be present. Further, chemical reactions may be slowed. The research presented herein aims to elucidate the biogeochemical processes that are affecting As speciation and solubility in the High Arctic soil ecosystem at Truelove Lowland, Devon Island, Nunavut.

3.0 ARSENIC ON DEVON ISLAND: A PRISTINE ECOSYSTEM

3.1 Introduction

Arsenic is a toxic trace element of contemporary concern due to its contamination of ground, surface and drinking waters throughout the world. Arsenic causes chronic health issues for many people including cancer and neurological disorders (Roy and Saha, 2002; Rodriguez et al., 2003). In the Canadian Sub-Arctic, the extraction of gold at sites such as the Royal Oak Giant Mine (Yellowknife, NWT), has led to surrounding surface sediment concentrations as high as 3821 mg kg^{-1} As (Mace, 1998). However, little is known about background As levels and cycling in the High Arctic.

The summer thaw in the High Arctic increases the complexity of As remediation when compared to temperate ecosystems. During the period from approximately late June to October when temperatures are sufficient to melt overlying snow, the ground surface becomes exposed to the sun's radiation and depressional areas become saturated with meltwater. At this time, there is a pulse of biogeochemical activity as well as a redistribution of components suspended in superpermafrost groundwater throughout the landscape (Quinton et al., 2004). Understanding the biogeochemical cycling of As in pristine areas is essential to successfully develop long-term sustainable management plans for disturbed and contaminated sites in the Arctic.

3.1.1 Atmospheric deposition of As

Contaminants such as mercury, cadmium and lead are deposited from the atmosphere in the Arctic (Poikolainen et al., 2004), but little consistent information is available on the deposition of As in the Canadian High Arctic. Natural emissions of As, mainly from volcanoes and forest fires contribute approximately $4.5 \cdot 10^7$ kg As yr^{-1} to the atmosphere, while anthropogenic input is approximately $2.8 \cdot 10^7$ kg As yr^{-1} (Chilvers, 1987). Shaw (1991) verified the presence of well-aged (10-100 d) metal-rich aerosols containing a mean concentration of 0.19 ng m^{-3} As (SD = 0.150) in Alaskan air masses. Therefore, it is plausible that some As be present in precipitation received by the Arctic.

3.1.2 The Truelove Lowland ecosystem

Whereas most of the islands in the Canadian Arctic Archipelago are classified as "Polar Deserts" receiving less than 10 cm of precipitation per year, Truelove Lowland on Devon Island is classified as a "Polar Oasis" (Bliss, 1977). The area is protected from harsh arctic winds by escarpments to the east and south, and the depressed landscape, developed as a result of isostatic rebound, is able to retain substantial surface water. As a result of enhanced moisture retention, the area supports greater biological diversity than most areas in the Canadian High Arctic (Bliss, 1977). These polar oases are an essential component of the High Arctic environment as they serve as habitat for a wide range of Arctic species.

In the early 1970s, the International Biological Project (IBP) set out to characterize various ecosystems around the world. Truelove Lowland was chosen to represent a

High Arctic ecosystem, resulting in a very comprehensive study comprising soils, geology, vegetation, hydrology, climate, and wildlife entitled "Truelove Lowland, Devon Island, Nunavut: A High Arctic Ecosystem" (Bliss, 1977) . Truelove Lowland encompasses approximately 43 km^2 in area and is found in the northeast portion of Devon Island (75° 33' N, 84° 40' W), Nunavut. The site is part of Canada's High Arctic and is underlain by continuous permafrost.

For the purpose of this research, the landscape on Truelove Lowland can be categorized into three main landscape positions: Raised Beach Crest (RBC), Lower Foreslope (LFS), and Wet Sedge Meadow (WSM). Raised beach crests are the result of the Arctic ocean having receded many years ago, leaving coarse sandy beaches in its wake (Walker and Peters, 1977). Today, in the areas of Truelove Lowland not covered by surface water, the topography gently undulates. Numerous catenas are composed of elevated RBCs sloping down to the LFS, then to the WSM landscape position.

3.1.3 Research hypothesis and objectives

The aim of the study conducted at Truelove Lowland was to gain information on the levels and biogeochemical cycling of As in soil and superpermafrost groundwater at a pristine site in the Canadian High Arctic. Previous work has not been undertaken on this topic. Similar studies in temperate regions indicate that Eh and pH are the dominant environmental factors controlling As solubility (Masscheleyn et al., 1991; Pfeifer et al., 2004). With the flooding of low-lying areas on Truelove Lowland during the summer thaw, it was hypothesized that a shift to reducing conditions would cause As solubilization via biological and chemical reducing processes, including reduction of

Fe(III) and arsenate. The provenance of As at Truelove Lowland was assumed to be of natural origin with the possibility of some atmospheric deposition.

The objectives of the study at Truelove Lowland were to: (i) Analyze snow and meltwater samples to determine whether As was introduced into the ecosystem from the atmosphere; (ii) Determine whether superpermafrost groundwater parameters including pH, Eh and temperature were correlated to As in groundwater; (iii) Assess the concentration and speciation of As in superpermafrost groundwater; and (iv) Determine which processes, chemical and biological, may be responsible for As solubility and speciation in low lying areas (WSM).

3.2 Materials and methods

3.2.1 Location of sample sites

Raised Beach Crest (RBC) - Lower Foreslope (LFS) - Wet Sedge Meadow (WSM) catenas were identified with similar slope and aspect in an attempt to minimize hydrologic and environmental factors that could affect As partitioning in the WSM. For example, catenas with greater slope may have superpermafrost groundwater flowing at a greater velocity and may be more prone to erosion. South-facing slopes may receive more direct radiation than north-facing slopes, and prevailing winds may increase the rate of evaporation at some sites. Samples were taken from the WSM at each of the six sites shown on Figure 3.1. The six sampling sites on Truelove Lowland were chosen to be used as replicates.

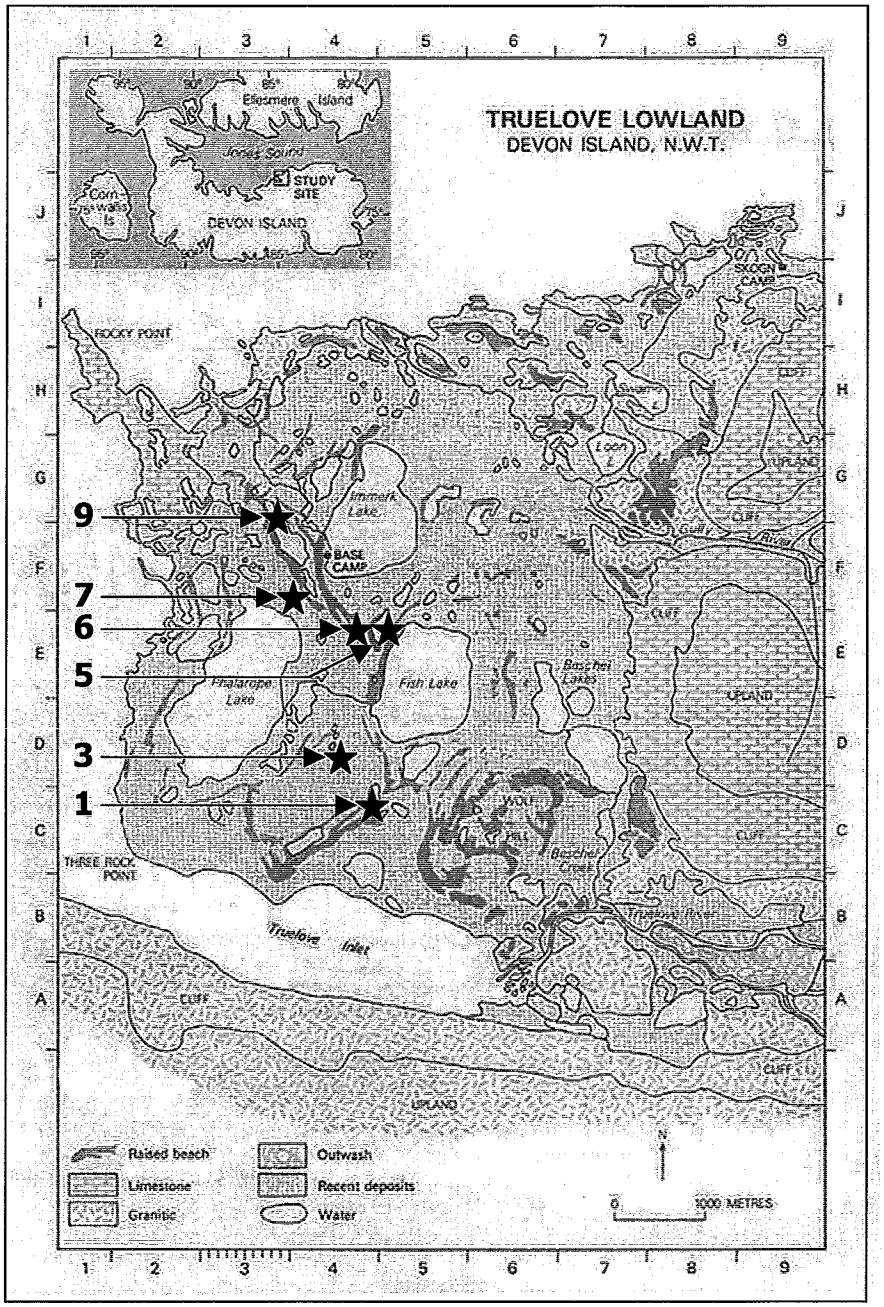

Figure 3.1 Numbers and stars represent sampling sites on the map of Truelove Lowland, Devon Island, NU. (adapted from Bliss (1977)).

3.2.2 Soils at Truelove Lowland, Devon Island, NU

All information on vegetation at Truelove Lowland was obtained from Muc and Bliss (1977) and soils information from Walker and Peters (1977) in "Truelove Lowland, Devon Island, Nunavut: A High Arctic Ecosystem" (Bliss, 1977). Soil classification is based on the Canadian System of Soil Classification, Third Edition (National Research Council, 1998). Soils are classified as Static and Turbic Cryosols. The RBC landscape position often displays a layer of gravel and rocks on the surface known as "desert pavement". The RBCs are typically classified as Brunisolic Turbic Cryosols. Approximately the first 10 cm of the RBC is Ahk underlain by a layer of variable depth of coarse sand (Ck) until the permafrost table (Cz). Vegetation of the RBC includes scattered cushion plant and lichen communities.

The LFS is characterized by microhummocks composed of a layer of organic material from the breakdown of cushion plants and moss (Of), followed by an Ahk, coarse sand (Ck), and permafrost (Cz). The WSM retains water that flows downslope from the RBC and LFS and supports vegetation adapted to submerged soils, mainly sedges, mosses and grasses including cottongrass. An organic layer (Of) is underlain by an Ahk, Bmk, Ck, and Cz. The Bmk and Ck in the WSM are slightly enriched in silt washed from raised landscape positions, and as a result the WSM is often hummocky. In all landscape positions parent material below overlying organic soil is classified as strongly to very strongly calcareous and contains approximately 65% sand, 25% silt, and 10% clay (Walker and Peters, 1977).

Sites for sampling snow, meltwater, groundwater, and soil were identified using the soils map prepared by Walker and Peters (1977). Sites were specifically chosen in

WSM areas in map units 31 and 61. Map unit 31 is characterized by Gleysolic Static Cryosols and average maximum thaw depth varies from 30 to 50 cm. The typical dull or bluish colours indicative of gleying and commonly associated with reducing conditions are seldom found in the mineral portions of these soils. Map unit 61 generally contains Gleysolic Turbic Cryosols. The soils in both map units 31 and 61 can also be classified as Fibric Organo Cryosols depending on the thickness of the overlying organic horizon (>40 cm). Table 3.1 shows chemical data for soils from map units 31 and 61. These two map units were selected for their relatively high Fe and SO_4 contents as compared to other soil types. Another desirable characteristic of map units 31 and 61 is the relatively shallow mineral horizon (i.e., within approximately 20 cm of the surface) in order to examine the biogeochemistry of As in both organic and mineral soil.

3.2.4 Water and soil sampling

3.2.4.1 Arsenic fractionation and speciation of water samples

To determine As partitioning between particulate and dissolved fractions, samples were separated into two aliquots. The first was unaltered and stored in a 15mL polystyrene Falcon® tube and was designated total As (T-As). The second aliquot was filtered through a 0.45μm Whatman® capsule filter (Clifton, New Jersey, U.S.A.) and stored in a 15mL Falcon® tube. The filtered sample was designated dissolved As (D-As). The speciation of As using a strong anion exchange resin was based on the method described by Le et al. (2000). The principle behind the strong anion-exchange resin is that when a filtered sample is adjusted to pH 4.5, the negatively charged arsenate

Table 3.1 Chemical data for selected Gleysolic Static and Turbic Cryosols within map units 31 and 61 (adapted from Bliss, 1977).

Horizon	Depth (cm)	pH	Org. C (%)	Total N (%)	$CaCO_3$ Equivalent (%)	Available nutrients ($mg\ kg^{-1}$)				Oxalate extractable	
						NO_3-N	P	K	SO_4-S	Fe (%)	Al (%)
Map unit 31 – Gleysolic Static Cryosol											
Of	23-0	6.2	26.1	2.24	n/a	0	5	105	50+	0.54	0.13
Ckg	0-5	7.6	0	0.04	35.5	0	1	18	21.2	0.62	0.02
Map unit 61 – Gleysolic Turbic Cryosol											
Ofy	18-0	7.2	25.9	2.21	1.3	n/a	n/a	n/a	n/a	0.40	0.02
Ckg	0-40	7.9	n/a	n/a	23.3	n/a	n/a	n/a	n/a	0.43	0.01
Ckgy	40-51	8.0	0.5	0.01	25.3	n/a	n/a	n/a	n/a	0.19	0.01

($H_2AsO_4^-$) will be held on the resin, while neutral arsenite ($As(OH)_3^0$) will pass through. The solution having passed through the resin was considered to contain only arsenite, and the resin was later eluted with 1.0N Omni*Trace*® HCl (EMD Chemicals Inc., Gibbstown, NJ) to remove adsorbed arsenate.

Silica-based anion-exchange cartridges (500 mg sorbent of 40-µm particle size and 60-Å pore size) were obtained from Supelco (Missisauga, ON, Canada). Cartridges were preconditioned with 50% methanol and deionized water before use. A 15 mL water sample was first filtered through a 0.45 µm Whatman capsule filter into a clean vessel. The sample was acidified to pH 4.5 with 1N Omni*Trace*® HCl (36-37%). The sample was then drawn into a Norm-Ject® 50 mL polypropylene syringe with a polyethylene plunger (Tuttlingen, Germany) and pushed through the anion-exchange resin cartridge. The water that passed through the resin was stored in a 15 mL Falcon® polystyrene tube. The resin cartridge was stored for elution with 1N OmniTrace® HCl upon return to the laboratory.

3.2.4.2 Snow sampling

Samples of snow were collected to determine if As was being deposited from the atmosphere. Sampling sites were chosen in accordance with sites for future meltwater and groundwater sampling (Figure 3.1). A 500 mL plastic graduated cylinder was used to remove 500 mL of snow that had accumulated in the WSM landscape position. Snow was placed in a Nalgene® bottle and allowed to melt at room temperature, then water samples were partitioned according to the above protocol (3.2.4.1).

3.2.4.3 Standing meltwater sampling

Ponded water from melted snow (meltwater) was collected to assess whether the melting process and pooling of water affected As concentration or partitioning. As snow melts and pools on the ground surface, there is potential for certain processes to cause As concentrations to decrease or increase. For example, photo-oxidation of arsenite in Fe-containing waters followed by precipitation of arsenate-Fe complexes can remove 45 to 78% of T-As from solution (Hug et al., 2001). Also, As in meltwater can sorb to binding sites on vegetation and minerals at the ground surface (Groudeva et al., 2004). Alternatively, As in meltwater could become concentrated as water evaporated, or it could desorb from vegetation and mineral surface sites if conditions became reducing (Sadiq, 1995).

Samples of meltwater at the chosen field sites were drawn through Teflon® tubing into a 50 mL Norm-Ject® syringe. As above (3.2.4.1), samples were partitioned into T-As, D-As, arsenate, and arsenite fractions. Three individual pools of meltwater at each site were sampled if there were enough pools present.

3.2.4.4 Groundwater sampling

Groundwater wells were installed once the soil had thawed sufficiently to be able to insert them to a depth that would hold them upright (~30cm) and were dug down further as the soil profile thawed. Wells were made of 5 cm diameter polyvinyl chloride (PVC) pipe with slits cut into the sides for entry of groundwater. The bottoms of the wells were capped to avoid water contact with underlying soil.

Three wells were installed at each of six different sites on Truelove Lowland in the WSM landscape position. The WSM was the only landscape position that consistently held sufficient groundwater for sampling. Wells were isolated with bentonite chips to avoid entrance of surface water. Wells were monitored approximately every 2 d. Water levels were measured and recorded with a plastic tape measure. Water temperature, Eh and pH were measured with an Orion 635 Advanced pHuture™MMS™ Meter (Reported accuracy of <±0.2°C (0 to 45°C); <0.1% of measured value, +3mV +1 digit; and 0.02±1 digit; for temperature, Eh, and pH, respectively). The Orion 635 Advanced pHuture™MMS™ measures Eh with a platinum electrode and values are automatically converted to standard hydrogen potential (SHE).

Three well volumes were evacuated from each well after parameter monitoring and prior to sampling to ensure fresh water samples. Water samples were fractionated into T-As, D-As, arsenate, and arsenite subsamples (3.2.4.1). Water samples were taken for analysis of Fe(III), Fe(II) and dissolved sulfide concentration and were filtered through a Whatman® 0.45µm capsule filter (3.2.6).

3.2.4.5 Soil sampling

Soil samples were taken shortly before leaving the field site and were kept at air temperature (~10°C) until they could be frozen. Samples were taken separately from overlying organic and underlying mineral soil. Four representative sites (5, 6, 7 and 9) (Figure 3.1) were sampled at the WSM landscape position. Soils from each field site and horizon were stored separately.

3.2.5 Arsenic analysis

Samples were analyzed for concentration of all As fractions using the Millenium Atomic Fluorescence Spectrometer (AFS) (Millenium Excalibur, PS Analytical Ltd., Kent, England). Hydrochloric acid was Omni*Trace*® (EMD™ Chemicals Inc., Darmstadt, Germany) and all water used for sample dilution, reagent blank, and reagent blank was Milli-Q® ultrapure water obtained with a Milli-R04 system (Millipore, Bedford, MA, USA).

The Millenium AFS employs a continuous flow hydride generation system for As detection (Corns et al., 1993). Three solutions must be made up for the analysis of As: (1) sodium tetrahydroborate (1.5% m v^{-1} $NaBH_4$) (J.T. Baker, Mallinckrodt Baker Inc., Phillipsburg, NJ, USA) in 0.1 mol L^{-1} NaOH (EM Science, Affiliate of Merck KgaA, Darmstadt, Germany), (2) 1 L of reagent blank composed of 300 mL Omni*Trace*® HCl (12N, 37%), 680 mL Milli-Q® ultrapure water, and 20 mL solution of 50% m v^{-1} potassium iodide (KI)(BDH Inc., Toronto, Canada) and 10% m v^{-1} ascorbic acid ($C_6H_8O_6$)(Alfa Aesar®, Ward Hill, MA, USA), and (3) prepared samples.

Samples were prepared for analysis of T-As by hand shaking in their original 15 mL Falcon® tube to re-suspend any precipitate, then left to sit for one h. Supernatant (9 ml) was pipetted into a 50 mL polystyrene Falcon® tube. To each 9 mL sample was added 6 mL of pure OmniTrace® HCl (12N, 37%), 4.5 mL Milli-Q® ultrapure water, and 0.4 mL 3.01 M potassium iodide (KI) and 0.57 M ascorbic acid ($C_6H_8O_6$) solution. Potassium iodide served to reduce any As in solution to arsenite, which forms the hydride necessary for spectrometric analysis. Samples for analysis of D-As and arsenite had been filtered through a 0.45μm Whatman® capsule filter, therefore it was not

necessary to re-suspend any precipitate. The amount of OmniTrace® HCl added to arsenate samples was normalized to account for elution from anion exchange resins with 1.0N OmniTrace® HCl (12N, 37%).

3.2.6 Quality assurance/quality control

Fresh $NaBH_4$ and reagent blank solutions were prepared daily. Standard solutions were prepared by appropriate dilution of stock 1000 mg L^{-1} As standard (EMD Chemicals Inc., Darmstadt, Germany). All equipment was adequately cleaned between samples and all glassware was soaked in 10% Omnitrace® nitric acid (initially 69-70% (15.9N), EMD Chemicals Inc., Darmstadt, Germany) prior to use and then rinsed five times with distilled water. In the field, samples from an off-site location with varying concentrations of As, including blanks, were treated in the same manner as field samples. Duplicate samples were taken at random in the field approximately every ten samples, and laboratory samples were randomly analyzed in duplicate. A complete QA/QC assessment of sampling containers, Norm-Ject® syringes, Whatman® capsule filters, and reagents was undertaken to determine whether As was being contributed or removed, or partitioning altered, during the sampling process (Appendix A).

The method detection limit (MDL) for the Millenium AFS was determined using United States Environmental Protection Agency (USEPA) Method 40 CFR Part 136: "Guidelines for Establishing Test Procedures for the Analysis of Pollutants". The USEPA defines the *method detection limit* as "the minimum concentration that can be determined with 99% confidence that the true concentration is greater than zero." (USEPA, 1998). The method detection limit for the AFS is calculated as follows:

$$MDL = 2.602 \cdot sd \quad (3.1)$$

Where 2.602 is the Student's t-value ($t_{15, 0.01}$) at the 0.01 level of probability and df = 15, and sd is the standard deviation ($\mu g\ L^{-1}$) of the measured As concentrations prepared in MilliΩ water. For samples analyzed using the Millenium Excalibur Atomic Fluorescence System™, the method detection limit was 0.011 μg As L^{-1} with n = 16 samples at 0.04 μg L^{-1}, mean recovery of 101.7% and the standard deviation was 0.0043 μg L^{-1} (Table 1, Appendix A). Ongoing precision expressed as relative percent difference between duplicates (RPD) for analysis of snow and meltwater was 42%, and the RPD for supermafrost groundwater samples was 23%. Complete QA/QC tables and procedures are available in Appendix A.

3.2.6 Analysis of other groundwater components

3.2.6.1 Spectrophotometric analysis of Fe(III) and Fe(II) in natural waters

Following the procedure of Takagai and Igarashi (2003), Fe(II) and Fe(III) were complexed with bathophenantholinedisulfonic acid disodium salt (98%) (BAP) (Lancaster Synthesis, Inc., Pelham, NH), and deferoxamine mesylate B (DFB) (Calbiochem, EMD Biosciences, La Jolla, CA), respectively. The siderophore solution was composed of $3 \cdot \times 10^{-3}$ μM BAP, 1.5×10^{-3} μM DFB, in 0.038 M KH_2PO_4 (Alfa Aesar, Ward Hill, MA) dissolved in Milli-Q® ultra-pure water. One milliliter of the siderophore solution was pipetted into each borosilicate glass vial (wide opening, screw-cap, 2 mL volume) (Agilent Technologies, Palo Alto, CA). Vials were capped with polypropylene screw caps with Teflon resin septa (Agilent Technologies, Palo Alto, CA)

inside an anaerobic chamber containing N_2. The N_2 headspace minimized sample contact with O_2 before complexation with the siderophores. Field samples were filtered through a 0.45μm Whatman® capsule filter then drawn into a 5 mL syringe fitted with a sterile 27G1/2 needle (Becton Dickinson & Co., Franklin Lakes, NJ). The needle was then used to pierce the Teflon septum and the sample was evacuated into the glass vial containing the siderophore solution.

Standards were prepared by serial dilution of solutions made with ferric chloride, 6-hydrate (Mallinckrodt Baker, Inc., Phillipsburg, NJ) for Fe(III), and ferrous sulfate heptahydrate (Merck, KgaA, Darmstadt, Germany) for Fe(II). Solutions of Fe(II) and Fe(III) were prepared directly in siderophore solution to avoid oxidation of Fe(II). Serial dilutions were prepared with Milli-Q® ultra-pure water. The Fe(II)-BAP solution has a red colour, and the Fe(III)-DFB solution is orange at high concentration and yellow at lower concentration. Standards of Fe(II), Fe(III) and mixed Fe(II) + Fe(III) were used to determine the concentrations of Fe(II) and Fe(III) in a sample.

Two hundred microlitres (200 μL) of each standard and sample was transferred to a sterile 96 well Microtest™ U-bottom polypropylene tissue culture plates (Falcon® Becton Dickinson, Franklin Lakes, NJ). After warming up the Emax precision microplate reader (Biolog, Hayward, CA) for 30 min, samples were analyzed spectophotometrically at 405 nm and 450 nm, and concentration calculations were based on different absorption wavelengths of the two complexes (Figure 3.2).

The principle behind the calculations for determination of Fe(II) and Fe(III) is that any difference in absorbance at 405 and 450 nm should be attributable to Fe(II)-BAP, and having prepared mixed standards, the absorbance contribution and hence the

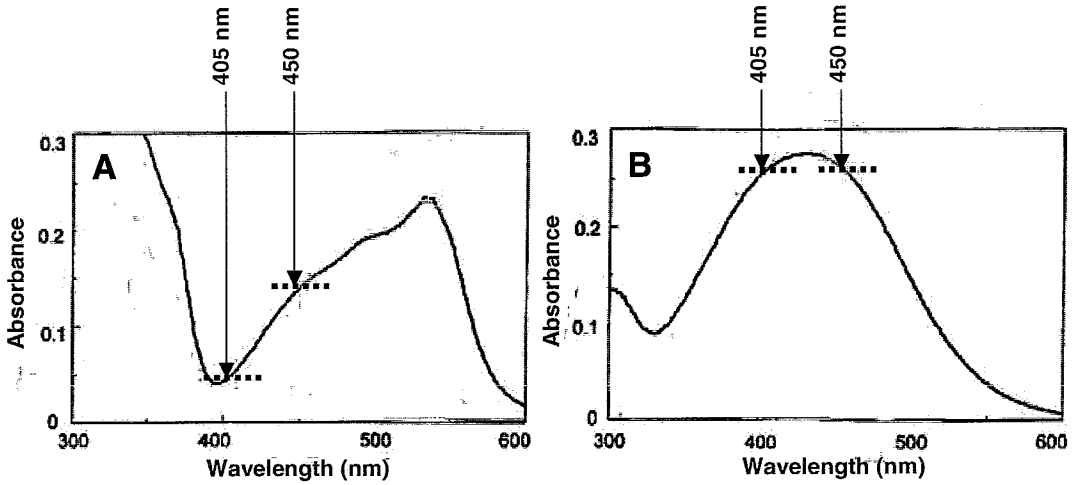

Figure 3.2 Absorbance spectra of Fe-siderophore complexes (A) Fe(II)-BAP ($[Fe(II)]_T=[Fe(III)]_T=1.0x10^{-5}$ mol L^{-1}, $[bathophen]_T = 1.0x10^{-4}$ mol L^{-1}) and (B) Fe(III)-DFB ($[Fe(II)]_T=[Fe(III)]_T=1.0x10^{-4}$ mol L^{-1}, $[DFB]_T = 2.0x10^{-4}$ mol L^{-1}) siderophore complexes at 405 and 450 nm (adapted from Takagai and Igarashi (2003)).

concentration of Fe(III) and Fe(II) can be differentiated. A complete description of the calculation method is provided in Appendix B.

The relationship between Fe concentration and absorptivity can be explained in light of Beer's law:

$$A = \varepsilon bc \tag{3.2}$$

where A is absorbance at the selected wavelength

ε is the molar absorptivity (L mol^{-1} cm^{-1})

b is the path length (cm)

c is the concentration of the compound in solution (mol L^{-1}).

To calculate the concentration of Fe(II) and Fe(III) in solution, the following calculations are based on the assumption that absorbance of Fe(III)-DFB is the same at 405 and 450 nm:

$$A_{405} = \varepsilon_{\lambda} b C_{Fe(II)405} + \varepsilon_{\lambda} b C_{Fe(III)405} \tag{3.3}$$

$$C_{Fe(III)405} = \frac{A_{405}}{\varepsilon_{\lambda} b} - C_{Fe(II)405} \tag{3.4}$$

$$A_{450} = \varepsilon_{\lambda} b C_{Fe(II)450} + \varepsilon_{\lambda} b C_{Fe(III)450} \tag{3.5}$$

$$C_{Fe(II)450} = \frac{A_{450}}{\varepsilon_{\lambda} b} - C_{Fe(III)450} \tag{3.6}$$

$$C_{Fe(II)450} = \frac{A_{450}}{\varepsilon_{\lambda} b} - \left(\frac{A_{405}}{\varepsilon_{\lambda} b} - C_{Fe(II)405} \right) \tag{3.7}$$

3.2.6.2 Spectrophotometric determination of hydrogen sulfide in natural waters

Following the procedure of Cline (1969), HS^- is complexed with "mixed diamine reagent" for spectrophotometric analysis. The mixed diamine reagent is prepared according to Table 3.2. Based on the estimated concentration of sulfide (μM), the corresponding amounts of N,N-dimethyl-ρ-phenylenediamine sulfate (diamine)

Table 3.2 Suggested reagent concentrations to be used in the determination of sulfide-sulfur in the stated concentration ranges (adapted from (Cline, 1969)).

Sulfide concentration (μM)	**Diamine concentration ($g \cdot 500\ mL^{-1}$)**	**$FeCl_3 \cdot 6H_2O$ ($g \cdot 500\ mL^{-1}$)**
1-3	0.5	0.75
3-40	2.0	3.0
40-250	8.0	12.0
250-1000	20.0	30.0

(Aldrich, Milwaukee, WI) and $FeCl_3 \cdot 6H_2O$ (Mallinckrodt Baker Inc., Phillipsburg, NJ) are dissolved in cool Omni*Trace*® HCl diluted to 50% (v/v). The reagent concentrations for the lower two ranges are in large excess to enhance reagent stability. Prior to sampling, one hundred microlitres of diamine reagent was pipetted into each 2-mL borosilicate vial (Agilent Technologies, Palo Alto, CA) before adding 1.5 mL of filtered sample or standard sulfide solution.

All standard preparation was carried out in an anaerobic chamber containing 100% N_2. Oxygen-free Milli-Q® ultrapure water was prepared by autoclaving followed by sparging with N_2 in an N_2-filled anaerobic chamber. Crystals of $Na_2S \cdot 9H_2O$ (BDH, Toronto, ON) were first washed with cooled oxygen-free water to remove oxidation products, then wiped dry with a cellulose tissue. A concentrated sulfide solution was prepared by dissolving the $Na_2S \cdot 9H_2O$ crystal in oxygen-free water. Appropriate volumes of the concentrated standard were pipetted into measured volumes of oxygen-free water in Solvent-Saver® scintillation borosilicate glass vials (VWR, West Chester, PA).

One and a half milliliters (1.5 mL) of standard was pipetted into a 2-mL glass vial containing 100 μL diamine reagent. After 30 min of reaction time, 200 μL of the reacted sample and diamine reagent was pipetted into a sterile 96 well Microtest™ U-bottom polypropylene tissue culture plate. After warming up the Emax precision microplate reader for 30 min, standards and samples were analyzed spectophotometrically at 650 nm. The concentration of sulfide in the sample was calculated using Beer's law outlined in equation (3.2).

3.2.7 Extraction of As, Fe and Mn in Soils from Truelove Lowland

3.2.7.1 Extraction of total Fe and total Mn in soil

The dithionite-citrate extraction enables quantification of Fe and Mn from finely divided hematite and goethite, amorphous inorganic Fe and Mn, organo-Fe and -Mn, and removes a portion of Fe and Mn from silicate minerals. This can be considered 'Total Fe' and 'Total Mn'. For analysis of Total Fe and Mn in soils from Truelove Lowland, organic and mineral soils from all sites (5, 6, 7 and 9) were dried in an oven at 105°C for 10 h. Two hundred and fifty (250) milligrams of dried soil was ground to pass through a 35 mesh sieve was placed into a 50 mL polypropylene centrifuge tube (BD Falcon®). Extractions were done in triplicate. A 0.68 M solution of sodium citrate ($Na_3C_6H_5O_7 \cdot 2H_2O$) was prepared by diluting 200 g of sodium citrate in 1 L of distilled water. To the soil in each centrifuge tube was added 12.5 mL of 0.68 M sodium citrate solution. To this mixture was added 0.2 g of sodium hydrosulfite ($Na_2S_2O_4$). Centrifuge tubes were capped tightly and placed in an end-over-end shaker. After 14 h the centrifuge tubes were removed from the shaker and centrifuged at 2000 rpm for 15 min. Centrifugate was pipetted into 15 mL centrifuge tubes for analysis using an atomic absorption spectrometer (Model 1200, Varian Techron) with an air-acetylene flame.

To give a convenient concentration for analysis and to reduce interference, samples for analysis of Fe were diluted with distilled water to a ratio of 1:16, and samples for analysis of Mn were diluted at a ratio of 1:2. Standards were prepared with 100 mg L^{-1} Fe standard solution (Hach chemicals, CA) and 1 mg mL^{-1} Mn standard (VWR International). The matrix of the standard solutions contained the same concentration of the extracting solution as the samples with equivalent dilution with distilled water.

3.2.7.2 Extraction poorly crystalline Fe oxides in Soil

Acid ammonium oxalate extractable Fe consists of poorly crystalline Fe oxides and organo-Fe complexes. This fraction of Fe is considered 'Poorly Crystalline Fe Oxides'. 0.2 M ammonium oxalate ($(NH_4)_2C_2O_4 \cdot H_2O$) solution was prepared by dissolving 14.15 g into 500 mL of distilled water. The 0.2 M oxalic acid ($H_2C_2O_4 \cdot 2H_2O$) solution was prepared separately by dissolving 12.6 g into 500 mL of distilled water. The ammonium oxalate and oxalic acid solutions were then combined in a ratio of 1:0.764.

Organic and mineral soils from four sites on Truelove Lowland (5, 6, 7 and 9) were dried and ground to pass a 35 mesh sieve. Soil (0.250 g) was placed into a 50 mL polypropylene centrifuge tube. There were three replicates. To each centrifuge tube was added 10 mL of the ammonium oxalate/oxalic acid mixture. Tubes were capped tightly and placed in an end-over-end shaker for five h in the dark. Tubes were then centrifuged for 20 min at 2000 rpm. The centrifugate was pipetted into clean 15 mL centrifuge tubes and diluted to a convenient concentration for analysis with 2000 mg L^{-1} NaCl. Iron standards were prepared in an equivalent matrix to that of the samples. Samples were run on an atomic absorption spectrometer (Model 1200, Varian Techron) with an air-acetylene flame.

3.2.7.3 Digest of total As in soil

Organic and mineral soils from all sites on Truelove Lowland (5, 6, 7, and 9) were dried at 105°C for 12 h. After cooling in a desiccator, soils were ground with a mortar and pestle and sieved through a 2 mm stainless steel sieve. Soil (1.000 ± 0.004 g) was

transferred into a clean 100 mL volumetric flask. There were three replicates of each soil. One milliliter of MilliΩ water was added to each volumetric flask to wet the soil followed by 12.0 mL of 36% m m^{-1} (12N) Omnitrace® hydrochloric acid and 4.0 mL of 69-70% (15.9N) Omnitrace® nitric acid. Excessive bubbling was controlled by adding several drops of n-dodecane. Flasks were placed on a cold heating mantle and heated gradually to a liquid temperature of 105°C with the digest gently refluxing. After heating at 105°C for 20 min, 5.0 mL of MilliΩ water was added to the digest, and heating continued for 10 min. Flasks were then removed from the heating mantle to cool. Digests were then diluted to 100 mL with MilliΩ water. After settling for 24 h, a portion of the supernatant was centrifuged at 3500 rpm for 20 min.

Samples were prepared as in section 3.2.4.1 for determination of T-As using the Millenium Excalibur AFS. Samples were diluted when necessary to achieve a convenient concentration for analysis.

3.2.7 Statistical analysis

Parametric data was analyzed using Analysis of Variance (ANOVA) with the General Linear Model (GLM). Data was evaluated for normality and heterogeneity for all ANOVA factors. The GLM was used to determine which factors affected As speciation and solubility, as well as interactions between factors. Non-parametric data was analyzed using Mood's Median test when only one factor was to be tested, and the Kruskal-Wallis test was used when several factors, such as different dates, were compared with one response variable, such as As concentration. A multiple comparison extension was performed to determine which values were significantly different from

one another at the 0.20 significance level. The multiple comparison extension uses the following formula:

$$|\overline{R_i} - \overline{R_j}| \leq \sqrt{\frac{N(N+1)}{12}\left(\frac{1}{n_i} + \frac{1}{n_j}\right)} \tag{3.11}$$

where $\overline{R_j}$ = mean rank of the jth group ($\Sigma_{Rj/nj}$)

z = critical value of z at 0.20 level of significance with k groups

N = total number of observations

n_j = number of observations in each group

Correlations between As concentrations and speciation with groundwater parameters and components were analyzed using Spearman's Rank Correlation for non-parametric data. All analysis was performed using MINITAB 14 Statistical Analysis software (Minitab Inc., State College, PA, U.S.A.).

Box and whisker plots are used to display non-parametric data. The illustration presented as Figure 3.3, adapted from Keith and Cooper (1974), is useful for interpreting a box and whisker plot.

3.3 Results

3.3.1 The summer thaw and sampling duration

For the purposes of this research, the summer thaw extends from Julian day 166 to 186 (June 12 to July 5, 2004). By July 5 the active layer at most sites was between 30 to 50 cm, which is considered the maximum thaw depth by Walker and Peters (1977)

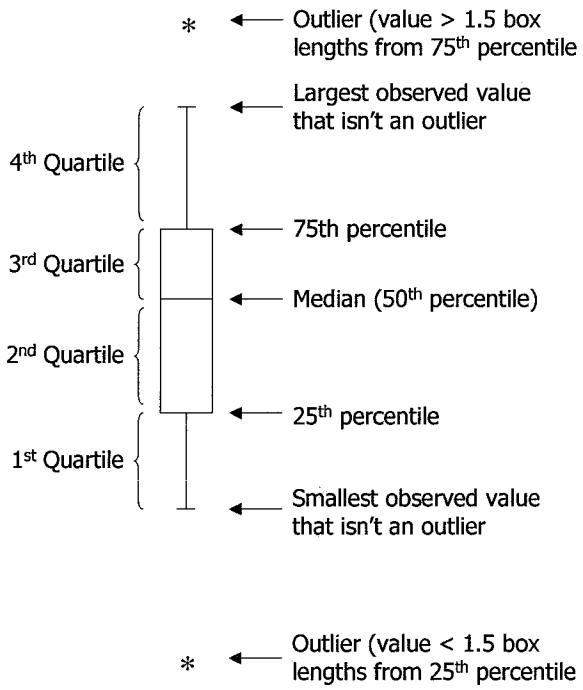

Figure 3.3 Box and whisker plot interpretive diagram (adapted from Keith and Cooper, 1974).

who classified the soils on Devon Island. Samples of snow, meltwater and groundwater weretaken at varying intervals from June 12 to July 5, 2004, and this was considered to be the sampling duration. All data for snow, meltwater and groundwater sampling are available in Appendix C.

3.3.2 Arsenic in soils from Truelove Lowland: Soil digestion

Strong correlation between total As and Fe suggests that As is bound in Fe-As complexes in soil. Table 3.3 shows the ranges and means of total As, Fe, Mn and poorly crystalling Fe oxides in soil extracts. Approximately 69 and 79% of Fe is in the form of poorly crystalline Fe oxides in mineral and organic soils, respectively. In organic soil, total As is strongly correlated with total Fe ($\rho = 0.815$, $P \leq 0.01$) and poorly crystalline Fe oxides ($\rho = 0.816$, $P \leq 0.01$) but is not correlated with total Mn ($P \geq 0.10$). In mineral soil, total As is also strongly correlated with total Fe ($\rho = 0.735$) ($P \leq 0.01$) and poorly crystalline Fe oxides ($\rho = 0.632$, $P \leq 0.05$), and is not correlated with total Mn ($P \geq 0.10$). Levels of poorly crystalline Fe oxides ($P \leq 0.10$) and total Mn ($P \leq 0.05$) are significantly higher in organic than mineral soil, but neither levels of total As nor total Fe are significantly different in organic and mineral soil ($P \geq 0.10$).

3.3.2 Arsenic in superpermafrost groundwater in relation to environmental conditions

In superpermafrost groundwater at Truelove Lowland, the concentrations of both T-As and D-As increase significantly over the summer thaw ($P \leq 0.01$) (Figure 3.4). The combined median T-As and D-As concentration for Julian days 184 and 186

Table 3.3 Range and average values of total As (HCl/HNO_3 digestion), total Fe (dithionate-citrate (DC)), poorly crystalline Fe oxides (ammonium-oxalate (AO)), and total Mn in soil extracts.

Soil Type	**Min.-Max./** Mean	**Total As (mg kg^{-1})**	**Total Fe (DC extraction) (g kg^{-1})**	**Poorly crystalline Fe oxides (AO extraction) (g kg^{-1})**	**Total Mn (DC extraction) (g kg^{-1})**
Mineral	Min.-Max.	0.05 – 1.49	0.34 – 1.28	0.33 – 0.76	0.003 – 0.05
Mineral	Mean	0.50 (SE = 0.16)	0.84 (SE = 0.11)	0.58 (SE = 0.05)	0.016 (SE = 0.005)
Organic	Min.-Max.	0.21 – 2.21	0.63 – 1.90	0.53– 1.45	0.01 – 0.07
Organic	Mean	0.34 (SE = 0.20)	1.02 (SE = 0.14)	0.81 (SE = 0.11)	0.03 (SE = 0.007)

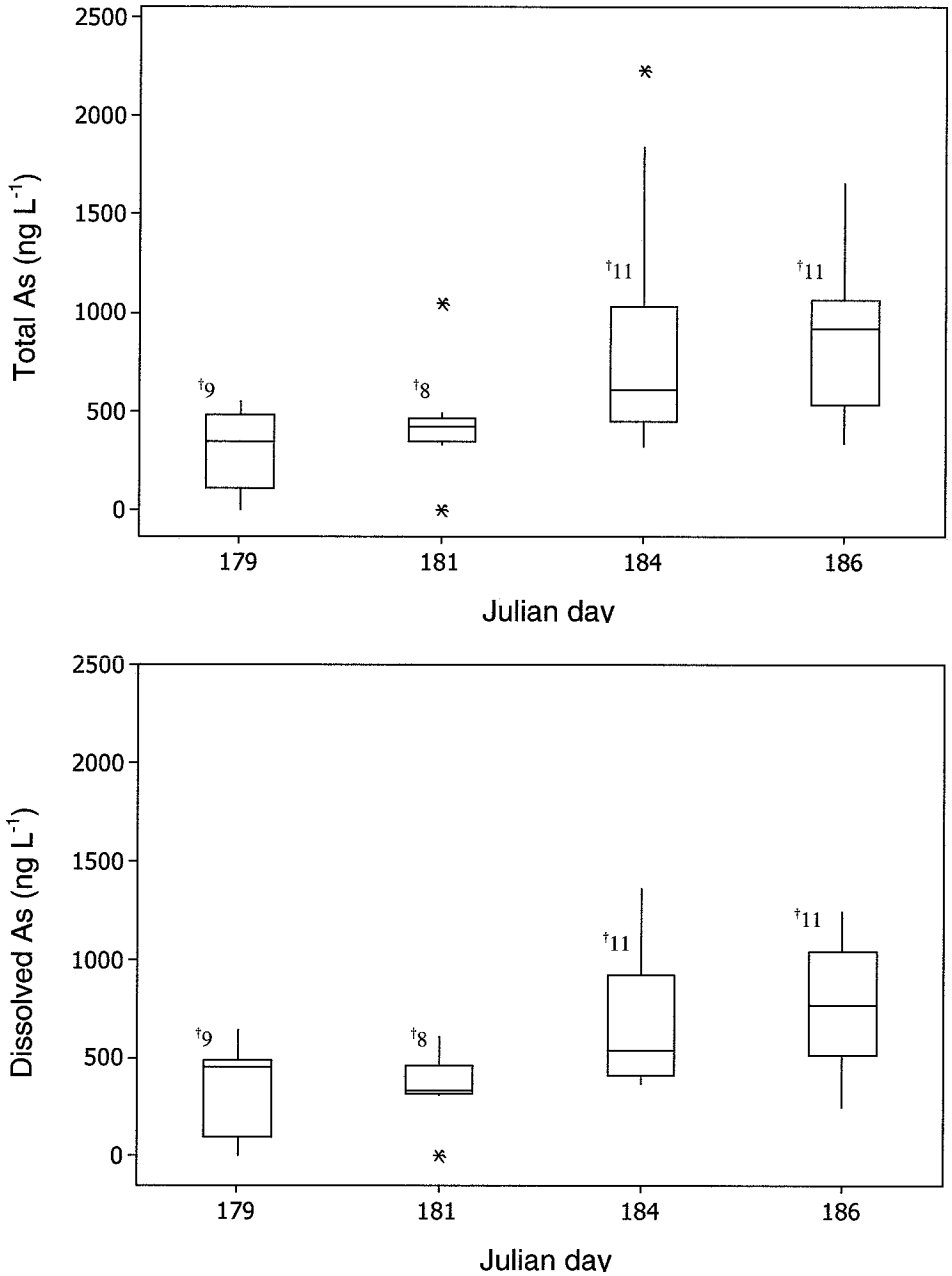

Figure 3.4 Box and whisker plots representing (A) total As (T-As) and (B) dissolved As (D-As) concentration in superpermafrost groundwater at Truelove Lowland. Data are pooled from all field sites for each sampling date. D-As samples were passed through a 0.45 μm Whatman® capsule filter.

†number of samples

†

approximately doubled that of Julian days 179 and 181 (765 vs. 382 ng L^{-1} and 655 vs. 390 ng L^{-1}, respectively). Concentrations of T-As and D-As did not differ significantly ($P \geq 0.20$), and particulate As (D-As subtracted from T-As) averaged only 3.1%.

From Julian day 179 to 186, arsenate decreased while arsenite increased (Figure 3.5). The average ratio of arsenite:arsenate increased over the sampling duration, suggesting that arsenate was being converted to arsenite (Figure 3.6). A shift to reducing conditions would cause arsenite to increase and could explain the rise in T-As concentration over time. If this were the case, we would also expect to see a decrease in Eh, an increase in Fe(II) and a decrease in Fe(III), and, if Eh were low enough (i.e, below -100 mV), an increase in sulfide might be observed.

Field results do not show a decrease in Eh measured with the Orion Pentrode ($P \geq 0.20$). Average Eh in groundwater was 388.9 mV (SE = 8.76). Weak Spearman rank correlations do exist between Eh and D-As (ρ_s = -0.205, $P \leq 0.20$) and arsenite (ρ_s = -0.259, $P \leq 0.10$) but are not strong enough to suggest causation. No correlations ($P \geq 0.20$) exist between T-As, D-As, arsenite or arsenate and Fe(III), Fe(II), or sulfide. Eh calculated from Fe(III) and Fe(II) averaged 172.7 (SE = 0.81), suggesting that conditions are aerobic. Eh calculations are provided in Appendix C.

Median concentrations of Fe(III), Fe(II) and sulfide over the entire sampling duration were 185 μM, 253 μM and 4.8 μM, respectively. While there are no significant correlations of these groundwater components with As fractions, a rise in Fe(III) concentration does occur over time ($P \leq 0.20$). No significant trends exist over time for Fe(II) or sulfide ($P \geq 0.20$).

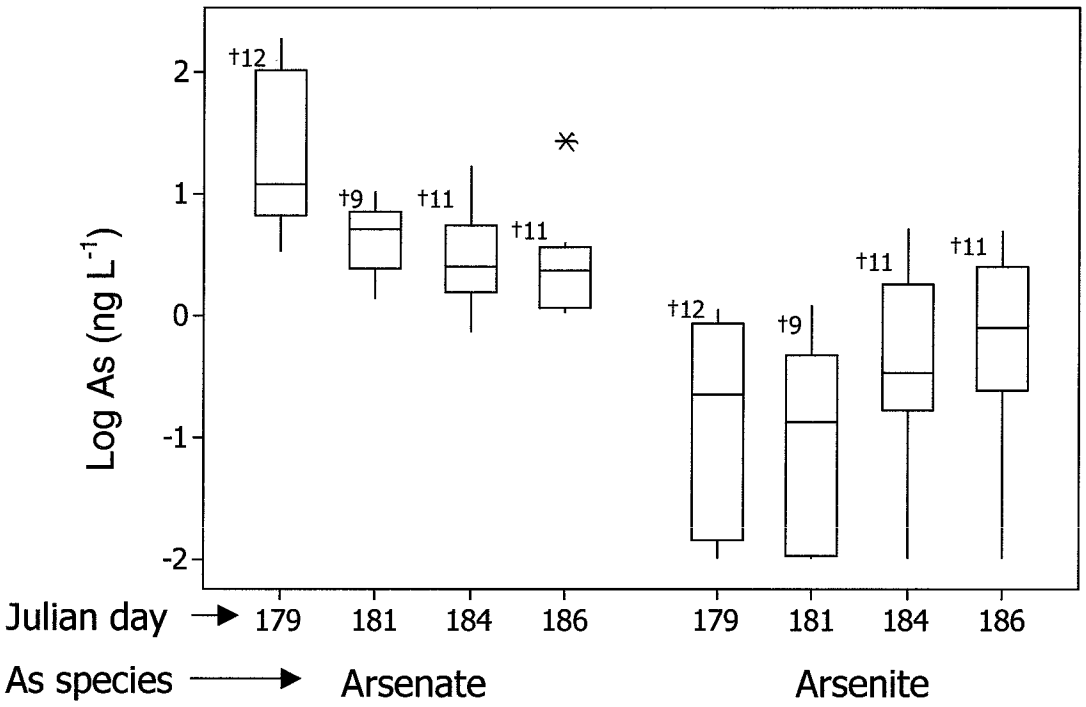

Figure 3.5 Box and whisker plots representing arsenate and arsenite concentration in superpermafrost groundwater at Truelove Lowland. Data are pooled from samples from all field sites for each sampling date. Samples for analysis of arsenate and arsenite were passed through a 0.45 μm Whatman® capsule filter.

†number of samples

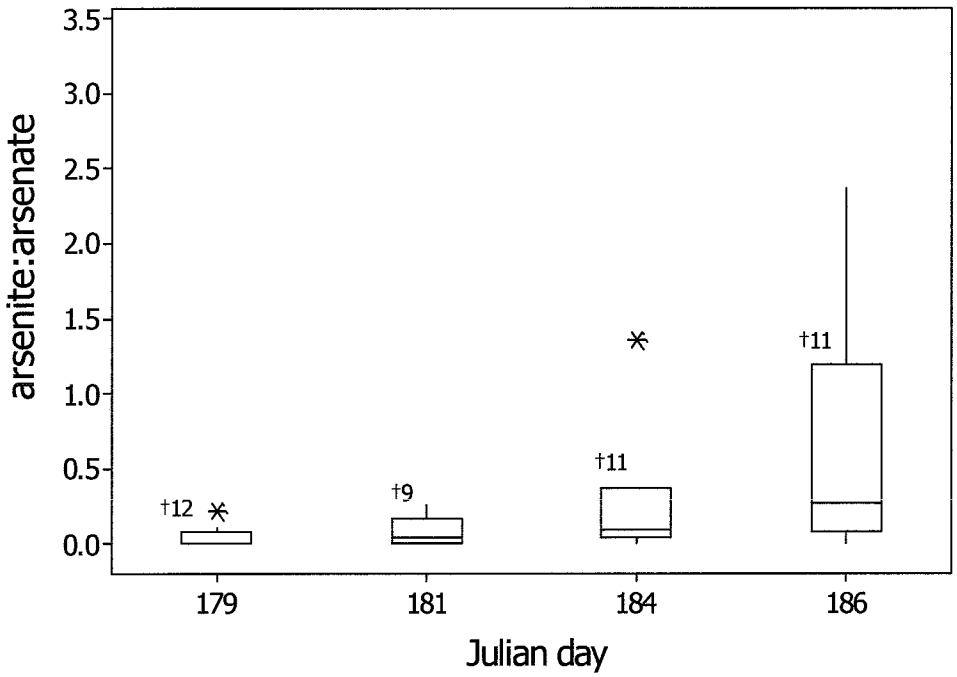

Figure 3.6 Box and whisker plots representing ratio values of arsenite:arsenate over the course of the summer thaw at Truelove Lowland. Amounts of arsenite and arsenate have been normalized for the volume of sample that passed through the strong anion exchange resin for As speciation. All samples were filtered through a Whatman® 0.45 μm capsule filter.

†number of samples

pH values decreased significantly over the sampling duration ($P \leq 0.05$) from an average of 7.8 on Julian day 179 to 7.3 on day 186 (Figure 3.7). A decrease in pH of such a small magnitude is not likely to affect sorption based on the pKa or sorption sites; however, a portion of mineral sites may become protonated, releasing bound As. Negative correlations exist between pH and T-As, D-As, and arsenite ($P \leq 0.05$). Spearman's rho values are –0.414, -0.454 and –0.324 for T-As, D-As, and arsenite, respectively.

Groundwater temperature rises to an average value of 6.66°C (n=11) from an average of 5.41°C (n=31, Julian days 179, 181 and 184) on Julian day 186. However, this rise is not statistically significant ($P \geq 0.20$). It is notable that the highest concentrations of T-As and D-As were present on Julian day 186. A rise in temperature could lead to As solubilization by accelerating chemical or biological reactions that solubilize As; however, definitive conclusions cannot be made to this effect.

3.3.3 Arsenic in snow and meltwater

The concentrations of T-As and D-As in snow averaged 29.3 (SE = 2.63) and 27.7 ng L^{-1} (SE = 4.49), respectively. Arsenic levels in snow did not change significantly over the sampling duration ($P \geq 0.20$). Average concentrations of T-As and D-As in snow are not significantly different ($P \geq 0.10$), indicating that there is very little particulate As. Thus, it appears that As in snow is dissolved in precipitation rather than a result of loess deposition on the snow surface. Relative to superpermafrost groundwater, snow contains very little T-As and D-As (Figure 3.8).

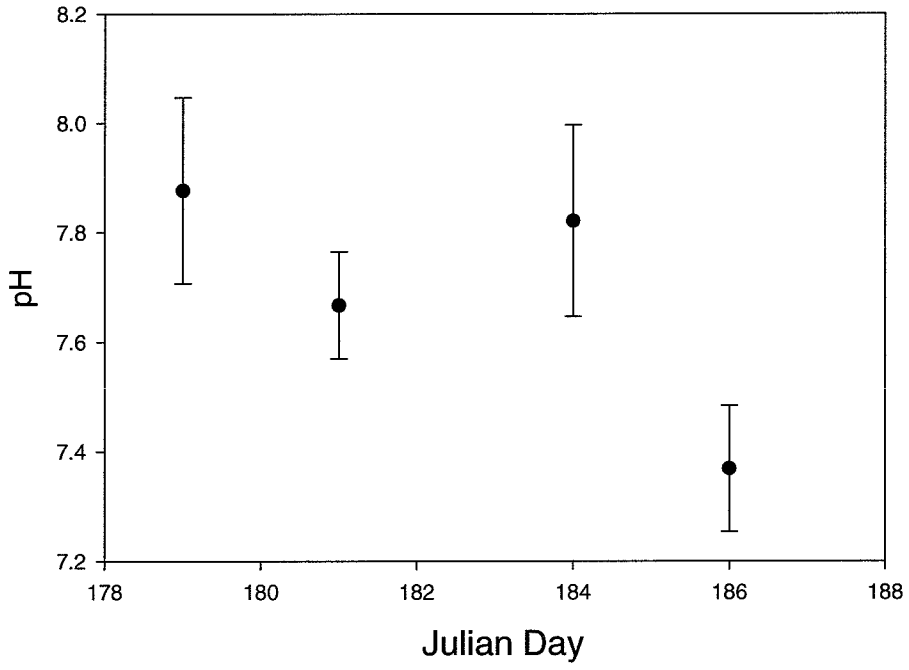

Figure 3.7 Mean pH values over the sampling duration (Julian day 179 to 186). Error bars represent standard error, n = 12.

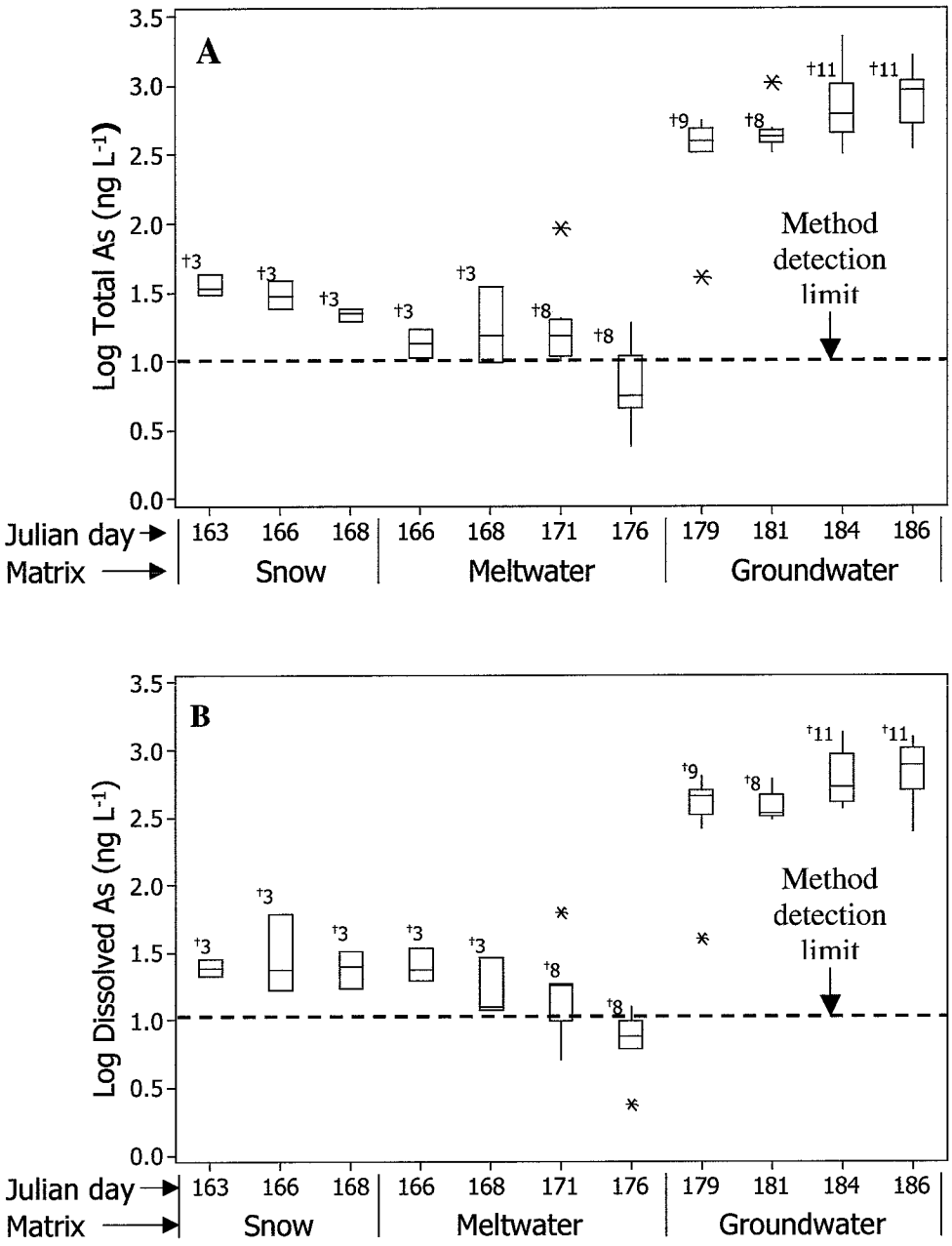

Figure 3.8 Box and whisker plots representing (A) total As (T-As) and (B) dissolved As (D-As) concentrations in snow, meltwater and superpermafrost groundwater at Truelove Lowland. D-As samples were filtered through a 0.45 μm Whatman® capsule filter. Data are pooled from samples from all field sites.

†number of samples

Arsenic concentration in standing meltwater was slightly lower than that in snow with mean T-As and D-As concentrations of 17.15 (SE = 3.84) and 16.00 (SE =2.66), respectively. There was a decreasing trend in As concentration in standing meltwater over time in both T-As ($P \leq 0.20$) and D-As ($P \leq 0.05$) (Figure 3.8). Levels of T-As in meltwater decreased from an average of 13.6 ng L^{-1} (SE = 1.23) on Julian day 166 to 10.6 ng L^{-1} (SE = 3.54) on Julian day 176 ($P \leq 0.05$), and levels of D-As in meltwater decreased from 25.6 ng L^{-1} (SE = 2.89) on Julian day 166 to 7.7 ng L^{-1} (SE = 1.16) on Julian day 176 ($P \leq 0.05$)(Figure 3.8). T-As and D-As in meltwater ranged from 2.4 to 91.8 ng L^{-1} and 2.4 to 62.5 ng L^{-1}, respectively.

Speciation of As in snow and standing meltwater samples was not reliable due to the trace levels of As present being so close to the MDL of the Millenium AFS. Eh and pH of meltwater did not change significantly by date nor site, and averaged 509 mV (SE = 25.4) and 8.76 (SE = 0.99), respectively. Neither Eh nor pH was correlated with As concentration in meltwater ($P \geq 0.10$).

3.4 Discussion

The increase in As concentration and specifically the increase in arsenite in groundwater while soil was flooded suggests that reducing conditions may have induced solubilization of As. However, the rise in arsenite occurred despite a decrease in measured Eh or an increase in Fe(II). In temperate ecosystems, an increase in As(III), Fe(II) and sulfide and a decrease in Eh and As(V) occur in soil porewater when soils in rice paddy fields are flooded (Takahashi et al., 2004). Chemical extraction of As in soils revealed that As is most likely bound in Fe oxide complexes.

Flooding in temperate soils generally results in reducing conditions, as anaerobic microbes reduce oxidized species and O_2 is consumed, often occurring in a matter of days (Sadiq, 1995). However, flooding of soils at Truelove Lowland did not produce the same result. It may be that Fe(III) reduction and subsequent lowering of Eh proceeds at a slower rate in cold temperatures, although Fe reducers are known to function at temperatures as low as 0°C (Stapleton et al., 2005).

At Truelove Lowland it does not appear that reductive dissolution of As-Fe complexes is the dominant process causing As solubilization. Based on the average measured Eh of 389 mV, the lack of Fe(II) and sulfide is not unusual. However, the rise in arsenite does not correspond with Eh indicating oxidizing conditions. One theory is that with the elevated pH of meltwater, As desorbs from mineral surfaces and becomes reduced in anaerobic soil microsites.

In the absence of reducing conditions, As can be desorbed from Fe oxides when competitive ligands are present (Jackson and Miller, 2000; Su and Puls, 2001). Jackson and Miller (2000) conducted experiments to determine the extraction efficiency of PO_4^{3-} and OH^- at removing arsenate and arsenite from goethite and amorphous Fe oxide. Results show that at pH 7, 0.1M OH^- was the more effective extractant with a maximum extraction efficiency of >80% arsenate but only ~5% arsenite from amorphous Fe oxides, and ~25% arsenate and ~30% arsenite from geothite. In contrast, 0.5 M PO_4^{3-} was able to extract arsenate to a maximum of 50% and arsenite to a maximum of 7% from amorphous Fe oxides, and 50% arsenate and ~30% arsenite from goethite. These results suggest that arsenate is more susceptible to desorption when competitive ligands are present. Thus, if aerobic water were constantly being replenished as occurs during the summer thaw, it is possible that negatively charged anions were desorbing As.

Fishback (2002) found that windblown loess from the escarpments surrounding Truelove Lowland resulted in a yearly flush of HCO_3^- into the soil, which may also act as a competitive ligand. Kim et al. (2000) found that the amount of As leached from rock was proportional to the $NaHCO_3$ concentration in solution. Within a 3 d incubation period, 1.5% of As was leached when rock was incubated in a 0.02M $NaHCO_3$ solution; when incubated in a 0.06M solution of $NaHCO_3$, 14.8% of As content in rock was leached. Alternatively, the elevated pH of meltwater (~8.5) could simply be inhibiting reduction of Fe(III) and thus slowing the reducing process (Masscheleyn et al., 1991).

The concentration of T-As in snow and standing meltwater sampled at Truelove Lowland was extremely low (Watras et al.) which is similar to the typical rainwater/snow concentration of 30 ng L^{-1} reported for temperate regions (Smedley and Kinniburgh, 2002). This suggests that the contribution of As from the atmosphere is relatively small, especially compared to the levels of As present in superpermafrost groundwater. Atmospheric As is likely not the main source of As on Truelove Lowland.

While no published information is available on As levels in snow, atmospheric concentrations of As in the Canadian High Arctic (Alert, Nunavut: 0.349 μg m^{-3}, n = 12, measured in 1989) (Landsberger et al., 1990) fall within the range of those found in the Russian Arctic (range: <0.06 to 8 μg m^{-3}) (Shevchenko et al., 2003). Atmospheric levels of As and other metals are extremely variable, both spatially and temporally, making it difficult to determine how much potential deposition of As could occur in precipitation. Thus, analysis of As and other metals in precipitation, especially snow, may be a more useful indicator of the amount of this contaminant entering an ecosystem.

3.5 Conclusions

There is not a clear explanation for the increase in As in superpermafrost groundwater over the sampling duration. Several possible explanations include desorption of weakly-bound As, competitive ligand exchange, and reductive dissolution of Fe-As complexes. The rise in arsenite concentration suggests that reducing processes are occurring, despite the lack of correlation with measured Eh, [Fe(II)], or sulfide. Further investigation is necessary to elucidate the mechanisms responsible for As solubilization at Truelove Lowland.

An almost negligible amount of the As found in superpermafrost groundwater is contributed from precipitation. Once the snow melts, however, levels of As in meltwater decrease, most likely due to sorption to vegetation and soil surfaces. If the binding strength of As to various surfaces is low, As may later become solubilized as environmental conditions change.

Determining natural levels of As in a soil ecosystem is crucial for developing regulations and remediation guidelines for allowable concentrations of As in soil and water. Understanding the biogeochemical cycling in the natural environment can also assist regulators in determining best management practices for contaminated sites. Further, determining concentrations of As in precipitation will help researchers and regulators assess whether natural areas could become contaminated by As from precipitation.

4.0 BIOGEOCHEMICAL CYCLING OF ARSENIC AT COLD TEMPERATURES: A LABORATORY INVESTIGATION

4.1 Introduction

Understanding the processes that control As solubilization in soil and groundwater is important from a regulatory and risk management perspective. Regulatory standards are often set for total As in soil and groundwater; however, the potential mobility of As must be taken into account. Changes in the natural environment may cause the form of As to change, making it more mobile and sometimes more toxic. In the Canadian High Arctic, the natural biogeochemical processes controlling As fate are not well understood. The Arctic climate and yearly melt are unique environmental phenomena that influence biological and chemical processes that control As solubilization. Controlled microcosm experiments help to elucidate the processes responsible for As movement from soil to water and provide more complete information for assessment of potential mobility.

In uncontaminated Florida soils, Chen et al. (2002) found that the highest As concentrations were found in soils that occur in wetlands, namely in the Gleysolic (Aquollic) and Organic (Histosolic) orders. Total As in these soils ranged from 0.5 to 11.7 mg kg^{-1} and 0.03 to 50.6 mg kg^{-1} in Organic and Gleysolic soils, respectively. Soils in WSM landscape positions at Truelove Lowland are generally classified as Fibric Organo Cryosols and Gleysolic Static Crysols (Walker and Peters, 1977), but the total

concentration of As in organic and mineral horizons of soils at Truelove Lowland is not known. Further, little information is available on the amount of As that is solubilized under natural environmental conditions in Arctic soil.

In temperate regions, the flooding of soil generates reducing conditions as O_2 is consumed in the soil ecosystem. In the High Arctic, the permafrost layer prevents vertical migration of water, facilitating the saturation of soil and limitation of O_2 diffusion from the surface. As Eh drops, anaerobic microbial processes including reduction of Fe(III) and arsenate are known to release As (Lovley, 1991; Dowdle et al., 1996; Fox and Doner, 2003; Takahashi et al., 2004).

During the summer thaw in the High Arctic, air temperature warms and soil thaws vertically. Throughout this process, the active layer is flooded with melt water that flows down slope, perched on the permafrost layer. At the beginning of the melt, the overlying organic layer is saturated, and as the active layer develops, water comes into contact with underlying mineral soil. In organic soil there are more carbon and nutrient sources for microbes (Kostka et al., 1999; Chatain et al., 2005), therefore the importance of microbial activity may be predominate in organic horizons. In mineral soil, chemical processes may be more important in controlling As fate. Thus, biological and chemical processes that contribute to As solubilization may occur at different times throughout the melt as organic and mineral horizons are sequentially exposed to superpermafrost groundwater.

It is hypothesized that soil flooding followed by anaerobic microbial processes caused solubilization of As in soil at Truelove Lowland. The objectives of this chapter are threefold: 1) To confirm the association of As with Fe oxides in soils from Truelove Lowland, 2) To determine how redox potential affects As solubility and partitioning, and

3) To determine the effect of pH on As solubility and partitioning. First, total Fe, Fe oxides and total As were extracted from soil from the four field sites on Truelove Lowland. Correlations were determined between As and Fe and/or Fe oxides. Second, microcosms incubated aerobically and anaerobically were sampled over time to observe trends in As solubility and partitioning. Third, a second set of microcosms were prepared with a pH adjustment and an As spike to further explore the role of pH and Eh in controlling As partitioning and speciation.

4.2 Materials and methods

4.2.1 Microcosm experiment

4.2.1.1 Microcosms with organic and mineral soil

Soil slurries were incubated under controlled conditions in 500 mL Nalgene® bottles (microcosms). Overlying organic and underlying mineral soils from sites 5, 6, 7 and 9 on Truelove Lowland, Devon Island, NU, were incubated in separate microcosms. Soil sub-samples were dried to determine moisture content, and based on this moisture content 6.75 g equivalent dry weight of mineral and organic soil from each site was placed into a 500 mL Nalgene® bottle. Soil aliquots to be used in microcosms were sorted manually to remove obvious coarse fragments and plant materials but were not sieved. Four treatments were assessed in triplicate: 1) mineral, aerobic incubation, 2) mineral, anaerobic incubation, 3) organic, aerobic incubation, and 4) organic, anaerobic incubation.

Two-hundred and seventy-five millilitres of distilled water was added to each microcosm that was to be incubated aerobically. Synthetic groundwater medium was not used as it may contain competitive ligands that would displace As, such as NO_3^-. One milliliter of 275 mM HEPES, Free Acid, ULTROL® Grade buffer (Calbiochem, Darmstadt, Germany) was added to each bottle to minimize pH differences between organic and mineral soil slurries. Caps were attached loosely to allow air exchange.

Anaerobic microcosms contained oxygen-free water, which was prepared by autoclaving water followed by N_2 sparging for 20 min and equilibration in a N_2-filled glovebox chamber. Once oxygen free water had cooled, 275 mL was added to each microcosm, followed by one milliliter of 275 mM HEPES buffer and one milliliter of 100 μM titanium(III) nitrilotriacetate (TiNTA) media reductant (Moench and Zeikus, 1983). Anaerobic microcosms were sealed tightly and inverted to minimize gas exchange. To ensure that Nalgene® bottles remained anaerobic for the duration of the experiment, one bottle was prepared with 275 mL of oxygen free distilled water, 1 mL of 275 mM HEPES buffer, 1 mL of 100 μM TiNTA reducing agent, and 1 mL Reazurin® indicator dye that turns pink in the presence of O_2. This bottle was opened in the N_2 -containing glovebox when anaerobic microcosms were sampled and closed the same way as anaerobic microcosms. The level of As in distilled water, HEPES buffer and TiNTA poising agent was below the detectable limit of the Millenium AFS (0.01 μg L^{-1}).

All aerobic and anaerobic microcosms were constantly shaken at 125 rpm in a rotating shaker to minimize diffusion gradients. Microcosms were kept at 10°C to mimic field conditions at Truelove Lowland. Sampling of microcosms containing mineral soil was carried out on days 1, 6, 11, 17 and 42. Sampling of microcosms

containing organic soil was carried out on days 1, 6, 11, 16 and 43. Sampling procedures for aerobic and anaerobic microcosms were identical; however, anaerobic microcosms were sampled and closed in an N_2 containing glovebox, while aerobic microcosms were sampled outside the glovebox.

Sampling of microcosms involved tightening of all caps and shaking vigorously, then measuring pH and Eh using an Orion Pentrode® 630 (Beverly, MA). Microcosms were left to sit upright for one h after shaking to allow suspended particles to settle. Supernatant was drawn through a Teflon tube attached to a Norm-Ject® 50 mL polypropylene syringe. 0.45 μm Whatman capsule filters were used to filter samples for analysis of D-As, Fe(II), Fe(III) and sulfide. Samples for analysis of T-As were not filtered, and particulate As was calculated by subtracting D-As from T-As.

4.2.1.2 Spiked microcosms

Spiked microcosms were prepared slightly differently than the pristine soil microcosms. Microcosms were prepared in glass serum bottles, and each time they were sampled, one bottle was sacrificed. Therefore, 15 serum bottles were used for each treatment (three repetitions and five sampling times) for each of four treatments: natural-aerobic, natural-anaerobic, spiked-aerobic, and spiked-anaerobic. Also, only mineral soil from site 7 was used and the soil was sieved before introducing into microcosms. The soil was sieved through a 4 mm sieve to remove coarse fragments. For each microcosm, 1.96 g of soil was placed into an 80 mL glass serum bottle. Sixty-five milliliters of distilled water and 1 mL of 275 mM HEPES buffer was added to each

serum bottle to be incubated aerobically, making a ratio of soil to water of approximately 1:34.

Oxygen was removed from distilled water for microcosms to be incubated anaerobically by boiling on a hotplate whilst sparging with N_2 gas for 30 mins. The water was cooled in an N_2-filled glovebox before adding to serum bottles containing soil. To each serum bottle was added 65 mL of oxygen-free water along with 1 mL of 275 mM HEPES buffer. A pH-buffered reductant, TiNTA, was added to each microcosm to be incubated anaerobically in the amount of 65 μL.

A subset of microcosms to be incubated aerobically and anaerobically was spiked with arsenate and arsenite to an initial concentration of 25 μg L^{-1} each arsenate and arsenite (total 50 μg L^{-1}). A concentrated solution was prepared with sodium arsenate ($Na_2HAsO_4 \cdot 7H_2O$) (Mallinckrodt Chemicals) in distilled water. A concentrated solution of arsenite was prepared with sodium arsenite ($NaAsO_2$) (Mallinckrodt Chemicals) in room temperature oxygen-free water in a N_2-filled glovebox. An appropriate amount of concentrated arsenite and arsenate was pipetted into each 'spiked' microcosm to a final concentration of 25 μg L^{-1} each arsenate and arsenite.

All microcosms were capped and shaken. Microcosms to be incubated anaerobically were capped with a rubber stopper and sealed with an aluminium cap within the N_2-filled glovebox. Microcosms to be incubated aerobically were capped and shaken, then a foam plug was inserted in the neck of the bottle to allow transfer of O_2. All microcosms were incubated at 10°C in a shaker rotating constantly at 125 rpm.

Sampling of microcosms containing mineral soil was carried out on days 1, 7, 14, 21 and 28. Sampling procedures for aerobic and anaerobic microcosms were identical; however, anaerobic microcosms were sampled in an N_2-filled glovebox, while aerobic

microcosms were sampled outside the glovebox. pH and Eh were measured using an Orion Pentrode® 630 (Beverly, MA). After shaking, microcosms were left to sit upright for one h after shaking to allow suspended particles to settle. Supernatant was drawn through a Teflon tube attached to a Norm-Ject® 50 mL polypropylene syringe. Whatman capsule filters, 0.45 μm, were used to filter samples for analysis of D-As, Fe(II), Fe(III) and sulfide.

At the low arsenic concentrations assessed in this study, the use of potassium iodide (KI) to reduce As(V) to As(III) for HG-AFS analysis proved problematic. It is commonly assumed that in a mixed solution of As(III) and As(V), As(V) will not contribute to HG-AFS signal. Thus, one uses KI to reduce As(V) to As(III). Then by difference, one can estimate As(V) and As(III). The Millenium HG-AFS detects 98.2% of the As(III) as well as 22.7% (0.227 = 1.215 ÷ 0.277) of As(V) present in solution without addition of KI (Appendix D). Thus, assuming that As in soil slurries is a combination of As(III) and As(V) (Sadiq, 1995), samples can be analyzed as follows:

$$\text{Response (no KI added)} = 0.9819\ \text{As(III)} + 0.277\ \text{As(V)} \quad (4.1)$$

$$\text{Response (KI added)} = 0.9819\ \text{As(III)} + 1.215\ \text{As(V)} \quad (4.2)$$

$$\text{Response (no KI added)} - \text{Response (KI added)} = 0.938\ \text{As(V)} \quad (4.3)$$

Once equation 4.3 is solved, then equation 4.2 will yield As(III) concentrations.

Samples for analysis of As were prepared as in section 3.2.4.1 for determination of all As fractions using the Millenium Excalibur AFS. Samples were diluted when necessary to achieve a convenient concentration for analysis. Relative percent difference (RPD) between duplicate samples from pristine microcosms was 11%, and from spiked microcosms RPD averaged 5%. Complete QA/QC tables are available in Appendix A.

4.3 Results

4.3.2 Microcosms with pristine soil incubated under aerobic and anaerobic conditions

4.3.2.1 Arsenic in microcosm supernatant in relation to environmental conditions

There is no clear trend in As concentration in supernatant with incubation time ($P \geq 0.10$). However, average levels of T-As are 61% lower in mineral microcosms and 17% lower in organic microcosms when incubated anaerobically versus aerobically (Figure 4.1). T-As concentration in anaerobic microcosms is only significantly lower in microcosms containing mineral soil ($P \leq 0.10$).

Concentrations of D-As follow a similar trend in microcosms containing mineral soil with an identical 61% less D-As in anaerobic versus aerobic microcosms ($P \leq 0.10$). In contrast, microcosms containing organic soil show a 48% increase in D-As ($P \leq 0.10$), suggesting that different processes are occurring in organic and mineral soils.

In organic microcosms, particulate As made up 71% of T-As under aerobic conditions, while only 44% under anaerobic conditions. In contrast, mineral microcosms incubated aerobically and anaerobically contained 30 and 24% particulate As, respectively. Thus, it appears that in organic soil, As partitioning between the particulate and dissolved phase was altered under reducing conditions, whereas this observation was not noted in mineral microcosms.

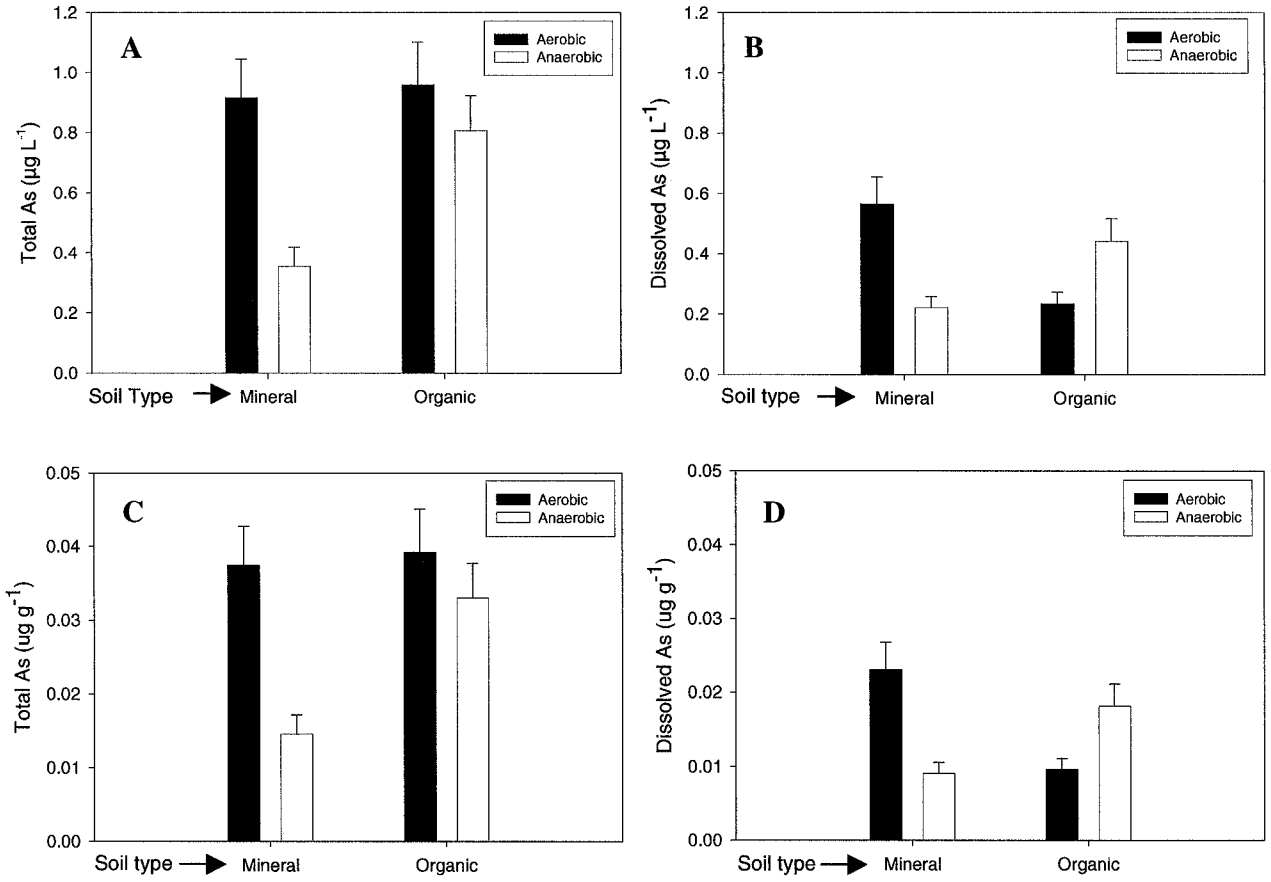

Figure 4.1 Average (A) total As (T-As) and (B) dissolved As (D-As) in supernatant from microcosms containing organic and mineral soil. Samples analyzed for D-As were filtered through a 0.45µm Whatman® capsule filter. Total As (C) and dissolved As (D) are also represented per soil weight. Microcosms were incubated under aerobic and anaerobic conditions for 42 days. Bars represent average response (n=60) from microcosms containing soil from sites 5,6,7, and 9 on Truelove Lowland, Devon Island, NU over the entire sampling duration. Error bars represent standard error of the estimate.

Average Eh as measured with the Orion Pentrode® (automatic conversion to Standard Hydrogen Electrode (SHE)) indicates that conditions in anaerobic microcosms were indeed reducing. Average Eh in microcosms incubated anaerobically was –33 (SE = 11.24) and 107 mV (SE = 10.75) in mineral and organic microcosms, respectively. Average Eh under aerobic conditions was 330 (SE = 2.66) and 422 mV (SE = 6.21) in microcosms containing mineral and organic soil, respectively. In microcosms containing mineral soil there was no correlation between Eh and T-As or D-As in microcosms incubated aerobically or anaerobically ($P \geq 0.10$) suggesting that Eh is not the dominating factor in As solubilization in mineral soil.

However, in microcosms containing organic soil, T-As and D-As were negatively correlated with Eh, with the strongest correlation occurring between D-As and Eh in anaerobic microcosms ($\rho = -0.433$, $P \leq 0.01$). This suggests that anaerobic processes are contributing to As solubilization in microcosms containing organic soil, i.e. as Eh decreased, As became solubilized. This interpretation is confirmed by the decrease in percentage particulate As. One might also expect to see a shift in As speciation toward arsenite; however, speciation of As was not possible due operational difficulties.

A rise in Fe(II) with decreasing Eh would suggest that reductive dissolution of Fe-As complexes was occurring in microcosms incubated anaerobically. Iron speciation supports measured Eh in that levels of Fe(II) are higher under anaerobic conditions in microcosms containing both organic and mineral soil ($P \leq 0.05$) (Figure 4.2). It appears that the source of Fe(III) that is being converted to Fe(II) is in particulate matter, as dissolved Fe(III) does not decrease (i.e. is not converted to Fe(II)) under anaerobic conditions. Most importantly, there is a very high correlation ($\rho = 0.699$, $P \leq 0.01$)

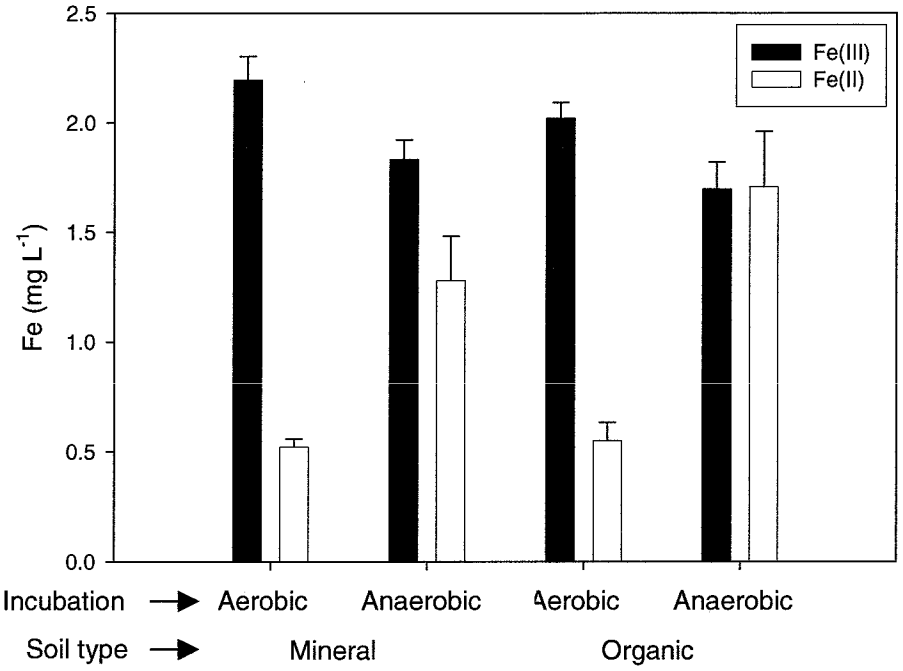

Figure 4.2 Average Fe(III) and Fe(II) in supernatant from microcosms. M1 = mineral soil incubated aerobically; M2 = mineral soil incubated anaerobically; O1 = organic soil incubated aerobically; O2 = organic soil incubated anaerobically. Bars represent the aveage (n = 60) from microcosms containing soil from sites 5,6,7, and 9 on Truelove Lowland, Devon Island, NU (n = 60) over the entire sampling duration. Error bars represent standard error of the estimate.

between D-As and Fe(II) under anaerobic conditions in microcosms containing organic soil. This suggests that As is associated with Fe minerals in organic soil, and that Fe(III) is being reduced to Fe(II) with subsequent release of D-As.

Average pH is notably lower in anaerobic compared to aerobic microcosms containing both mineral and organic soil. In microcosms containing mineral soil, average aerobic pH was 7.92 (SE = 0.04) whereas anaerobic pH was 6.82 (SE = 0.03). Organic microcosms had aerobic supernatant pH of 7.34 (SE = 0.05) and anaerobic pH of 6.64 (SE = 0.03). The cause of decreased pH in anaerobic microcosms was the addition of an acidic reducing agent (TiNTA). Correlations between pH and T-As in microcosms containing mineral soil are positive in microcosms incubated aerobically ($\rho = 0.339$, $P \leq 0.01$) and anaerobically ($\rho = 0.287$, $P \leq 0.05$). In microcosms containing organic soil, T-As and pH are positively correlated ($\rho = 0.430$, $P \leq 0.01$) under aerobic conditions, but no significant correlation exists under anaerobic conditions.

The higher pH in aerobic microcosms could be causing increased T-As as compared to anaerobic microcosms, possibly as Fe-oxide minerals near their PZC around pH 8 (Carrillo and Drever, 1998). To clarify this possibility, a further experiment with aerobic and anaerobic microcosms that were buffered to equal pH was conducted. A subset of microcosms in this experiment were spiked with 50 $\mu g\ L^{-1}$ (25 $\mu g\ L^{-1}$ each arsenate and arsenite) to provide insight on whether there was enhanced mobilization of As under aerobic conditions, as is suggested by the pH theory, or enhanced sequestration under anaerobic conditions. As the microcosms containing mineral soil showed the most marked decrease in T-As under anaerobic conditions, the "spiked microcosms" contained only mineral soil.

4.3.3 Spiked microcosms

4.3.3.1 pH in spiked microcosms

Average pH in the second set of microcosms was 7.82 (SE = 0.02) and 7.77 (SE = 0.01) in those incubated aerobically and anaerobically, respectively. Despite the homogeneity of pH, average T-As under anaerobic conditions was 50 and 45% lower than aerobic conditions in natural and spiked microcosms, respectively. Natural and spiked microcosms incubated anaerobically also had 58 and 31% lower average D-As than when incubated aerobically (Figure 4.3).

4.3.3.2 Arsenic partitioning in relation to redox status

Eh in aerobic microcosms ranged between 386 and 465 with an average of 403 mV (SE = 3.47). Eh in anaerobic microcosms ranged between 24 and 109 and averaged 101 mV (SE = 4.55). Eh in aerobic and anaerobic microcosms did not change significantly over time ($P \leq 0.10$).

Over the 28-d incubation, T-As in supernatant decreased, reaching equilibrium after approximately 20 d in both natural and spiked microcosms (Figure 4.4). In natural microcosms, T-As decreased by 78% in aerobic microcosms and 67% in anaerobic microcosms over the incubation duration of 28 d. The average equilibrium concentrations of T-As in aerobic and anaerobic microcosms are not significantly different ($P \geq 0.10$). This suggests that equivalent amounts of As are able to be sorbed under both aerobic and anaerobic conditions, but that the rate of sorption is faster under reducing conditions.

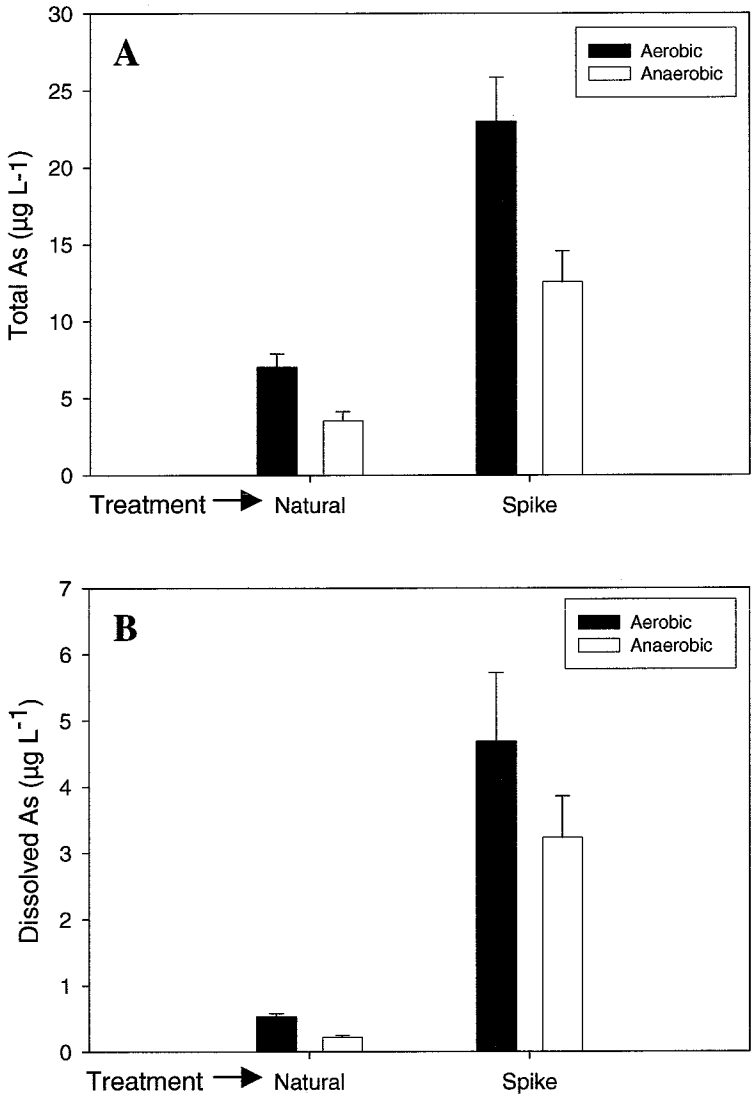

Figure 4.3 Average (A) total As (T-As) and (B) dissolved As (D-As) in supernatant from spiked and natural microcosms. 'Natural' microcosms contain no additional As; 'Spiked' microcosms were spiked to a final concentration of 25 µg L^{-1} arsenite and 25 µg L^{-1} arsenate. Bars represent average concentrations of T-As and D-As in samples taken from microcosms containing mineral soil from site 7 on Truelove Lowland, Devon Island, NU over the entire sampling duration (n = 15). Error bars represent standard error of the estimate.

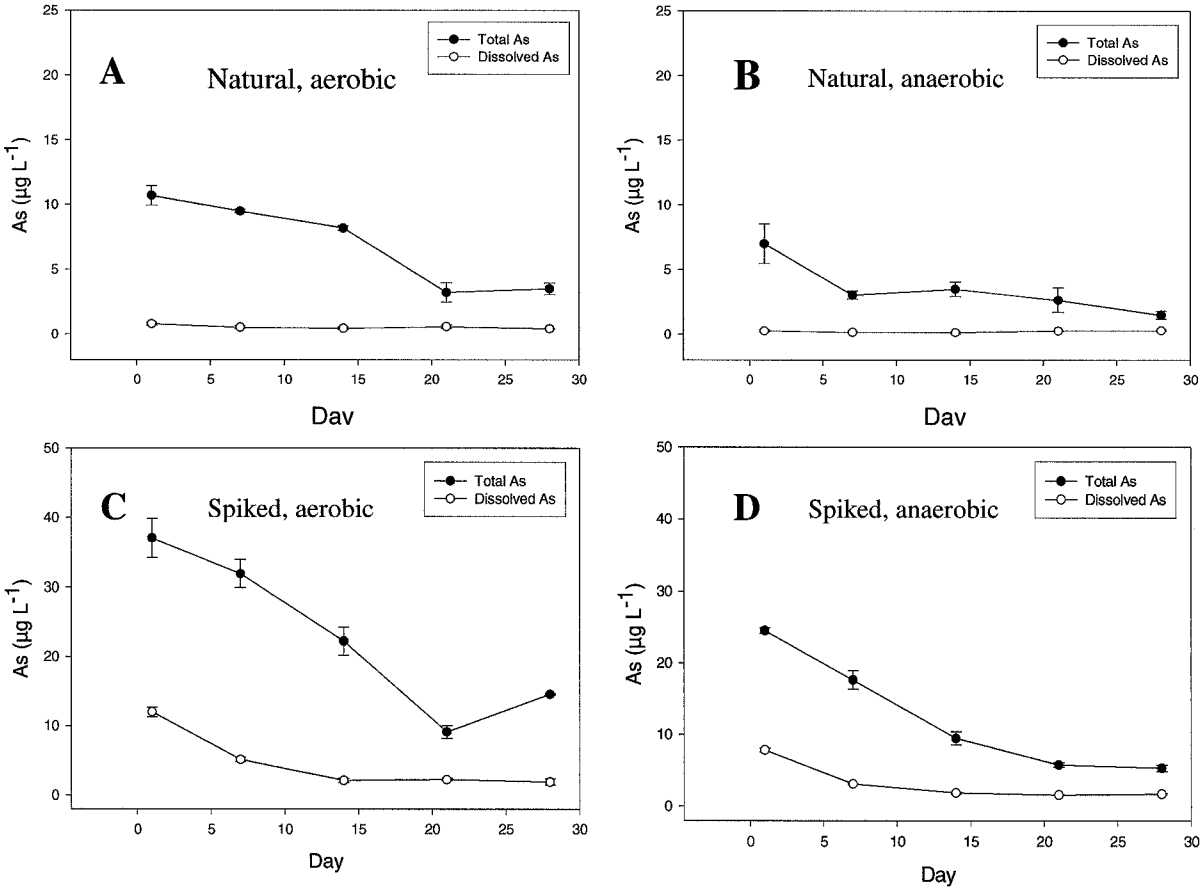

Figure 4.4 Total and dissolved As in microcosm supernatant over the sampling duration in microcosms containing mineral soil. 'Natural' microcosms contain no additional As; 'Spiked' microcosms were spiked to a final concentration of 25 µg L^{-1} arsenite and 25 µg L^{-1} arsenate. (A) Natural, aerobic; (B) Natural, anaerobic; (C) Spike, aerobic; and (D) Spike, anaerobic. Samples for D-As were filtered through a 0.45 µm Whatman® capsule filter. Error bars represent standard error of the estimate, n=3.

In spiked microcosms, T-As decreased by 61 and 78% in anaerobic and aerobic microcosms, respectively. The equilibrium concentrations of T-As in supernatant was higher in aerobic microcosms ($P \leq 0.05$), suggesting that significantly more As is sequestered under reducing conditions.

4.3.3.3 Arsenic speciation trends over the sampling duration

In natural microcosms under aerobic conditions, most As is in the arsenate form and it takes approximately 20 d to reach equilibrium (Figure 4.5). In natural anaerobic microcosms, it appears that equilibrium is reached within approximately 7 d. Arsenite levels do not increase in anaerobic microcosms, suggesting that compounds to which As is sorbed, interpreted to be Fe oxides, are not being reduced. This may be attributed to a scarcity of available carbon or nutrients to support a population of anaerobic microorganisms that would accelerate the reduction of Fe(III).

In spiked microcosms under aerobic conditions, it appears that arsenite was first converted to arsenate during the first 14 d followed by a sharp drop in T-As around day 21 (Figure 4.5). Approximately 10 $\mu g\ L^{-1}$ of arsenite sorbed immediately when water was introduced into microcosms, while arsenate disappeared from solution much more slowly. In spiked microcosms incubated anaerobically, arsenite disappeared rapidly from solution, most likely via sorption to soil particles.

4.4 Discussion

In both natural and spiked microcosms, T-As decreased when incubated anaerobically. In microcosms containing mineral soil, this decrease was particularly

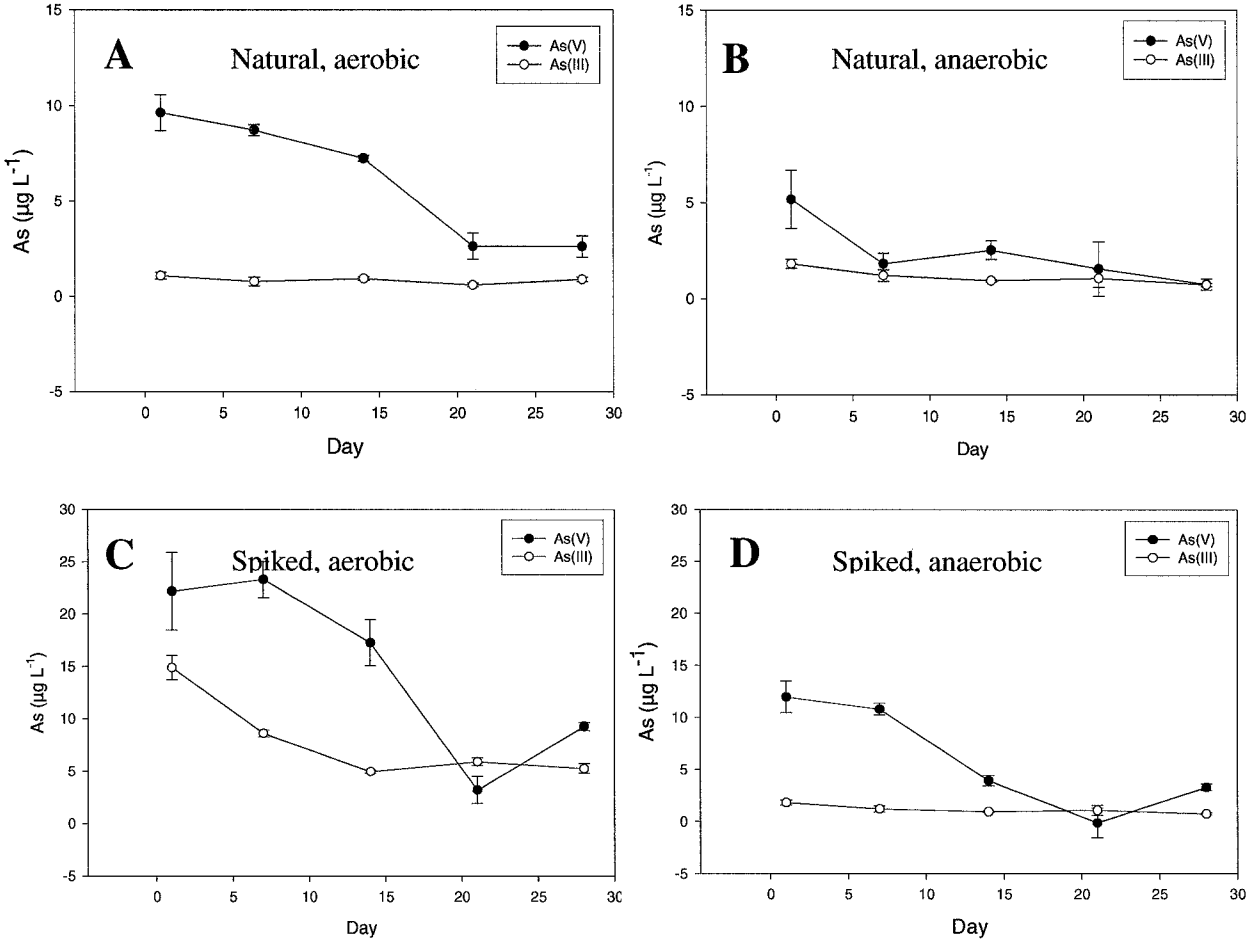

Figure 4.5 Arsenate and arsenite fractions of total As (T-As) in microcosm supernatant over the sampling duration in microcosms containing mineral soil (M7). 'Natural' microcosms had no As added, while 'Spike' had a concentration of 50 µg L^{-1} added on day 0. (A) Natural, aerobic; (B) Natural, anaerobic; (C) Spike, aerobic; and (D) Spike, anaerobic. Samples for D-As were filtered through a 0.45 µm Whatman® capsule filter. Error bars represent standard error, n=3.

pronounced, and the spike experiment verified that sequestration of As was occurring under anaerobic conditions rather than enhanced mobilization under aerobic conditions. In microcosms containing mineral soil there was little difference in the partitioning of As; T-As and D-As decreased equally. In microcosms containing organic soil, there was a change in partitioning with an increase in D-As and a decrease in T-As. This phenomenon suggests that different processes are occurring in organic and mineral soil slurries under anaerobic incubation.

The rise in D-As in microcosms containing organic soil is consistent with results observed in rice paddy soils, which contain similar quantities of organic matter (Takahashi et al., 2004). The flooding of rice paddy soils generates reducing conditions as O_2 is consumed by anaerobic microorganisms. This is followed by a solubilization of As as Fe-As compounds are reduced via chemical and biological mechanisms (Kocar et al., 2005; Lengke and Tempel, 2005).

The reduction of available electron acceptors can also cause a decrease in Eh into the zone of SO_4^{2-} reduction (< -200 mV) (Lefroy et al., 1993). Under these conditions arsenite can precipitate with Fe(II) and sulfide as FeAsS (Lengke and Tempel, 2005). The microcosms in this study did not exhibit this activity, and the decrease in T-As is not likely due to precipitation of FeAsS. It is possible that the oligotrophic nature of High Arctic soils limits microbial activity and prevents the decrease in Eh required for precipitation of FeAsS compounds (Chatain et al., 2005; Stapleton et al., 2005).

Several authors have observed a decrease in T-As under anaerobic incubation via processes other than precipitation of FeAsS minerals. One possible mechanism for the decrease in T-As under anaerobic conditions could be preferential sorption of arsenite to ferrihydrite (Sadiq, 1995). Herbel and Fendorf (2004) found that reaction of 1.5 mM

arsenite or arsenate with ferrihydrite-coated sands resulted in mass loadings of 318.2 mg arsenite kg^{-1} and 201.7 mg arsenate kg^{-1}, resulting in nearly twofold greater sorption of arsenite.

The preferential sorption of arsenite has also been documented by Raven et. al (1998) with arsenite loading on 2-line ferrihydrite reaching adsorption density of 0.60 mol As · mol Fe^{-1}, while the maximum arsenate adsorption density reached only 0.25 mol As mol Fe^{-1}. Further, it was found that the rate of arsenite sorption was greater than arsenate; after 96 h exposure, 98% of arsenite and only 71% of arsenate was sorbed to ferrihydrite. After 24 h, 98% of both arsenite and arsenate had sorbed to ferrihydrite. The theory of preferential sorption of arsenite to ferrihydrite is supported by the spiked microcosms, where the rate of sorption was greater for arsenite than arsenate.

The preferential sorption of arsenite to ferrihydrite requires that ferrihydrite persist while arsenate is being converted to arsenite. It is likely that some Fe(III) is converted to Fe(II) under these conditions, as the dissimilatory reduction of Fe(III) provides more energy than reduction of arsenate, and thus Fe(III) would be preferentially reduced (Newman et al., 1998). Under the redox conditions encountered in the anaerobic microcosms (~ -100 to +100 mV), the formation of mixed Fe(II) and Fe(III) oxides, commonly referred to as green rust minerals, is quite likely (Su and Puls, 2004; Lien and Wilkin, 2005; Thoral et al., 2005). Both arsenate and arsenite have been found to sorb substantially to green rust minerals, and the presence of these minerals under reducing conditions may explain the sequestration of T-As in microcosms incubated anaerobically (Thoral et al., 2005).

4.5 Conclusions

During the summer thaw in the High Arctic, thawing of the overlying organic layer in depressional areas occurs while the underlying mineral layer remains frozen. Results from this study suggest that some solubilization of As may occur in the organic layer, perhaps due to activity of anaerobic microbes. However, scarcity of nutrients and perhaps labile C and cold temperatures are presumed to limit anaerobic microbial activity. As the active layer develops, meltwater is exposed to the underlying mineral layer, which, according the this study, would provide sorption sites for T-As or D-As. If the As is in the arsenite form, preferential sorption to ferrihydrite may occur, or green rust may form as some Fe(III) is converted to Fe(II), providing sorption sites for both arsenite and arsenate.

Understanding the potential fate of natural As in soil, especially during the summer thaw, will allow development of more comprehensive regulations for remediation of Arctic sites contaminated with As. The use of microcosms in this study provided some insight into potential mobility of As under simulated field conditions. Further experiments including analysis of soil slurries incubated anaerobically using X-ray diffraction (XRD) could validate the theory of sorption to green rust minerals. Further monitoring of As in groundwater during the summer thaw at other pristine locations in the High Arctic would also help to validate these experiments and provide more detailed information for regulators.

5.0 SUMMARY AND CONCLUSIONS

In this study, T-As levels in superpermafrost groundwater at a site in the High Arctic doubled over the course of the summer thaw. This increase was not due to snow input as levels in snow were negligible. This increase in T-As did not correspond with a decrease in Eh, nor a rise in soluble Fe(II). It did, however, correspond with a shift in As speciation from arsenate to arsenite suggestive of reducing conditions. In the absence of predominant reducing conditions, the highly alkaline nature of the melting snow and concomitant large input of HCO_3^- may have played an important role in the increase of As in groundwater during the summer thaw.

Laboratory studies found that D-As release under anaerobic conditions depended on the organic matter content of soil, with organic soils releasing D-As under reducing conditions and mineral soils sequestering D-As. In temperate soils, the release of D-As from organic soils is greatly accelerated due to the activity of anaerobic microbes. In northern soils, the same phenomenon may occur, with greater microbiological activity in organic soils where there is more labile C and nutrients than in mineral soil.

The sequestration of As in mineral soil is postulated to have occurred due to preferential sorption of arsenite to ferrihydrite or possibly to green rust minerals present under anaerobic conditions. Supporting this, arsenite sequestration occurred to a greater extent compared to arsenate, which is in agreement with the relative affinities of these two species for ferrihydrite.

This evidence suggests that the As cycle on Truelove Lowland is dominated by the desorption of As due to HCO_3^- input each year during the spring melt linked to the

sorption of As to ferrihydrite or green rust present in underlying mineral soils. The sequential thawing of the soil's active layer and large inputs of HCO_3^- are unique to northern environments. Thus, this delicate balance of two sorbing processes should be born in mind in northern development. Large inputs of soluble organic matter or nutrients could cause increased solubilization and mobility of D-As during the summer thaw when soils become flooded.

In the Canadian Arctic there are a number of sites that are heavily contaminated with As. Among these is the Royal Oak Giant Mine in Yellowknife, NWT, where 237,000 tonnes of AsO_3 dust is stored in underground chambers. Arsenic has leached from these chambers into the soil, groundwater, and surface water, causing widespread contamination in a sensitive ecosystem. With the expansion of mining and industrial development in the Canadian Arctic, a better understanding of natural levels and biogeochemical cycling of contaminants such as As is required to develop strategies and guidelines for remediation of sites such as the Giant Mine.

During the summer thaw in the High Arctic there is a pulse of biological activity as the snow melts and the soil's active layer develops. Low-lying topographical areas receive meltwater from elevated landscape positions, resulting in the ponding of water. In temperate soils, flooding of soil is followed by a decrease in Eh and often results in solubilization of As via reductive dissolution of Fe oxides. In soil, As is most commonly associated with Fe minerals such as Fe oxides under aerobic conditions (McGeehan et al., 1998; Cummings et al., 1999). In the High Arctic, the effects of flooding of low-lying areas on As partitioning is not known. It is hypothesized that flooding of soil during the summer thaw will result in reducing conditions and solubilization of As, leading to increased mobility in surface water.

The goal of the study described in this thesis was to characterize the biogeochemical cycling of As in soil and superpermafrost groundwater at a pristine site in the High Arctic. The specific objectives included:

(1) Determining the concentration of As in snow, meltwater and superpermafrost groundwater at Truelove Lowland on Devon Island, Nunavut during the summer thaw and the correlation of As with Eh, pH, [Fe(III)], [Fe(II)] and sulfide; and

(2) Using microcosms to incubate soil slurries under aerobic and anaerobic conditions in the laboratory to elucidate the dominant biogeochemical processes controlling As fate.

To achieve objective (1), samples of snow, meltwater and superpermafrost groundwater were taken for analysis of T-As, D-As, arsenite and arsenate. Superpermafrost groundwater samples were taken over the duration of the summer thaw and parameters including Eh, pH and temperature were also measured. Samples were taken for analysis of redox-sensitive ions Fe(III), Fe(II) and sulfide.

The most important finding of the field study was that T-As in superpermafrost groundwater nearly doubled as the summer thaw progressed. Further investigation revealed that arsenate decreased while arsenite increased over the sampling duration. This suggests that reductive dissolution of As minerals in soil was occurring, and was a likely mechanism for solubilization of As. However, in superpermafrost groundwater at Truelove Lowland, measured Eh did not indicate that conditions were reducing (> 300 mV), and a rise in Fe(II) was not seen as would be expected with reductive dissolution of Fe oxides. T-As concentration was not correlated with Eh, Fe(III), Fe(II) or sulfide, despite the rise in arsenite indicative of reducing conditions.

One possibility for contradictory the redox indicators is that equipment or sampling procedures were not accurately reflecting the soil's redox status. For example, it is often difficult to sample dissolved Fe(III) and Fe(II). Fe(III) is often found in the form $Fe(OH)_3$ and can precipitate between pH 4 and 11 (Collins and Buol, 1970; Kirk, 2004; Moldovan and Hendry, 2005). Also, depending on solution Eh and pH, Fe(II) and sulfide may not be suspended in solution; Fe-S will precipitate under reducing conditions below approximately -100 mV (Rittle et al., 1995). Thus, concentrations of Fe(III), Fe(II) and sulfide may not have been accurately measured.

Further complicating assessment of redox status, it can also be difficult to accurately assess Eh with a platinum electrode. Yan et al. (2004) found that 10 m of standing water in a piezometer was necessary to obtain reliable downhole Eh measurements with a Pt electrode, as O_2 from the surface was introduced into the water column by the electrode. Piezometers on Truelove Lowland were capturing superpermafrost groundwater only, and generally held a water column less than 30 cm. Some authors suggest placing the Pt electrode directly in sediment and equilibrating for up to four h (Bennett and Dudas, 2003), which was not possible in capped piezometers and given time constraints. Finally, Eh in soil microsites may be reducing even if the overall soil solution does not show decreased Eh (Renault and Stengel, 1994).

In the absence of reducing conditions and reductive dissolution of Fe oxides, the rise in As over the summer thaw could be due to desorption of weakly-bound As. In some aquifers, As desorption is enhanced by competitive ligands such as phosphate (PO_4^{3-}), nitrate (NO_3^-), bicarbonate (HCO_3^-), and hydroxide (OH^-) (Jackson and Miller, 2000; Kim et al., 2000; Su and Puls, 2001). In temperate ecosystems, large inputs of PO_4^{3-} and NO_3^-, generally from agricultural systems, are required to mobilize As from soil surface

sites, and these nutrients are generally limiting in soil at Truelove Lowland (<10 mg kg^{-1} and <1 mg kg^{-1} for NO_3^- and PO_4^{3-}, respectively) (Walker and Peters, 1977). Carbonate (HCO_3^-), however, is contributed continually as loess from nearby escarpments (Fishback, 2002), and for this reason snow and meltwater pH was measured at between 8 and 9. High concentrations of HCO_3^- in snow and meltwater could have caused the observed increase of As in superpermafrost groundwater at Truelove Lowland by competitive ligand exchange.

From the field study alone, the mechanisms controlling As fate in low-lying areas of the landscape are not clear. To further understand the processes governing As fate in flooded soil, a microcosm experiment simulating conditions at Truelove Lowland was conducted in the laboratory. Organic and mineral soils from Truelove Lowland were made into slurries in Nalgene® bottles (microcosms) and incubated at 10°C under aerobic and anerobic conditions. Two microcosm experiments were run; one set of microcosms was unspiked and the other was spiked with 25 μg L^{-1} arsenate and arsenite (50 μg L^{-1} total). Samples of supernatant were taken over the period of incubation at varying intervals and were analyzed for T-As, D-As, arsenate, arsenite, Fe(III), Fe(II) and sulfide. Eh and pH of slurries were also measured.

The unspiked microcosm study highlighted the importance of organic matter to the fate of As in Arctic soils. As release under anaerobic conditions differed considerably between organic and mineral soils. Only in organic soil was an increase is D-As observed under anaerobic conditions. Further, in organic microcosms, Eh was negatively correlated with both T-As and D-As, while D-As and Fe(II) were positively correlated. This suggests that decreasing Eh and reduction of Fe(III) in Fe oxides was the mechanism causing release of As in organic microcosms under anaerobic conditions.

Microbial activity is known to enhance reductive dissolution of Fe oxides, and in organic microcosms, it is possible that more labile C and nutrients were available for anaerobic microbes than in mineral soil. In microcosms containing mineral soil, D-As decreased under anaerobic conditions, most likely as a result of sorption to Fe compounds.

A subset of microcosms in the second experiment using mineral soil was spiked with 25 $\mu g\ L^{-1}$ arsenate and arsenite (50 $\mu g\ L^{-1}$ total) to determine whether As was being sequestered under anaerobic conditions or solubilized under aerobic conditions. Results of the spiked microcosm study confirmed that T-As was being sequestered under anaerobic conditions rather than solubilized under aerobic conditions. Spiked arsenite sorbed rapidly under anaerobic conditions, while sorption of arsenate occurred at a slower rate. Further, upon initial addition of water to microcosms, spiked arsenite was converted to arsenate, and sorption of As was delayed.

Several authors have found that arsenite has a greater affinity for ferrihydrite than does arsenate (Sadiq, 1995; Raven et al., 1998; Moldovan and Hendry, 2005). Results from the spiked microcosm study suggest that under anaerobic conditions, arsenate is converted to arsenite, followed by a decrease in soluble arsenite. An extraction of total Fe and poorly crystalline Fe oxides from mineral soil showed that approximately 70% of Fe was in the form of poorly crystalline Fe oxides. Therefore, it is possible that when soluble arsenite decreased, it was sorbing to ferrihydrite in soil.

Alternatively, the formation of green rust minerals under anaerobic conditions could provide abundant binding sites for both arsenite and arsenate, thus explaining enhanced sequestration under anaerobic conditions. Analysis of soil incubated anaerobically using X-ray diffraction or scanning electron microscopy would be useful to determine if green

rust minerals are forming, and whether As sorption to these minerals is the dominant mechanism of sequestration (Su and Puls, 2001; Su and Puls, 2004). Analysis of the compounds formed under aerobic and anaerobic conditions would allow a more comprehensive understanding of As sorption in soil.

Further studies in both the field and laboratory would be useful in elucidating the processes that are occurring in the High Arctic soil ecosystem. In the field, an extended stay until the end of July would be beneficial to continue monitoring superpermafrost groundwater to determine whether T-As decreases when groundwater encounters mineral soil. Also, a complete assessment of cations and anions in groundwater would be useful for geochemical modeling purposes and as part of a further laboratory experiment to determine whether competitive ligands are contributing to As desorption in the field. A hydrologic assessment to determine the volume of water flowing through the active layer is also recommended.

In the laboratory, a further assessment in the role of microorganisms in controlling As partitioning and speciation would also be beneficial for understanding the biogeochemical cycling of As in soil of the High Arctic. Similar microcosm experiments have included amendments of a C source and nutrients to determine whether stimulation of microbes enhances As solubilization, particularly in the form of D-As (Chatain et al., 2005). In terms of industrial development, understanding the role that C and nutrient amendment plays in contaminant fate is crucial for waste management, and an experiment similar to that mentioned above would be helpful in determining the impact of organic material on As cycling in the High Arctic.

6.0 LIST OF REFERENCES

Ahmann, D., L.R. Krumholz, H.F. Hemond, D.R. Lovley, and F.M. Morel. 1997. Microbial mobilization of arsenic from sediments of the Aberjona watershed. Environmental Science & Technology 31:2923-2930.

Anawar, H.M., J. Akai, K. Komaki, H. Terao, T. Yoshioka, T. Ishizuka, S. Safiullah, and K. Kato. 2003. Geochemical occurrence of arsenic in groundwater of Bangladesh: sources and mobilization processes. Journal of Geochemical Exploration 77:109-131.

Aposhian, H.V. 1989. Biochemical toxicology of arsenic. In: Hodgson, E., Bend, J.R., Philpot, R.M. (Eds.), Reviews in Biochemical Toxicology. Elsevier, New York, pp. 265-299.

Bartrip, P. 1992. A pennurth of arsenic for rat poison - the Arsenic Act, 1851 and the prevention of secret poisoning. Medical History 36:53-69.

Bencko, V., P. Rossner, H. Havrankova, A. Puzanova, and M. Tucek. 1978. Effects of the combined action of selenium and arsenic on mice versus suspension culture of mice fibroblasts. In: Fouts, J.R., Gut, I. (Eds.), Industrial and Environmental Xenobiotics. In vitro versus in vivo biotransformation and toxicity. Excerpta Medica. Oxford, pp. 312-316.

Bennett, B., and M.J. Dudas. 2003. Release of arsenic and molybdenum by reductive dissolution of iron oxides in a soil with enriched levels of native arsenic. Journal of Environmental Engineering and Science 2:265-272.

Bliss, L.C. 1977. Truelove Lowland, Devon Island, Canada: A High Arctic Ecosystem. The University of Alberta Press, Edmonton.

Carrillo, A., and J.I. Drever. 1998. Adsorption of arsenic by natural aquifer material in the San Antonio El Triunfo mining area, Baja California, Mexico. Environmental Geology 35:251-257.

Chatain, V., R. Bayarda, F. Sanchez, P. Moszkowicz, and R. Gourdona. 2005. Effect of indigenous bacterial activity on arsenic mobilization under anaerobic conditions. Enviroment International 31:221-226.

Chattopadhyay, M.A., and M.V. Jagannadham. 2001. Maintenance of membrane fluidity in Antarctic bacteria. Polar Biology 24:321-331.

Chilvers, D.C., and Peterson, P.J. 1987. Global cycling of arsenic, p. 279– 301., *In* and T. C. Hutchison, Meema, K.M. (Eds.), eds. Lead, Mercury, Cadmium and Arsenic in the Environment. Scientific Committee on Problems of the Environment (SCOPE) 31. John Wiley & Sons, New York.

Clark, I.D., and K.G. Raven. 2004. Sources and circulation of water and arsenic in the Giant Mine, Yellowknife, NWT, Canada. Isotopes in Environmental and Health Studies 40:114-128.

Cline, J.D. 1969. Spectrophotometric determination of hydrogen sulfide in natural waters. Limnology and Oceanography 14:454-458.

Collins, J.F., and S.W. Buol. 1970. Patterns of iron and manganese precipitation under specified Eh-Ph conditions. Soil Science 110:157-166.

Corns, W.T., P.B. Stockwell, L. Ebdon, and S.J. Hill. 1993. Development of an atomic fluorescence spectrometer for hydride-forming elements. Journal of Analytical Atomic Spectroscopy 8:71-77.

Cui, W.N., L.F. del Pino, T.C. Voice, K. Chou, and D.P. Kamdem. 2005. Speciation of arsenic and chromium in the leachate from chromated copper arsenate (CCA) type C treated southern pine (Pinus spp.). Holzforschung 59:199-204.

Cummings, D.E., F.J. Caccavo, S. Fendorf, and R.F. Rosenzweig. 1999. Arsenic Mobilization by the dissimilatory Fe(III)-reducing bacterium *Shewanella alga BrY*. Environmental Science & Technology 33:723-729.

Deming, J.W. 2002. Psychrophiles and polar regions. Current Opinion in Microbiology 5:301-309.

Dixon, H.B.F. 1997. The biochemical action of arsonic acids especially as phosphate analogues. Advanced Inorganic Chemistry 44:191-227.

Dowdle, P.R., A.M. Laverman, and R.S. Oremland. 1996. Bacterial dissimilatory reduction of arsenic(V) to arsenic(III) in anoxic sediments. Applied and Environmental Microbiology 62:1664-1669.

Dzombak, D.A., and F.M.M. Morel. 1987. Development of a database for modeling adsorption of inorganics on iron and aluminum-oxides. Environmental Progress 6:133-137.

Ellenhorn, M.J. 1997. Ellenhorn's Medical Toxicology: Diagnosis and treatment of human poisoning. 2nd ed. Wilkins & Wilkins, Baltimore.

Evangelou, V.P., and Y.L. Zhang. 1995. A Review - Pyrite oxidation mechanisms and acid-mine drainage prevention. Critical Reviews in Environmental Science and Technology 25:141-199.

Fendorf, S., M.J. Eick, P.R. Grossl, and D.L. Sparks. 1997. Arsenate and chromate retention mechanisms on geothite. 1. Surface structure. Environmental Science & Technology 31:315-320.

Fendorf, S., M.J. La Force, and G. Li. 2004. Temporal changes in soil partitioning and bioaccessibility of arsenic, chromium, and lead. Journal of Environmental Quality 33:2049-2055.

Fishback, L. 2002. Establishing the provenance of catchment-derived pond sediments: Truelove Lowland, Devon Island, NU.. Ph.D. dissertation., University of Western Ontario, London, ON, Canada.

Fox, P.M., and H.E. Doner. 2003. Accumulation, release, and solubility of arsenic, molybdenum, and vanadium in wetland sediments. Journal of Environmental Quality 32:2428-2435.

Frankenberger, W.T.J. 2002. Environmental Chemistry of Arsenic, p. 1-26, *In* J. O. Nriagu, ed. Arsenic in the Environment. Dekker, New York.

Gadd, G.M. 1993. Microbial formation and transformation of organometallic and organometalloid compounds. FEMS Microbiology Reviews 11:297-316.

Goldberg, S., and C.T. Johnston. 2001. Mechanisms of arsenate adsorption on amorphous oxides evaluated using macroscopic measurements, vibrational spectroscopy, and surface complexation modeling. Journal of Colloid and Interface Science 234:204-216.

Groudeva, V.I., S.N. Groudev, and A.D. Stoyanova. 2004. Treatment of acid drainage in a uranium deposit by means of a natural wetland. Nukleonika 49:S17-S20.

Harris, S.A., H.M. French, J.A. Heginbottom, G.H. Johnston, B. Ladanyi, D.C. Sego, and R.O. van Everdingen. 1988. Glossary of permafrost and related ground-ice terms. National Research Council of Canada, Associate Committee on Geotechnical Research, Ottawa, Technical Memorandum No. 142. 156 pp.

Huang, P.M. 1975. Retention of arsenic by hydroxy-aluminium on surfaces of micaceous mineral colloids. Soil Science Society of America Proceedings 39:271-274.

Huang, R.J., Z.X. Zhuang, Y.R. Wang, Z.Y. Huang, X.R. Wang, and F.S.C. Lee. 2005. An analytical study of bioaccumulation and the binding forms of mercury in rat body using thermolysis coupled with atomic absorption spectrometry. Analytica Chimica Acta 538:313-321.

Hudson-Edwards, K.A., H.E. Jamieson, J.M. Charnock, and M.G. Macklin. 2005. Arsenic speciation in waters and sediment of ephemeral floodplain pools, Rios Agrio-Guadiamar, Aznalcollar, Spain. Chemical Geology 219:175-192.

Hug, S.J., L. Canonica, M. Wegelin, D. Gechter, and U. Von Gunten. 2001. Solar oxidation and removal of arsenic at circumneutral pH in iron containing waters. Environmental Science & Technology 35:2114-2121.

Hughes, M.F. 2002. Arsenic toxicity and potential mechanisms of action. Toxicology Letters 133:1-16.

Jackson, B.P., and W.P. Miller. 2000. Effectiveness of phosphate and hydroxide for desorption of arsenic and selenium species from iron oxides. Soil Science Society of America Journal 64:1616-1622.

Keith, V., and M. Cooper. 1974. Non-parametric design and analysis University of Ottawa Press, Ottawa.

Kenney, L.J., and J.H. Kaplan. 1988. Arsenate substitutes for phosphate in the human red blood cell sodium pump and anion exchanger. Journal of Biological Chemistry 263:7954-7960.

Kim, J., J. Nriagu, and S. Haack. 2000. Carbonate ions and arsenic dissolution by groundwater. Environmental Science & Technology 34:3094-3100.

Kirk, G.A. 2004. The Biogeochemistry of Submerged Soils. John Wiley & Sons, Ltd., Chichester, West Sussex, England.

Kocar, B., K. Tufano, Y. Masui, B. Stewart, M. Herbel, and S. Fendorf. 2005. Arsenic mobilization influenced by iron reduction and sulfidogenesis. Geochimica Et Cosmochimica Acta 69:A466-A466.

Koons, R.D., and D.M. Grant. 2002. Compositional variation in bullet lead manufacture. Journal of Forensic Sciences 47:950-958.

Kostka, J.E., B. Thamdrup, R. Nohr Glud, and D.E. Canfield. 1999. Rates and pathways of carbon oxidation in permanently cold Arctic sediments. Marine Ecology Progress Series 180:7-21.

Landsberger, S., S.J. Vermette, and L.A. Barrie. 1990. Multielemental composition of the Arctic aerosols. Journal of Geophysical Research-Atmospheres 95:3509-3513.

Laverman, A.M., J. Switzer-Blum, J.K. Schaefer, E.J.P. Phillips, D.R. Lovley, and R.S. Oremland. 1995. Growth of strain SES-3 with arsenate and other diverse electron acceptors. Applied and Environmental Microbiology 61:3556-3561.

Lefroy, R.D.B., S.S.R. Samosir, and G.J. Blair. 1993. The Dynamics of sulfur, phosphorus and iron in flooded soils as affected by changes in Eh and pH. Australian Journal of Soil Research 31:493-508.

Lengke, M.F., and R.N. Tempel. 2005. Geochemical modeling of arsenic sulfide oxidation kinetics in a mining environment. Geochimica Et Cosmochimica Acta 69:341-356.

Lien, H.L., and R.T. Wilkin. 2005. High-level arsenite removal from groundwater by zero-valent iron. Chemosphere 59:377-386.

Lin, X.L., D. Alber, and R. Henkelmann. 2004. Elemental contents in Napoleon's hair cut before and after his death: did Napoleon die of arsenic poisoning? Analytical and Bioanalytical Chemistry 379:218-220.

Lovley, D.R. 1991. Dissimilatory Fe(III) and Mn(IV) reduction. Microbiological Reviews 55:259-287.

Mace, I.S. 1998. A study of arsenic contamination from the Royal Oak Giant Mine, Yellowknife, Northwest Territories., Royal Military College of Canada, Kingston, ON.

Manning, B.A., S. Fendorf, and S. Goldberg. 1998. Surface structures and stability of arsenic(III) on geothite: spectroscopic evidence for inner-sphere complexes. Environmental Science & Technology 32:2383-2388.

Manning, B.A., and S. Goldberg. 1996. Modeling arsenate competitive adsorption on kaolinite, montmorillonite and illite. Clays and Clay Minerals 44:609-623.

Masscheleyn, P.H., R.D. Delaune, and W.H. Patrick. 1991. Effect of redox potential and Ph on arsenic speciation and solubility in a contaminated soil. Environmental Science & Technology 25:1414-1419.

McGeehan, S.L., S.E. Fendorf, and D.V. Naylor. 1998. Alteration of arsenic sorption in flooded-dried soils. Soil Science Society of America Journal 62:828-833.

McKenzie, R.M. 1981. The surface charge on manganese dioxides. Australian Journal of Soil Research 19:41-50.

Merwin, I., P.T. Pruyne, J.G. Ebel, K.L. Manzell, and D.J. Lisk. 1994. Persistence, phytotoxicity, and management of arsenic, lead and mercury residues in old orchard soils of New York State. Chemosphere 29:1361-1367.

Moldovan, B.J., and M.J. Hendry. 2005. Characterizing and quantifying controls on arsenic solubility over a pH range of 1 - 11 in a uranium mill-scale experiment. Environmental Science & Technology 39:4913-4920.

Morel, F.M.M., and J.G. Hering. 1993. Principles and applications of aquatic chemistry. Wiley, New York.

Muc, M., and L.C. Bliss. 1977. Plant communities of Truelove Lowland, p. 143-153, *In* L. C. Bliss, ed. Truelove Lowland, Devon Island: A High Arctic Ecosystem. The University of Alberta Press, Edmonton, AB.

National Research Council, A.a.A.-F.C. 1998. The Canadian System of Soil Classification, Third Edition. Third ed. NRC Research Press, Ottawa.

Ndiokwere, C.L. 1985. The dispersal of arsenic, chromium and copper from a wood treatment factory, and their effect on soil, vegetation and crops. International Journal of Environmental Studies 24:231-237.

Newman, D.K., D. Ahmann, and F.M.M. Morel. 1998. A brief review of microbial arsenate respiration. Geomicrobiology Journal 15:255-268.

Nordstrom, D.K. 2002. Public health - Worldwide occurrences of arsenic in ground water. Science 296:2143-2145.

Nriagu, J.O. 1994. Arsenic in the environment. Wiley, New York.

O'Connor, R., M. O'Connor, K. Irgolic, J. Sabrsula, H. Gurleyuk, R. Brunette, C. Howard, J. Garcia, and J. Brien. 2005. Transformations, air transport, and human impact of arsenic from poultry litter. Environmental Forensics 6:83-89.

Oremland, R.S., P.R. Dowdle, S. Hoeft, J.O. Sharp, J.K. Schaefer, L.G. Miller, J.S. Blum, R.L. Smith, N.S. Bloom, and D. Wallschlaeger. 2000. Bacterial dissimilatory reduction of arsenate and sulfate in meromictic Mono Lake, California. Geochimica Et Cosmochimica Acta 64:3073-3084.

Oremland, R.S., and J.F. Stolz. 2003. The Ecology of Arsenic. Science 300:939-944.

Pfeifer, H.R., A. Gueye-Girardet, D. Reymond, C. Schlegel, E. Temgoua, D.L. Hesterberg, and J.W.Q. Chou. 2004. Dispersion of natural arsenic in the Malcantone watershed, Southern Switzerland: field evidence for repeated sorption-desorption and oxidation-reduction processes. Geoderma 122:205-234.

Poikolainen, J., E. Kubin, J. Piispanen, and J. Karhu. 2004. Estimation of the long-range transport of mercury, cadmium, and lead to Northern Finland on the basis of moss surveys. Arctic Antarctic and Alpine Research 36:292-297.

Quinton, W.L., S.K. Carey, and N.T. Goeller. 2004. Snowmelt runoff from northern alpine tundra hillslopes: major processes and methods of simulation. Hydrology and Earth System Sciences 8:877-890.

Randall, S.R., D.M. Sherman, and K.V. Ragnarsdottir. 2001. Sorption of As(V) on green rust (Fe-4(II)Fe-2(III)(OH)(12)SO4 center dot 3H(2)O) and lepidocrocite (gamma-FeOOH): Surface complexes from EXAFS spectroscopy. Geochimica Et Cosmochimica Acta 65:1015-1023.

Rattner, H. 1943. The treatment of early syphilis - By the concurrent administration of arsenic and bismuth in a period of five days. Journal of the American Medical Association 122:986-989.

Raven, K.P., A. Jain, and R.H. Loeppert. 1998. Arsenite and arsenate adsorption on ferrihydrite: Kinetics, equilibrium, and adsorption envelopes. Environmental Science & Technology 32:344-349.

Reichl, F.X., L. Szinicz, H. Kreppel, and W. Forth. 1988. Effect of arsenic on carbohydrate metabolism after single or repeated injection in guinea pigs. Archives of Toxicology 62:473-475.

Renault, P., and P. Stengel. 1994. Modeling oxygen diffusion in aggregated soils: I. Anaerobiosis inside the aggregates. Soil Science Society of America Journal 58:1017-1023.

Rittle, K.A., J.I. Drever, and P.J.S. Colberg. 1995. Precipitation of arsenic during bacterial sulfate reduction. Geomicrobiology Journal 13:1-11.

Rochette, E.A., B. Bostick, G.C. Li, and S. Fendorf. 2000. Kinetics of arsenate reduction by dissolved sulfide. Environmental Science & Technology 34:4714-4720.

Rochette, E.A., G.C. Li, and S.E. Fendorf. 1998. Stability of arsenate minerals in soil under biotically generated reducing conditions. Soil Science Society of America Journal 62:1530-1537.

Rodriguez, V.M., M.E. Jimenez-Capdeville, and M. Giordano. 2003. The effects of arsenic exposure on the nervous system. Toxicology Letters 145:1-18.

Romero, F.M., M.A. Armienta, and A. Carrillo-Chavez. 2004. Arsenic sorption by carbonate-rich aquifer material, a control on arsenic mobility at Zimapan, Mexico. Archives of Environmental Contamination & Toxicology 47:1-13.
Rosen, B.P. 2002. Biochemistry of arsenic detoxification. FEMS Letters 529:86-92.
Roy, P., and A. Saha. 2002. Metabolism and toxicity of arsenic: A human carcinogen. Current Science 82:38-45.
Ryden, B.E. 1977. Hydrology of Truelove Lowland, p. 107-137, *In* L. C. Bliss, ed. Truelove Lowland, Devon Island, Canada: A High Arctic Ecosystem. The University of Alberta Press, Edmonton.
Sadiq, M. 1990. Arsenic chemistry in marine environments: A comparison between theoretical and field observations. Marine Chemistry 31:285-297.
Sadiq, M. 1995. Arsenic chemistry in soils: An overview of thermodynamic predictions and field observations. Water Air and Soil Pollution 93:117-136.
Scott, N., K.M. Hatlelid, N.E. MacKenzie, and D.E. Carter. 1993. Reactions of arsenic (III) and arsenic (V) species with glutathione. Chemical Research in Toxicology 6:102-106.
Shaw, G.E. 1991. Aerosol Chemical-Components in Alaska Air Masses .1. Aged Pollution. Journal of Geophysical Research-Atmospheres 96:22357-22368.
Sheridan, P.P., H. Lanasik, J.M. Coombs, and J.E. Brenchley. 2000. Approaches for deciphering the structural basis of low temperature enzyme activity. Biochimica et Biochimica Acta (BBA)/Protein Structure and Molecula Enzymology 1543:417-433.
Shevchenko, V., A. Lisitzin, A. Vinogradova, and R. Stein. 2003. Heavy metals in aerosols over the seas of the Russian Arctic. The Science of the Total Environment 306:11-25.
Shigeno, K., K. Naito, N. Sahara, M. Kobayashi, S. Nakamura, S. Fujisawa, K. Shinjo, A. Takeshita, R. Ohno, and K. Ohnishi. 2005. Arsenic trioxide therapy in relapsed or refractory Japanese patients with acute promyelocytic leukemia: Updated outcomes of the phase II study and postremission therapies. International Journal of Hematology 82:224-229.
Smedley, P.L., and D.G. Kinniburgh. 2002. A review of the source, behaviour and distribution of arsenic in natural waters. Applied Geochemistry 17:517-568.
Smith, A.H., C. Hopenhayn-Rich, M.N. Bates, H.M. Goeden, I. Hertz-Picciotto, H.M. Duggan, R. Wood, M.J. Kosnett, and M.T. Smith. 1992. Cancer risks from arsenic in drinking water. Environmental Health Perspectives 97:259-267.
Sparks, D.L. 2003. Environmental Soil Chemistry. Second ed. Academic Press: An imprint of Elsevier Science, San Diego, California.
Sposito, G. 1984. The Surface Chemistry of Soils. Oxford University Press; Oxford [Oxfordshire]: Clarendon Press, New York.
Stapleton, R.D., Z.L. Sabree, A.V. Palumbo, C.L. Moyer, A.H. Devol, Y. Roh, and J.Z. Zhou. 2005. Metal reduction at cold temperatures by Shewanella isolates from various marine environments. Aquatic Microbial Ecology 38:81-91.
Stumm, W. 1992. Chemistry of the solid-water interface John Wiley & Sons, New York.
Stumm, W., and J.J. Morgan. 1996. Aquatic chemistry: chemical equilibria and rates in natural waters. 3rd ed. Wiley, New York.

Su, C., and R.W. Puls. 2001. Arsenate and arsenite removal by zerovalent iron: Effects of phosphate, silicate, carbonate, borate, sulfate, chromate, molybdate, and nitrate, relative to chloride. Environmental Science & Technology 35:4562-4568.

Su, C.M., and R.W. Puls. 2004. Significance of iron(II,III) hydroxycarbonate green rust in arsenic remediation using zerovalent him in laboratory column tests. Environmental Science & Technology 38:5224-5231.

Swiggart, R.C., Whitehea.Cj, F.E. Kellogg, and A. Curley. 1972. Wildlife kill resulting from misuse of arsenic acid herbicide. Bulletin of Environmental Contamination and Toxicology 8:122-&.

Szinicz, L., and W. Forth. 1988. Effects of As_2O_3 on gluconeogenesis. Archives of Toxicology 61:444-449.

Tadanier, C.J., M.E. Schreiber, and J.W. Roller. 2005. Arsenic mobilization through microbially mediated deflocculation of ferrihydrite. Environmental Science & Technology 39:3061-3068.

Takagai, Y., and S. Igarashi. 2003. Simultaneous determination of Iron(II) and Iron(III) by micellar electrokinetic chromatography using an off-line selective complexing reaction. Analytical Sciences 19:1207-1209.

Takahashi, Y., R. Minamikawa, K.H. Hattori, K. Kurishima, N. Kihou, and K. Yuita. 2004. Arsenic behavior in paddy fields during the cycle of flooded and non-flooded periods. Environmental Science & Technology 38:1038-1044.

Thoral, S., J. Rose, J.M. Garnier, A. Van Geen, P. Refait, A. Traverse, E. Fonda, D. Nahon, and J.Y. Bottero. 2005. XAS study of iron and arsenic speciation during Fe(II) oxidation in the presence of As(III). Environmental Science & Technology 39:9478-9485.

Turpeinen, R., M. Pantsar-Kallio, M. Haggblom, and T. Kairesalo. 1999. Influence of microbes on the mobilization, toxicity and biomethylation of arsenic in soil. Science of the Total Environment 236:173-180.

USEPA. 1996. Method 1632: Inorganic Arsenic in Water by Hydride Generation Quartz Furnace Atomic Absorption, Washington.

USEPA. 1998. Guidelines establishing test procedures for the analysis of pollutants, 40 CFR 136. U.S. Gov. Print Office, Washington, DC, U.S.A.

Vahter, M., and G. Concha. 2001. Role of metabolism in arsenic toxicity. Pharmacology & Toxicology 89:1-5.

Vanysek, P. 1995. Electrochemical series., p. 8-21, *In* D. R. Lide, ed. CRC handbook of chemistry and physics, 76th Ed. CRC Press, Boca Raton, FL.

Walker, B.D., and T.W. Peters. 1977. Soils of Truelove Lowland and Plateau, p. 31-60, *In* L. C. Bliss, ed. Truelove Lowland, Devon Island, Canada: A High Arctic Ecosystem. University of Alberta Press, Edmonton.

Watras, C.J., K.A. Morrison, A. Kent, N. Price, O. Regnell, C. Eckley, H. Hintelmann, and T. Hubacher. 2005. Sources of methylmercury to a wetland-dominated lake in northern Wisconsin. Environmental Science & Technology 39:4747-4758.

WHO. 2001. Environmental Health Criteria 224: Arsenic and arsenic compounds, 2nd ed. World Health Organization, Geneva.

Williams, P.J., and M.W. Smith. 1989. The Frozen Earth: Fundamentals of Geocryology. Cambridge University Press, Cambridge.

Yan, X.P., R. Kerrich, and M.J. Hendry. 2000. Distribution of arsenic(III), arsenic(V) and total inorganic arsenic in porewaters from a thick till and clay-rich aquitard

sequence, Saskatchewan, Canada. Geochimica & Cosmochimica Acta. 62:2637-2648.

Yang, J.K., M.O. Barnett, J.L. Zhuang, S.E. Fendorf, and P.M. Jardine. 2005. Adsorption, oxidation, and bioaccessibility of As(III) in soils. Environmental Science & Technology 39:7102-7110.

Zhender, A.J.B., and W. Stumm. 1988. Geochemistry and biogeochemistry of anaerobic habitats., p. 1-38, *In* A. J. B. Zhender, ed. Biology of anaerobic microorganisms. Wiley, New York.

Zobrist, J., P.R. Dowdle, J.A. Davis, and R.S. Oremland. 2000. Mobilization of arsenite by dissimilatory reduction of adsorbed arsenate. Environmental Science & Technology 34:4747-4753.

APPENDIX A

According to United States Environmental Protection Agency (USEPA) protocol, Quality Control and Quality Assurance (QA/QC) analysis of sampling and analytical measurement of arsenic was undertaken. Method 1632: Inorganic Arsenic in Water by Hydride Generation Quartz Furnace Atomic Absorption (USEPA, 1996) and *40 CFR 136* Guidelines establishing test procedures for the analysis of pollutants (USEPA, 1998) outline the necessary procedures for ensuring analytical integrity. While EPA Method 1632 outlines procedures for analysis of As using Hydride Generation Quartz Furnace Atomic Absorption, the method employed using the Millenium Excalibur Atomic Fluorescence System™ (AFS) is based on the same mechanism of hydride generation.

The QA/QC protocol for this study involved determining the method detection limit for the AFS, ensuring sampling and analysis equipment was neither contributing nor sorbing As, and assessing detection reliability on an ongoing basis.

A.1 Establishment of method detection limit (MDL)

The method detection limit (MDL) for the Millenium Excalibur Atomic Fluorescence System™ (AFS) was determined using United States Environmental Protection Agency (USEPA) Method 40 CFR Part 136: "Guidelines for Establishing Test Procedures for the Analysis of Pollutants". The USEPA defines the *method detection limit* as "the minimum concentration that can be determined with 99% confidence that the true concentration is greater than zero." (USEPA, 1998). The method detection limit for the AFS is calculated as follows:

$$MDL = (t_{n-1, 0.01}) \cdot sd \quad (A.1)$$

Where the Student's t-value at the 0.01 level of probability for 16 samples is 2.602, and 'sd' is the standard deviation of 16 samples of a particular concentration. According to EPA protocol, the concentration used for determination of the MDL should be approximately three times the standard deviation of seven blanks. The standard deviation of seven blanks run on the AFS was 0.0132, and the concentration of 0.04 μg L^{-1} was analyzed for this reason (Table A.1). For samples analyzed using the AFS, the method detection limit was 0.011 μg As L^{-1} with n = 16 samples at 0.04 μg L^{-1}, and the standard deviation was 0.0043 μg L^{-1}. Mean recovery of samples used to determine the MDL is 101.7%.

A.2 Equipment blanks

Analysis of trace metals requires that materials in the sampling equipment neither contribute nor sorb As. This was tested by passing MilliΩ ultrapure water (blank) and an As solution of 5 μg L^{-1} through syringes and filters. Storage containers including Falcon® tubes, Nalgene® bottles, and glass serum bottles were placed in a rotating shaker for one week containing MilliΩ ultrapure water and an As solution of 5 μg L^{-1} (Table A.2).

Table A.1 AFS detected concentration in duplicate samples for determination of the method detection limit.

Sample #	Concentration ($\mu g\ L^{-1}$)	AFS output ($\mu g\ L^{-1}$)	% Recovery
1	0.04	0.0431	107.8371
2	0.04	0.0456	114.1114
3	0.04	0.0351	87.87172
4	0.04	0.0432	108.1478
5	0.04	0.0480	120.1491
6	0.04	0.0469	117.4745
7	0.04	0.0395	98.78613
8	0.04	0.0415	103.9432
9	0.04	0.0325	81.49797
10	0.04	0.0422	105.6555
11	0.04	0.0374	93.57327
12	0.04	0.0380	95.01687
13	0.04	0.0365	91.40991
14	0.04	0.0412	103.1756
15	0.04	0.0422	105.6555
16	0.04	0.0374	93.57327
		Average: 0.0407	101.7424
		St. Dev.: 0.0043	
		Variance: $1.868 \cdot 10^{-5}$	

Table A.2 Equipment blanks and sorption test.

Equipment	Rep	True conc. (ug L^{-1})	Detected conc. (ug L^{-1})	Recovery (%)
Syringe	1	0	0.01	*
	2	0	0.02	*
	3	0	-0.02	*
	1	5	5.15	103
	2	5	5.07	101.4
	3	5	5.02	100.4
Filter	1	0	0.03	*
	2	0	0.04	*
	3	0	-0.02	*
	1	5	4.96	99.2
	2	5	4.98	99.6
	3	5	4.95	99
Nalgene bottle	1	0	0.03	*
	2	0	0.02	*
	3	0	0.03	*
	1	5	5.1	102
	2	5	5.07	101.4
	3	5	4.99	99.8
Glass serum bottle	1	0	-0.01	*
	2	0	0.02	*
	3	0	0.03	*
	1	5	5.13	102.6
	2	5	5.07	101.4
	3	5	5.09	101.8
Falcon tube	1	0	0.02	*
	2	0	-0.03	*
	3	0	-0.01	*
	1	5	5.12	102.4
	2	5	5.15	103
	3	5	5.2	104
			Average:	101.4

A.3 Ongoing precision in field and microcosm samples

Ongoing precision was assessed during analysis of samples from the field and microcosms including sample duplicates and blanks (Table A.3). For approximately each 10 to 12 samples analyzed, one duplicate was run as well as a random standard. Relative percent difference is presented as well as percent recovery of standard solution for each set of samples. Field blanks were carried in the field and treated in the same way as a field sample and returned an average concentration of 0.02 μg L^{-1} (SE = 0.0001).

Relative percent difference between a sample and a duplicate is calculated as follows:

$$\text{Re}\textit{lative percent difference} = \left(\frac{|S1 - S2|}{(S1 + S2)} \right) * 200 \qquad \text{(A.2)}$$

where S1 is the sample and S2 is the duplicate.

Percent recovery is determined using the following formula:

$$\%\ \text{Recovery} = \left(\frac{\text{observed concentration}}{\text{known concentration}} \right) * 100 \qquad (3)$$

Table A.3 Relative percent difference between duplicates and percent recovery for snow, meltwater, groundwater and microcosm samples.

Sample Batch	Sample/ Reference Material	Date Collected	Julian Date	Analyte	MATRIX DUPLICATES Rep 1 (ug L^{-1})	Rep 2 (ug L^{-1})	Mean (ug L^{-1})	Abs value	RPD (%)	TRUE conc. (ug L^{-1})	Observed conc. (ug L^{-1})	Recovery (%)
Snow & Meltwater	121	12-Jun-04	163	T-As	0.042	0.031	0.0365	0.011	30.137	0.5	0.53	106.000
	152	15-Jun-04	166	D-As	0.61	0.72	0.665	0.11	16.541	0	0.02	*
	261	15-Jun-04	166	D-As	0.02	0.032	0.026	0.012	46.154	1.5	1.5	100.000
	252	17-Jun-04	168	D-As	0.012	0.011	0.0115	0.001	8.696	2	2.08	104.000
	233	20-Jun-04	171	D-As	0.063	0.034	0.0485	0.029	59.794	1	0.96	96.000
	274	25-Jun-04	176	T-As	0.011	0.012	0.0115	0.001	8.696	1	0.98	98.000
	274	25-Jun-04	176	D-As	0.009	0.002	0.0055	0.007	127.273	2	1.99	99.500
								Average:	42.470		Average:	100.583
Groundwater	563	29-Jun-04	179	T-As	0.019	0.033	0.026	0.014	53.846	0.6	0.68	113.333
	571	1-Jul-04	181	T-As	0.17	0.166	0.168	0.004	2.381	0.3	0.37	123.333
	563	4-Jul-04	184	T-As	0.05	0.045	0.0475	0.005	10.526	0	0.015	*
	571	6-Jul-04	186	T-As	0.29	0.3	0.295	0.01	3.390	0.3	0.3	100.000
	532	29-Jun-04	179	D-As	0.027	0.052	0.0395	0.025	63.291	0.03	0.05	166.667
	572	1-Jul-04	181	D-As	0.0104	0.013	0.0117	0.0026	22.222	0.09	0.09	100.000
	523	4-Jul-04	184	D-As	0.046	0.049	0.0475	0.003	6.316	0.06	0.07	116.667
	551	6-Jul-04	186	D-As	0.039	0.02	0.0295	0.019	64.407	0.12	0.12	100.000
	532	29-Jun-04	179	As(V)	11.21	11.6	11.405	0.39	3.420	0	0.01	*
	571	1-Jul-04	181	As(V)	0.432	0.461	0.4465	0.029	6.495	0.03	0.04	133.333
	553	4-Jul-04	184	As(V)	1.68	1.71	1.695	0.03	1.770	0.3	0.04	13.333
	511	6-Jul-04	186	As(V)	0.16	0.17	0.165	0.01	6.061	0.6	0.06	10.000
	563	29-Jun-04	179	As(III)	0.095	0.076	0.0855	0.019	22.222	0.9	0.1	11.111
	562	1-Jul-04	181	As(III)	0.127	0.086	0.1065	0.041	38.498	0.12	0.11	91.667

Sample Batch	Sample/ Reference Material	Date Collected	Julian Date	Analyte	MATRIX DUPLICATES Rep 1 (ug L^{-1})	Rep 2 (ug L^{-1})	Mean (ug L^{-1})	Abs value	RPD (%)	TRUE conc. (ug L^{-1})	Observed conc. (ug L^{-1})	Recovery (%)
	591	4-Jul-04	184	As(III)	0.243	0.135	0.189	0.108	57.143	0.06	0.07	116.667
	591	6-Jul-04	186	As(III)	0.56	0.53	0.545	0.03	5.505	0.09	0.09	100.000
								Average:	22.968		Average:	92.579
Pristine	M173	28-Nov-04		T-As	0.84	0.86	0.85	0.02	2.352941176	1	1	100.000
Microcosms	M292	28-Nov-04		T-As	1.5	1.45	1.475	0.05	3.389830508	2	1.92	96.000
	M191	28-Nov-04		D-As	0.22	0.22	0.22	0	0	1	1.15	115.000
	M293	28-Nov-04		D-As	0.42	0.42	0.42	0	0	0.5	0.48	96.000
	O172	30-Nov-04		T-As	0.22	0.18	0.2	0.04	20	0	0.01	*
	O253	30-Nov-04		T-As	0.7	0.68	0.69	0.02	2.898550725	1	1.09	109.000
	O171	30-Nov-04		D-As	0.65	0.67	0.66	0.02	3.03030303	0	0.03	*
	O292	30-Nov-04		D-As	0.4	0.44	0.42	0.04	9.523809524	0.5	0.54	108.000
	M163	3-Dec-04		T-As	0.46	0.48	0.47	0.02	4.255319149	1	1.03	103.000
	M273	3-Dec-04		T-As	0.15	0.18	0.165	0.03	18.18181818	0	0.05	*
	M153	3-Dec-04		D-As	0.42	0.39	0.405	0.03	7.407407407	0.5	0.6	120.000
	M263	3-Dec-04		D-As	0.29	0.26	0.275	0.03	10.90909091	0	0.08	*
	O172	5-Dec-04		T-As	0.31	0.37	0.34	0.06	17.64705882	1	0.93	93.000
	O291	5-Dec-04		T-As	1.41	1.48	1.445	0.07	4.844290657	0	0.004	*
	O162	5-Dec-04		D-As	0.46	0.59	0.525	0.13	24.76190476	0.5	0.46	92.000
	O251	5-Dec-04		D-As	0.1	0.16	0.13	0.06	46.15384615	1.5	1.63	108.667
	M151	8-Dec-04		T-As	0.85	0.9	0.875	0.05	5.714285714	1	1.02	102.000
	M271	8-Dec-04		T-As	4.36	4.2	4.28	0.16	3.738317757	4	3.75	93.750
	M191	8-Dec-04		D-As	0.73	0.72	0.725	0.01	1.379310345	0.5	0.46	92.000
	M291	8-Dec-04		D-As	0.22	0.2	0.21	0.02	9.523809524	1.5	1.63	108.667
	O191	10-Dec-04		T-As	0.94	0.86	0.9	0.08	8.888888889	2	1.96	98.000
	O293	10-Dec-04		T-As	0.32	0.19	0.255	0.13	50.98039216	1.5	1.41	94.000
	O172	10-Dec-04		D-As	0.15	0.12	0.135	0.03	22.22222222	1	0.91	91.000
	O263	10-Dec-04		D-As	0.63	0.54	0.585	0.09	15.38461538	0	-0.03	*
	M172	8-Jan-05		T-As	0.73	0.69	0.71	0.04	5.633802817	1	1.1	110.000
	M291	8-Jan-05		T-As	0.22	0.33	0.275	0.11	40	0	0.04	*

Sample Batch	Sample/ Reference Material	Date Collected	Julian Date	Analyte	MATRIX DUPLICATES					TRUE conc. (ug L^{-1})	Observed conc. (ug L^{-1})	Recovery (%)
					Rep 1 (ug L^{-1})	Rep 2 (ug L^{-1})	Mean (ug L^{-1})	Abs value	RPD (%)			
	M153	8-Jan-05		D-As	0.97	1.07	1.02	0.1	9.803921569	2	1.99	99.500
	M272	8-Jan-05		D-As	0.16	0.16	0.16	0	0	0	0.06	*
	O152	11-Jan-05		T-As	0.74	0.77	0.755	0.03	3.973509934	3	2.79	93.000
	O272	11-Jan-05		T-As	0.89	0.88	0.885	0.01	1.129943503	0	0.04	*
	O161	11-Jan-05		D-As	0.65	0.62	0.635	0.03	4.724409449	1	1.07	107.000
	O271	11-Jan-05		D-As	0.42	0.42	0.42	0	0	2	2.12	106.000
								Average:	11.20167501		Average:	101.547
Spiked Microcosms	11N3	27-May-05		T-As	10.89	11.14	11.015	0.25	2.26963232	0	-0.07	*
	12S1	27-May-05		T-As	25.78	23.94	24.86	1.84	7.401448109	15	15.33	102.200
	21N2	2-Jun-05		D-As	0.71	0.72	0.715	0.01	1.398601399	1	0.97	97.000
	22S2	2-Jun-05		T-As	18.36	18.4	18.38	0.04	0.217627856	25	26.56	106.240
	32N3	9-Jun-05		T-As	2.38	2.38	2.38	0	0	4	4.4	110.000
	32S3	9-Jun-05		D-As	2.08	2.07	2.075	0.01	0.481927711	10	9.81	98.100
	42N2	16-Jun-05		T-As	4.42	4.54	4.48	0.12	2.678571429	1	0.93	93.000
	41S2	16-Jun-05		D-As	1.84	2.4	2.12	0.56	26.41509434	9	9.36	104.000
	51N1	23-Jun-05		D-As	0.37	0.4	0.385	0.03	7.792207792	1.5	1.65	110.000
	51S1	23-Jun-05		T-As	14.43	14.56	14.495	0.13	0.896860987	12	12.65	105.417
								Average:	4.955197194		Average:	102.884

APPENDIX B

The derivation for an alternative method for calculating concentrations of Fe(III) and Fe(II) in solution is as follows:

$$Abs_{450} = Fe(III) + Fe(II) \tag{B.1}$$

$$Abs_{405} = Fe(III) + \left(\frac{m_{abs405nm}}{m_{abs450nm}}\right) Fe(II) \tag{B.2}$$

$$Abs_{450} - Abs_{405} = \left[1 - \left(\frac{m_{abs405nm}}{m_{abs450nm}}\right)\right] Fe(II) \tag{B.3}$$

$$Fe(II) = \frac{Abs_{450} - Abs_{405}}{1 - \left(\frac{Fe(II)m_{abs405nm}}{Fe(II)m_{abs450nm}}\right)} \tag{B.4}$$

$$Abs_{450} = Fe(III) + \frac{1}{\left[1 - \left(\frac{m_{abs405nm}}{m_{abs450nm}}\right)\right]} \left(Abs_{450} - Abs_{405}\right) \tag{B.5}$$

$$Fe(III) = Abs_{450} - \left[\left(\frac{1}{\left[1 - \left(\frac{Fe(II)m_{abs405nm}}{Fe(II)m_{abs450nm}}\right)\right]}\right)\left(Abs_{450} - Abs_{405}\right)\right] \tag{B.6}$$

where Abs_{450} is the absorbance of a solution containing both Fe(III) and Fe(II) at 450 nm; Abs_{405} is the absorbance of a solution containing both Fe(III) and Fe(II) at 405 nm; $m_{abs405nm}$ is the slope of the standard curve of a mixed solution at 405 nm; and $m_{abs450nm}$ is the slope of the standard curve of a mixed solution at 450 nm.

The following steps outline the calculation of [Fe(II)] and [Fe(III)]:

1) Standard curves for Fe(III)-DFB and Fe(II)-Bap at both 405 and 450 nm are obtained and expressed in the form $y = mx$ for each curve where y represents absorbance, m is the slope of the trendline, x is the concentration in solution, and b is the intercept. NB: The standard curves for Fe(II) at 405 and 450 nm must

have their intercept set to zero; the standard curves for Fe(III) should not be set to zero. Four different slope coefficients are available from standard curves: Fe(III)$m_{abs405nm}$, Fe(III)$m_{abs450nm}$, Fe(II)$m_{abs405nm}$ and Fe(II)$m_{abs450nm}$. A second set of mixed standards must be prepared with known concentrations of Fe(III)-DFB and Fe(II)-Bathophen at different concentrations. Mixed standards are analyzed spectrophotometrically at 405 and 450 nm. "Abs_{405}" and "Abs_{450}" represent absorption of mixed standards at each wavelength.

2) Separate absorption of Fe(II) and Fe(III) in mixed standards must now be differentiated using the following formulas:

$$Fe(III) = Abs_{450nm} - \left[\left(\frac{1}{1-\left(\frac{Fe(II)m_{abs405nm}}{Fe(II)m_{abs450nm}}\right)}\right)\left(Abs_{450nm} - Abs_{405nm}\right)\right] \quad \text{(B.7)}$$

$$Fe(II) = \frac{Abs_{450nm} - Abs_{405nm}}{1-\left(\frac{Fe(II)m_{abs405nm}}{Fe(II)_{mabs450nm}}\right)} \quad \text{(B.8)}$$

3) Plot separate graphs for Fe(III) and Fe(II) with calculated absorbance (equations 3.2 and 3.3) on the y-axis and the actual concentration in solution on the x-axis. Add a trend line to obtain the linear equation $y = mx + b$.

4) To determine [Fe(III)] and [Fe(II)] concentration in samples, rearrange the linear equation to solve for x using the graphs produced in step 3.

APPENDIX C

Table C.1 All data from analysis of snow, meltwater and superpermafrost groundwater from Truelove Lowland, Devon Island, NU.

Matrix	Site	Rep/Well	Date	Julian day	Water column** (cm)	T-As (ng L^{-1})	D-As (ng L-1)	As V (ng L-1)	As (III) (ng L-1)	pH	measured Eh (mV)	Temperature (°C)	Fe(III) (µM)	Fe(II) (µM)	Total Fe (µM)	calculated Eh (mV)***	S^{2-} (µM)
S	7	-	12-Jun-04	163	-	33.25	28.62	-	-	10.27	-	-	-	-	-	-	-
S	5	-	12-Jun-04	163	-	42.88	21.28	-	-	10.45	-	-	-	-	-	-	-
S	6	-	12-Jun-04	163	-	30.46	24.22	-	-	10.37	-	-	-	-	-	-	-
S	7	-	15-Jun-04	166	-	38.69	16.44	-	-	10.51	-	-	-	-	-	-	-
S	6	-	15-Jun-04	166	-	23.54	23.47	-	-	10.22	-	-	-	-	-	-	-
S	5	-	15-Jun-04	166	-	29.66	61.00	-	-	10.33	-	-	-	-	-	-	-
S	7	-	17-Jun-04	168	-	23.86	17.14	-	-	8.86	-	-	-	-	-	-	-
S	6	-	17-Jun-04	168	-	19.42	24.49	-	-	9.38	-	-	-	-	-	-	-
S	5	-	17-Jun-04	168	-	22.27	32.22	-	-	9.35	-	-	-	-	-	-	-

Matrix	Site	Rep/Well	Date	Julian day	Water column** (cm)	T-As (ng L-1)	D-As (ng L-1)	As V (ng L-1)	As (III) (ng L-1)	pH	measured Eh (mV)	Temperature (°C)	Fe(III) (µM)	Fe(II) (µM)	Total Fe (µM)	calculated Eh (mV)***	S^{2-} (µM)
MW	7	-	15-Jun-04	166	-	13.31	34.12	-	-	8.97	-	7.9	-	-	-	-	-
MW	6	-	15-Jun-04	166	-	10.54	23.53	-	-	8.22	-	8.9	-	-	-	-	-
MW	5	-	15-Jun-04	166	-	17.03	19.26	-	-	8.7	-	10.9	-	-	-	-	-
MW	5	-	17-Jun-04	168	-	9.62	11.71	-	-	7.63	-	7.8	-	-	-	-	-
MW	6	-	17-Jun-04	168	-	15.02	28.68	-	-	7.32	-	8.6	-	-	-	-	-
MW	7	-	17-Jun-04	168	-	34.71	12.29	-	-	9.12	-	10.3	-	-	-	-	-
MW	9	-	20-Jun-04	171	-	11.91	18.59	-	-	8.59	-	8	-	-	-	-	-
MW	7	-	20-Jun-04	171	-	16.55	17.79	-	-	7.5	-	7.59	-	-	-	-	-
MW	6	-	20-Jun-04	171	-	9.99	18.22	-	-	8.47	-	8.93	-	-	-	-	-
MW	5	-	20-Jun-04	171	-	17.97	9.30	-	-	8.94	-	7.98	-	-	-	-	-
MW	4	-	20-Jun-04	171	-	20.29	11.71	-	-	8.64	-	8.99	-	-	-	-	-

Matrix	Site	Rep/Well	Date	Julian day	Water column** (cm)	T-As (ng L^{-1})	D-As (ng L-1)	As V (ng L-1)	As (III) (ng L-1)	pH	measured Eh (mV)	Temperature (°C)	Fe(III) (µM)	Fe(II) (µM)	Total Fe (µM)	calculated Eh (mV)***	S^{2-} (µM)
MW	3	-	20-Jun-04	171	-	10.37	62.52	-	-	9.31	-	7.8	-	-	-	-	-
MW	2	-	20-Jun-04	171	-	91.79	17.78	-	-	8.91	-	6.7	-	-	-	-	-
MW	1	-	20-Jun-04	171	-	13.85	5.06	-	-	8.46	-	7.2	-	-	-	-	-
MW	9	-	25-Jun-04	176	-	18.99	6.03	-	-	8.87	-	7.3	-	-	-	-	-
MW	7	-	25-Jun-04	176	-	10.64	9.77	-	-	9.14	-	6.5	-	-	-	-	-
MW	6	-	25-Jun-04	176	-	4.50	6.18	-	-	8.4	-	10.8	-	-	-	-	-
MW	5	-	25-Jun-04	176	-	2.36	9.39	-	-	7.96	-	12	-	-	-	-	-
MW	4	-	25-Jun-04	176	-	5.51	6.50	-	-	8.95	-	12.3	-	-	-	-	-
MW	3	-	25-Jun-04	176	-	5.46	8.63	-	-	8.99	-	10.5	-	-	-	-	-
MW	2	-	25-Jun-04	176	-	7.03	12.48	-	-	7.95	-	9.78	-	-	-	-	-
MW	1	-	25-Jun-04	176	-	30.00	2.36	-	-	8.36	-	10.1	-	-	-	-	-

Matrix	Site	Rep/Well	Date	Julian day	Water column** (cm)	T-As (ng L^{-1})	D-As (ng L-1)	As V (ng L-1)	As (III) (ng L-1)	pH	measured Eh (mV)	Temperature (°C)	Fe(III) (µM)	Fe(II) (µM)	Total Fe (µM)	calculated Eh (mV)***	S^{2-} (µM)
GW	1	1	28-Jun-04	179	6	40.00	40.00	-	0.00	7.77	319	6.5	148.80	251.11	399.91	169.03	3.13
GW	1	2	28-Jun-04	179	7	330.00	440.00	-	0.00	8.25	326	6	125.86	192.02	317.87	169.61	3.14
GW	3	1	28-Jun-04	179	7	340.00	640.00	-	88.25	6.89	326	4.8	415.90	359.98	775.88	172.87	3.14
GW	3	2	28-Jun-04	179	6	550.00	470.00	-	3.49	7.03	365	5	185.64	253.19	438.83	170.26	3.14
GW	6	1	28-Jun-04	179	9	430.00	490.00	-	24.50	7.45	394	5.8	205.24	336.13	541.37	169.20	4.79
GW	6	2	28-Jun-04	179	12	480.00	510.00	648.62	70.30	8.16	442	4.6	47.62	13.69	61.30	179.21	4.79
GW	6	3	28-Jun-04	179	8	0.00	0.00	649.62	95.29	8.11	432	6.4	27.16	0.21	27.37	200.07	8.10
GW	7	1	28-Jun-04	179	10	520.00	460.00	568.75	19.98	8.43	455	4.6	144.84	211.72	356.55	169.86	1.49
GW	7	2	28-Jun-04	179	10	0.00	0.00	419.91	0.00	8.47	463	5.1	186.92	340.28	527.20	168.60	8.10
GW	7	3	28-Jun-04	179	14	480.00	420.00	1117.84	19.59	8.16	465	6.5	54.40	23.02	77.42	176.98	6.45
GW	9	1	28-Jun-04	179	10	330.00	260.00	264.99	26.58	8.06	325	6.5	467.70	349.61	817.31	173.71	1.49

Matrix	Site	Rep/Well	Date	Julian day	Water column** (cm)	T-As (ng L^{-1})	D-As (ng L-1)	As V (ng L-1)	As (III) (ng L-1)	pH	measured Eh (mV)	Temperature (°C)	Fe(III) (µM)	Fe(II) (µM)	Total Fe (µM)	calculated Eh (mV)***	S^{2-} (µM)
GW	9	3	28-Jun-04	179	12	350.00	460.00	366.06	110.76	7.13	381	4.9	92.66	129.81	222.47	170.10	3.14
GW	1	1	30-Jun-04	181	4	410.00	350.00	158.01	59.36	7.73	273	6.3	183.42	314.36	497.78	168.94	8.10
GW	1	2	30-Jun-04	181	5	440.00	320.00	672.92	38.13	8	278	5.3	153.90	152.62	306.52	172.09	3.14
GW	3	1	30-Jun-04	181	5	420.00	610.00	251.80	15.74	7.41	298	4.3	443.66	492.69	936.35	171.44	6.45
GW	6	1	30-Jun-04	181	6	440.00	310.00	339.91	11.56	7.68	388	5.77	50.40	23.02	566.00	176.54	9.76
GW	6	2	30-Jun-04	181	4	370.00	480.00	472.80	127.18	7.68	388	5.77	207.30	328.87	566.00	169.39	3.14
GW	7	1	30-Jun-04	181	10	330.00	320.00	330.28	1.19	8.14	458	4.4	294.42	366.20	660.62	170.79	3.14
GW	7	2	30-Jun-04	181	10	490.00	330.00	750.09	0.00	7.75	455	5.2	75.44	35.46	110.90	176.38	3.14
GW	7	3	30-Jun-04	181	15	1050.00	450.00	85.67	18.82	7.84	461	5.4	271.06	461.59	732.64	168.98	3.14
GW	9	1	30-Jun-04	181	4	0.00	0.00	487.49	0.00	7.77	354	5.1	534.20	531.05	1065.25	172.07	8.10
GW	3	3	03-Jul-04	184	6	450.00	420.00	517.35	61.56	7.28	466	4.8	263.66	389.01	652.67	169.80	1.49

Matrix	Site	Rep/Well	Date	Julian day	Water column** (cm)	T-As (ng L^{-1})	D-As (ng L-1)	As V (ng L-1)	As (III) (ng L-1)	pH	measured Eh (mV)	Temperature (°C)	Fe(III) (µM)	Fe(II) (µM)	Total Fe (µM)	calculated Eh (mV)***	S^{2-} (µM)
GW	5	1	03-Jul-04	184	14	2230.00	1360.00	557.03	231.13	7.2	301	3.6	249.67	303.94	566.06	172.72	5.12
GW	5	2	03-Jul-04	184	12	1840.00	920.00	308.99	90.33	7.1	372	3.8	356.84	522.76	879.60	169.85	8.10
GW	5	3	03-Jul-04	184	11	910.00	410.00	1196.52	23.37	7.06	394	5.6	144.60	240.75	385.34	169.11	8.10
GW	6	3	03-Jul-04	184	4	320.00	370.00	143.10	0.00	8.83	356	4.5	230.04	170.24	400.28	173.77	6.45
GW	7	1	03-Jul-04	184	12	370.00	410.00	191.46	23.88	8.32	422	6.1	37.88	16.80	54.67	176.71	18.02
GW	7	2	03-Jul-04	184	12	470.00	430.00	91.25	21.78	8.45	420	7	37.56	20.94	58.50	175.40	0.01
GW	7	3	03-Jul-04	184	12	600.00	540.00	264.48	8.78	8.4	425	6.4	356.98	644.06	1001.04	168.65	4.79
GW	9	1	03-Jul-04	184	10	1030.00	1230.00	115.63	243.27	8.04	358	6.8	85.24	128.77	214.01	169.67	3.14
GW	9	2	03-Jul-04	184	13	610.00	890.00	110.37	511.88	8.2	358	6.8	166.10	59.30	225.40	177.96	9.76
GW	9	3	03-Jul-04	184	13	710.00	710.00	394.30	39.25	7.2	370	5.3	242.00	313.32	555.32	170.56	4.79
GW	1	1	05-Jul-04	186	7.5	610.00	770.00	147.96	134.24	6.82	391	8.4	1338.74	1813.58	3152.32	170.30	0.01

Matrix	Site	Rep/Well	Date	Julian day	Water column** (cm)	T-As (ng L^{-1})	D-As (ng L-1)	As V (ng L-1)	As (III) (ng L-1)	pH	measured Eh (mV)	Temperature (°C)	Fe(III) (µM)	Fe(II) (µM)	Total Fe (µM)	calculated Eh (mV)***	S^{2-} (µM)
GW	1	3	05-Jul-04	186	8	530.00	1060.00	203.80	78.66	7.03	353	5.5	532.60	448.11	980.71	173.03	1.49
GW	3	2	05-Jul-04	186	6	920.00	1040.00	247.18	14.08	6.69	450	7.2	355.70	556.97	912.67	169.46	6.45
GW	5	1	05-Jul-04	186	13.5	910.00	550.00	170.20	207.23	7.25	342	4.3	207.04	325.76	532.80	169.43	14.72
GW	5	3	05-Jul-04	186	7	1090.00	510.00	206.64	24.00	7.33	395	5.7	124.28	141.21	265.49	171.31	6.45
GW	7	1	05-Jul-04	186	11.5	1040.00	520.00	1987.32	0.00	7.38	468	6.6	93.72	70.71	164.43	173.66	8.10
GW	7	2	05-Jul-04	186	10	450.00	250.00	73.70	29.26	7.59	459	7.2	744.78	841.06	1585.84	171.34	0.01
GW	7	3	05-Jul-04	186	14.5	340.00	430.00	113.56	31.06	7.51	473	8.4	119.02	86.26	205.28	173.89	8.10
GW	9	1	05-Jul-04	186	9.5	1070.00	1240.00	369.31	562.79	7.93	371	6.8	151.14	175.43	326.57	171.18	3.14
GW	9	2	05-Jul-04	186	10	1660.00	900.00	247.62	479.39	7.39	355	6.6	61.36	10.58	71.93	182.15	1.49
GW	9	3	05-Jul-04	186	10	1030.00	820.00	104.50	208.62	7.35	377	6.6	520.58	623.33	1143.91	171.00	1.49

* Matrices of snow (S), meltwater (W) and superpermafrost groundwater (GW).
** Water column inside polyvinyl chloride tube with 5 cm inner diameter \
*** Eh is calculated according to the following formula using concentrations of Fe(II) and Fe(III) (Kirk, 2004):

$$pe = pe^{\circ} - \frac{1}{n\left(\log\frac{[red]}{[ox]}\right)} \tag{C.1}$$

$$Eh = pe\left(\frac{2.303RT}{F}\right) \tag{C.2}$$

where pe^{o} is 13.0 (Kirk, 2004) assuming $Fe^{3+}+e^{-} \rightarrow Fe^{2+}$, R = 1.98722 cal K^{-1} mol^{-1}, T = 298K, F = 96484.6 C mol^{-1}.

APPENDIX D

Arsenic speciation was determined by analyzing samples without pre-reducing to arsenite with potassium iodide, allowing the determination of mostly arsenite. A consistent fraction of arsenate is also able to be detected by the AFS as seen in Figure C.1. For determination of standard curved, an arsenate solution was prepared with sodium arsenate ($Na_2HAsO_4 \cdot 7H_2O$) (Mallinckrodt Chemicals) in distilled water, and an arsenite solution was prepared with sodium arsenite ($NaAsO_2$) (Mallinckrodt Chemicals) in room temperature oxygen-free water in a N_2-filled glovebox

At the low arsenic concentrations assessed in this study, the use of potassium iodide (KI) to reduce As(V) to As(III) for HG-AFS analysis proved problematic. It is commonly assumed that in a mixed solution of As(III) and As(V), As(V) will not contribute to HG-AFS signal. Thus, one uses KI to reduce As(V) to As(III). Then by difference, one can estimate As(V) and As(III). The Millenium HG-AFS detects 98.2% of the As(III) as well as 22.7% (0.227 = 1.215 ÷ 0.277) of As(V) present in solution without addition of KI (Figure 1). Thus, assuming that arsenic in soil slurries is a combination of As(III) and As(V) (Sadiq, 1995), samples can be analyzed as follows:

Response (no KI added) = 0.9819 As(III) + 0.277 As(V) (4.1)

Response (KI added) = 0.9819 As(III) + 1.215 As(V) (4.2)

Response (no KI added) – Response (KI added) = 0.938 As(V) (4.3)

Once equation 5 is solved, then equation 4 will yield As(III) concentrations.

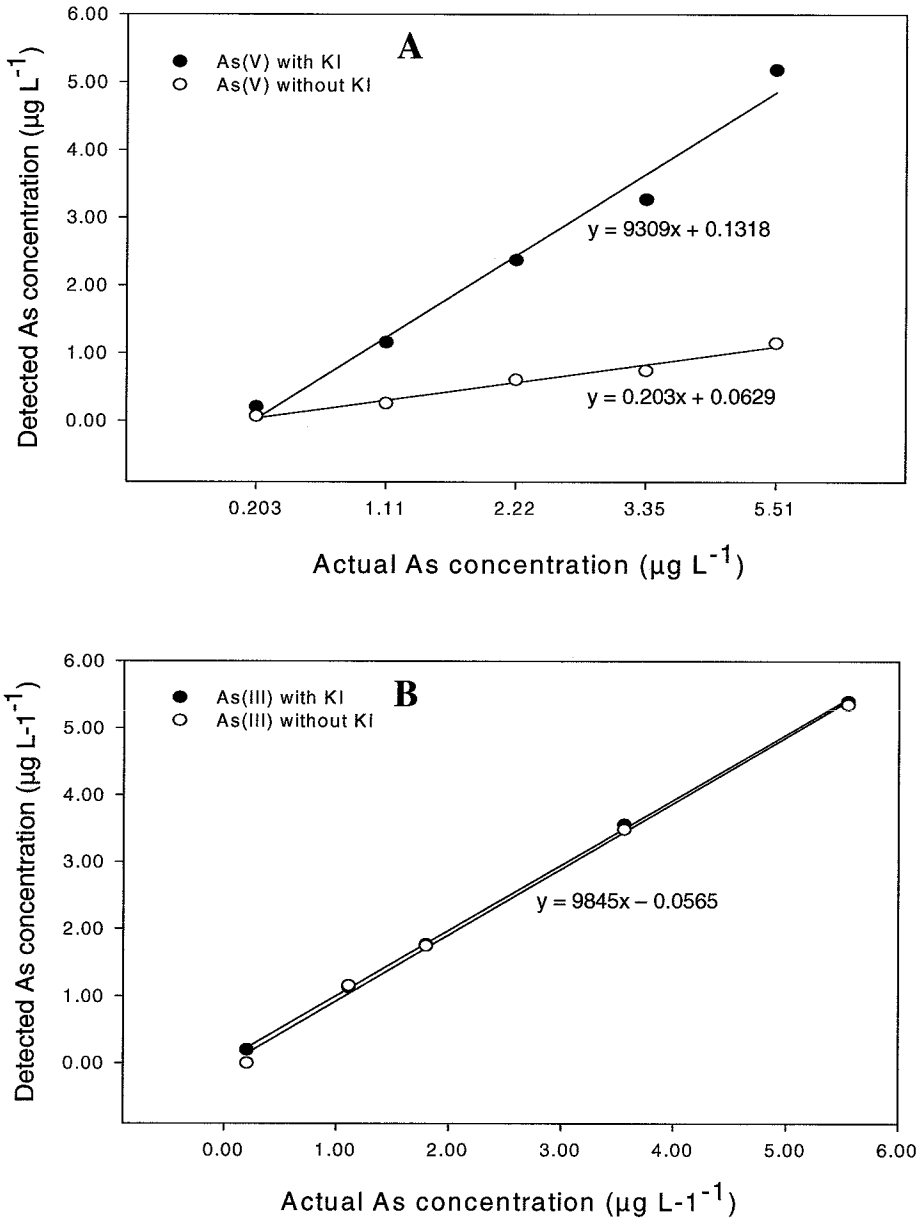

Figure D.1 Arsenic detected by the Millenium AFS for (A) arsenate (As(V)) and (B) arsenite (As(III)) with and without the reducing agent KI. The Millenium AFS detects 100% of the As(III) but only 22.7% of As(V) present in solution without addition of KI.